RESIDUAL STRESSES PRODUCED DURING SHARP BENDING OF WIDE SHEETS

RESIDUAL STRESSES PRODUCED DURING SHARP BENDING OF WIDE SHEETS

by

DEVENDRA K. TYAGI, B.Sc.(HONS.)
B.Sc. Civil & Municipal Eng. (HONS.)

A Thesis

Submitted to the Faculty of Graduate Studies

in Partial Fulfilment of the Requirements

for the Degree

Master of Engineering

McMaster University

1971

MASTER OF ENGINEERING
(Civil Engineering)

McMASTER UNIVERSITY
Hamilton, Ontario

TITLE: Residual Stresses Produced During Sharp Bending of Wide Sheets

AUTHOR: Devendra K. Tyagi, B.Sc.(Hons.)
Banaras Hindu University

B.Sc. Civil & Municipal Engineering (Hons.)
Banaras Hindu University

SUPERVISOR: Dr. Robert M. Korol

NUMBER OF PAGES: xvi, 149

SCOPE AND CONTENTS:

Manufacturing processes such as cold-bending flat sheet to a small radius produces a rather complex residual stress state through the thickness of light gauge structural steel sections. When the load-application device is released the sheet exhibits a phenomenon called "spring-back".

The purpose of this research was to develop an exact method of computing the residual stresses in a wide sheet of ideal plastic metal after spring back and subsequently to study their effect on the behaviour of cold-formed sections. An approximate analysis based on the assumption of elastic spring back is presented for comparison purposes. It is demonstrated that plastic flow occurs within a thin core of sheet below the neutral axis and that the spring back is not completely elastic beyond a certain curvature. Such behaviour is particularly significant in cases where the radius of bend is of the same order as the thickness. An exact analysis based

on a more realistic approach is then performed considering the adjustments in the stress components due to the plastic core. Computer programs have been developed to calculate the residual stresses associated with any given radius of bend. It is found that the choice of one yield criterion rather than the other does not have any effect on the present analysis and the stress components for Von Mises' material are $(2/\sqrt{3})$ times the components for Tresca's material. Furthermore, the effect of lateral stretching on the behaviour of cold-formed sections is briefly viewed.

The purpose of the experimental work in this thesis was to verify the validity of some of the assumptions made in the analysis.

Conclusions are drawn and suggestions made for further research.

ACKNOWLEDGEMENTS

The author wishes to express his deepest gratitude and sincere appreciation to Dr. Robert M. Korol for his guidance and encouragement throughout the course of this research.

The financial support of the National Research Council of Canada and the scholarship and teaching assistantship awarded by McMaster University are gratefully acknowledged.

Especially recognized is the skill and the patience of Mrs. Suzanne McQueen, who typed the manuscript of this thesis.

Thanks are also due to my parents for their patience, general assistance and advice.

Devendra K. Tyagi

TABLE OF CONTENTS

CHAPTER		PAGE
I	INTRODUCTION	1
	1.1 Preliminaries	1
	1.2 Cold-Forming	3
	1.3 Literature Survey	8
	1.4 Current Work	12
II	SHEET BENDING ANALYSIS	17
	2.1 Mathematical Formulation of the Problem	20
	2.2 Von Mises Criterion	25
	2.3 Tresca Criterion	27
	2.4 Moment Required to Bend the Sheet	29
III	SPRING-BACK ANALYSIS	34
	3.1 Approximate Analysis—Completely Elastic	35
	3.1.1 Residual Stresses	41
	3.2 Validity of the Assumption of Elastic Spring-Back	42
	3.3 Exact Analysis — Plastic Core	44
	3.3.1 Stresses in Plastic Zone	46
	3.3.2 Unloading Stresses in Elastic Zones	47
	3.3.3 Residual Stresses	53
	3.3.4 Determination of Unknowns-c,ρ,γ and k	60

Chapter		Page
IV	VALIDITY OF ASSUMPTIONS AND EXPERIMENTAL WORK	69
	4.1 Stress-Strain Curves	71
	4.2 Measurement of Lateral Strains During Bending Operation	76
	4.3 Verification of Plane Strain Condition	81
	4.4 Verification of Virtual Constancy of Physical Dimensions During Spring-Back	85
V	RESULTS AND DISCUSSIONS	93
	5.1 Plots of Residual Stress Components	93
	5.2 Geometric Representation of Stress Path and Residual Stress Distribution	107
	5.3 Effect of Longitudinal Stretching on the Behaviour of Cold-Formed Sections	117
VI	CONCLUSIONS AND RECOMMENDATIONS FOR FURTHER RESEARCH	120
APPENDIX		
A	COMPUTER PROGRAMS FOR CALCULATING BENDING, SPRING-BACK, RESIDUAL AND DEVIATORIC STRESS COMPONENTS	123
	A.1 Designations	123
	A.2 Flow Chart for Approximate Analysis' Program	126

		Page
	A.3 Flow Chart for Exact Analysis' Program	127
	A.4 Computer Program--Approximate Analysis	130
	A.5 Computer Program--Exact Analysis	133
BIBLIOGRAPHY		143

LIST OF FIGURES

FIGURE	TITLE	PAGE
1.1	Air-Press-Braking	6
1.2	Schematic Diagram of a Typical Sheet Bending Press	7
2.1	Geometry of the Bent Sheet Showing the System of Axes Used	18
2.2	Stresses on a Typical Volume Element	23
2.3	Circumferential Stress (σ_θ) Distribution for a/t=3.0, ν=.3	30
3.1	Geometry of Curved Sheet	37
3.2	Stresses on a Typical Element	37
3.3	Elastic and Plastic Residual Stress Zones After Spring-Back	45
3.4	Unloading Strains in Sheet	48
3.5	Enlarged view of Fig. 3.4	49
3.6	Sheet Thickness Divided in m Parts	59
4.1	Dimensions of the Tension Specimen	70
4.2	Stress-Strain Curves for Alcon 2S-H14	75
4.3	Bending Press	77
4.4	Position of Strain Gauge on the Sheet	80
4.5	Sheet Bend Around the Rod	82
4.6	Non-Alignment of Strain Gauge	82

Figure	Title	Page
4.7	Geometry of Element for a/t=1.0 (a) Before Spring-Back (b) After Spring-Back	86
5.1	Residual Stress Distributions for a/t=1.5	94
5.2	Exact Residual Stress Distributions for a/t=2.0, ν=.3	95
5.3	Exact Residual Stress Distributions for a/t=3.0, ν=.3	96
5.4	Exact Residual Stress Distributions for a/t=4.0, ν=.3	97
5.5.	Exact Residual Stress Distributions for a/t=5.0, ν=.3	98
5.6	Residual Stress Distributions for a/t=6.0, ν=.3	99
5.7	Exact Residual Stress Distributions for a/t=25.0, ν=.3	100
5.8(a)	Projection of σ'_θ on π Plane	109
5.8(b)	Representation of Stress Components on π Plane	109
5.9	Stress Paths of Extreme Fibres During Bending and Spring Back (a/t=1.5, ν=.3)	111
5.10	Geometric Representation of Residual Stress Distribution on the Plane of Deviatoric States of Stress and Subsequent Stretching for a/t=1.5, ν=.3	113

Figure	Title	Page
5.11	Geometric Representation of Residual Stress Distribution on the Plane of Deviatoric States of Stress for a/t=25.0, ν=.3	115
5.12	Geometric Representation of Residual Stress Distribution on the Plane of Deviatoric States of Stress for a/t=1.5,ν=.5.	116

LIST OF PHOTOGRAPHS

PHOTOGRAPH	TITLE	PAGE
4.1	Specimens for Tension Test	89
4.2	Bending Press	90
4.3	Specimen for Sheet Bending Test	91
4.4	Experimental Set-up for Bending Test	92

LIST OF TABLES

TABLE NO.	TITLE	PAGE
4.1	Test Data for Tension Test (Specimen in the Direction of Rolling)	72
4.2	Test Data for Tension Test (Specimen at 45° to the Direction of Rolling)	73
4.3	Test Data for Tension Test (Specimen at 135° to the Direction of Rolling)	74
4.4	Results of Tensile Test	76
5.1	Residual Circumferential stress (σ_θ^R) at Critical Fibres (Exact Method, ν=0.3)	102
5.2	Residual Radial Stress (σ_r^R) at Critical Fibres (Exact Method, ν=0.3)	103
5.3	Residual Lateral Stress (σ_z^R) at Critical Fibres (Exact Method, ν=0.3)	104
5.4	Position of Neutral Axis and Thickness of Plastic Core	105

NOMENCLATURE

θ, r, z	Coordinates in circumferential, radial and axial direction
a	Radius of curvature of the concave (inner) boundary of the plastically bent sheet
b	Radius of curvature of the convex (outer) boundary of the plastically bent sheet
a^s	Radius of curvature of inner fibre after spring back
r	Radius of curvature of any general fibre
r_n	Radius of curvature of the neutral surface
r_n^s	Radius of curvature of the neutral surface after spring back
ρ	Radius to inner elastic-plastic boundary
c	Radius to NN, the fibre where unloading circumferential strain is zero (Fig. 3.5)
t	Thickness
x	Distance between inner fibre and NN (Fig. 3.5)
y	Distance of any general fibre from NN
d	Thickness of each small division of total sheet thickness (=t/m)
Δr	Differential increment in r

m	Number of parts in which sheet thickness is divided
j	Boundary of any general division of the thickness (j=0 at r=a and j=m at r=b)
$d\theta$	Differential angle between plane sections
d_θ^s	Differential angle after spring back
δ	Angle between strain gauge and the axis of bending
$\delta d\theta$	Rotation of a plane section
ν	Poisson's ratio
E	Young's modulus of elasticity
α	$= \frac{E}{1-\nu^2}$
β	$= \frac{2\nu-1}{1-\nu}$
γ	$= \frac{\alpha a \varepsilon_{\theta_i}^s}{x}$
ϕ	Airy's stress function
$d\lambda$	Scalar constant in Prandtl-Reuss equation
N	Constant for a particular geometry of sheet, defined by equation [3.10]
V	$= \frac{t^2}{N}(-\frac{2a^2b^2}{r^2} \ln \frac{b}{a} + b^2 - a^2)$

A, B, C, D, k	Constants of integration
σ_y	Uniaxial stress necessary to cause plastic flow
σ_θ, σ_r, σ_z	Normal stresses in circumferential, radial and axial direction
σ_{max}, σ_{min}, σ_{int}	Maximum, minimum and intermediate principal stresses
σ_θ^s , σ_r^s, σ_z^s	Spring-back or unloading normal stresses
σ_θ^R , σ_r^R, σ_z^R	Residual normal stresses
$\bar{\sigma}$	Hydrostatic or mean stress component, $(\sigma_\theta + \sigma_r + \sigma_z)/3$
σ_θ', σ_r', σ_z'	Deviatoric stress components such as $\sigma_\theta' = \sigma_\theta - \bar{\sigma}$
σ'_{max}, σ'_{int}, σ'_{min}	Deviatoric components of maximum, intermediate and minimum principal stresses
σ'_{ij}	Deviatoric stress tensor
$\sigma^s_{\theta_\rho}$	Unloading circumferential stress at $r = \rho$
$\sigma^R_{\theta_\rho}$	Residual circumferential stress at $r = \rho$
$\sigma^s_{r_\rho}$	Unloading radial stress at $r = \rho$
$\sigma^s_{r_{r_n}}$	Unloading radial stress at $r=r_n$
$\sigma^R_{r_\rho}$	Residual radial stress at $r = \rho$

$\sigma^R_{r_{r_m}}$	Residual radial stress at $r=r_n$
$\sigma^s_{\theta_j}$	Unloading circumferential stress at j^{th} boundary.
$\sigma^s_{r_j}$	Unloading radial stress at j^{th} boundary
$\sigma^s_{r_m}$	Unloading radial stress at m^{th} boundary i.e. at r=b
$\Delta\sigma^s_r$	Differential increment in σ^s_r
$\Delta\sigma^s_{r_j}$	Differential increment in, σ^s_r at j^{th} boundary
ε_y	Uniaxial strain when yielding commences
ε_θ, ε_r, ε_z	Normal strains in circumferential, radial and axial direction [natural strain, $\varepsilon=\ln(1+e)$]
e	Engineering strain [(change in lenth)/(original length)]
ε^P_{max}, ε^P_{min}, ε^P_{int}	Maximum, minimum and intermediate principal strains
ε^s_θ, ε^s_r, ε^s_z	Spring back or unloading, normal strains
ε^R_θ, ε^R_r, ε^R_z	Residual normal strains
$\varepsilon^s_{\theta_i}$	Unloading circumferential strain at inner fibre
$d\varepsilon^P_{ij}$	Plastic strain increment tensor
M_p	Fully plastic moment per unit width

M^s	Spring back or unloading moment per unit width
M_1	$= \int_a^\rho \sigma_\theta^s \, r \, dr$
M_2	$= \int_{r_n}^b \sigma_\theta^s \, r \, dr$
M_3	$= -\sigma_y [-\frac{t^2}{4} + \frac{1}{2}(r_n^2-\rho^2)\ln(ak)]$
F_1	$= \int_a^\rho \sigma_\theta^s \, dr$
F_2	$= \int_{r_n}^b \sigma_\theta^s \, dr$
F_3	$= -\sigma_y \ln(ak)(r_n-\rho)$

CHAPTER I

INTRODUCTION

1.1 Preliminaries

An elastic perfectly plastic material responds differently in the plastic and elastic states of behaviour. These distinct states are separated by the elastic limit of the material. The behaviour of a metal and the related laws are simple and well defined in the elastic range but are rather complex and sometimes misunderstood in the plastic range.

In the design of structures and machines the yield point may be used as the criterion of failure of a structural or mechanical member. However, as is known, the material retains carrying capacity and is not destroyed, even if it has been stressed beyond its yield point. On the contrary, most metals after once having been stressed beyond their yield points have a greater resistance to deformation than they had prior to such treatment.[1,2,3,4,8,22,30] The plastic phenomenon makes it possible to fabricate a variety of structural shapes by a vast number of methods.

Since the very beginning of the structural use of the ferrous metals, desired shaping has been achieved either in the hot state (hot rolling, casting etc.) or by cold-forming of plate, sheet or strip. The development of both

methods started around the middle of the last century, with cold-formed steel construction having developed rather more rapidly during the last 30-35 years.

The structural members used in light-gage steel construction are produced by various cold-forming processes. Closed shapes such as rectangular and square, hollow structural steel sections are cold-formed from the round pipes in some steel mills.[3] During fabrication, metal plates are often cold formed to small radii-a fabrication procedure that may plastically strain the plates large amounts. The "minimum bend radius" or maximum curvature, to which a given metal can be formed without failure varies within wide limits, depending upon the "breadth-to-height ratio" of the cross-section. Sangdahl, Aul and Sachs[5] reported that for sections whose breadth is greater than their height, minimum bend radius generally increases with increasing breadth-to-height ratio.

During the fabrication process, initially flat sheets are permanently deformed into desired shapes by different cold forming methods (to be discussed later) and the sheets are subjected to a complex history of loading. When the load-application device is released, the sheet tries to return to its initial flat shape and exhibits a phenomenon called "spring back".

The analysis and determination, of residual stresses and strains after spring back, is desirable and would be helpful if such sections are to be used for structural purposes.

1.2 Cold-Forming

Various authors[1,2,3,4] have reported the change in the mechanical properties of the metal sheets after such sheets were cold-formed to structural shapes for light gage steel construction. The cold working usually increases the yield and ultimate strengths and decreases ductility. These changes in the mechanical properties depends upon the chemical composition of steel or any other ductile metal, its prior cold work and metallurgical histories and the magnitude of the plastic strains. Karren[2] reported that the yield strength of corners cold formed by roll-form or press brake, was up to 102% larger than the virgin yield strength of the metal. The increase in ultimate tensile strength was reported to be up to 47%. Alexander Chajes, S.J. Britvec and George Winter[1] attributed these changes to: strain hardening, strain aging and Bauschinger effect.

Cold forming can be carried out with steels previously furnished with a variety of surface coatings, metallic (galvanized, aluminized etc) as well as plastic without

damaging the surface to give better aesthetic and architectural appearance as well as to provide improved corrosion protection. Cold forming permits the fabrication of a vast number of shapes, the majority of which could not be produced by hot-rolling. Cold forming has been responsible for the "light gauge steel construction"[4] in which the thickness of cold-formed members is generally smaller than that of hot-rolled members.

The hot-rolled steels are sharp yielding whereas cold-worked steels are "gradual yielding" due to the residual stresses induced and by cold-working itself. Karren[2] pointed out that the stress-strain curves of corner specimens are gradual yielding because of the varying amounts of plastic strain throughout the corner. He added that the effect of the residual stresses from cold working and that of residual cooling stresses in hot-rolled sections, are the same though their origin and distribution are quite different. The effect is to round the stress-strain curve at the "knee" and produce a reduced effective proportional limit.

Cold-formed members are used as: girders, joists, studs, columns, floor and wall panels and as roof decks, in many standardized steel buildings. Improved shapes are continually being developed for use.

The various cold-forming methods have been reported by many authors[2,15,16,17,18,20,21,24,26]. These methods as used in the fabrications of light gauge structural members and could be divided into two main groups

(1) roll-forming and

(2) brake-forming.

Roll-forming is a mass-production process and requires a number of roll stands. As the section passes successive stations in the rolling assembly, it is changed gradually from a flat sheet to the required shape. Roll design is still not a fully developed field and often the number of rolls required for a particular shape depends upon the skill and experience of the designer.

Brake forming is rather a straight bending, semi-manually operated process. It requires a standard set of tools, dies and punches for almost any shape which can be brake-formed. The process is slow and can only be used for a limited production rate. The process is subdivided into "air-press-braked" and "coin-press-braked". In the latter, both the punch and die match the final desired shape and to eliminate spring-back the sheet is "coined" or "bottomed" in the die. The variety of shapes that can be used for dies in "air" press-braking is somewhat limited since the corners are bent sharper than the final desired angle to allow for spring-back. Considerable pressure is developed on the

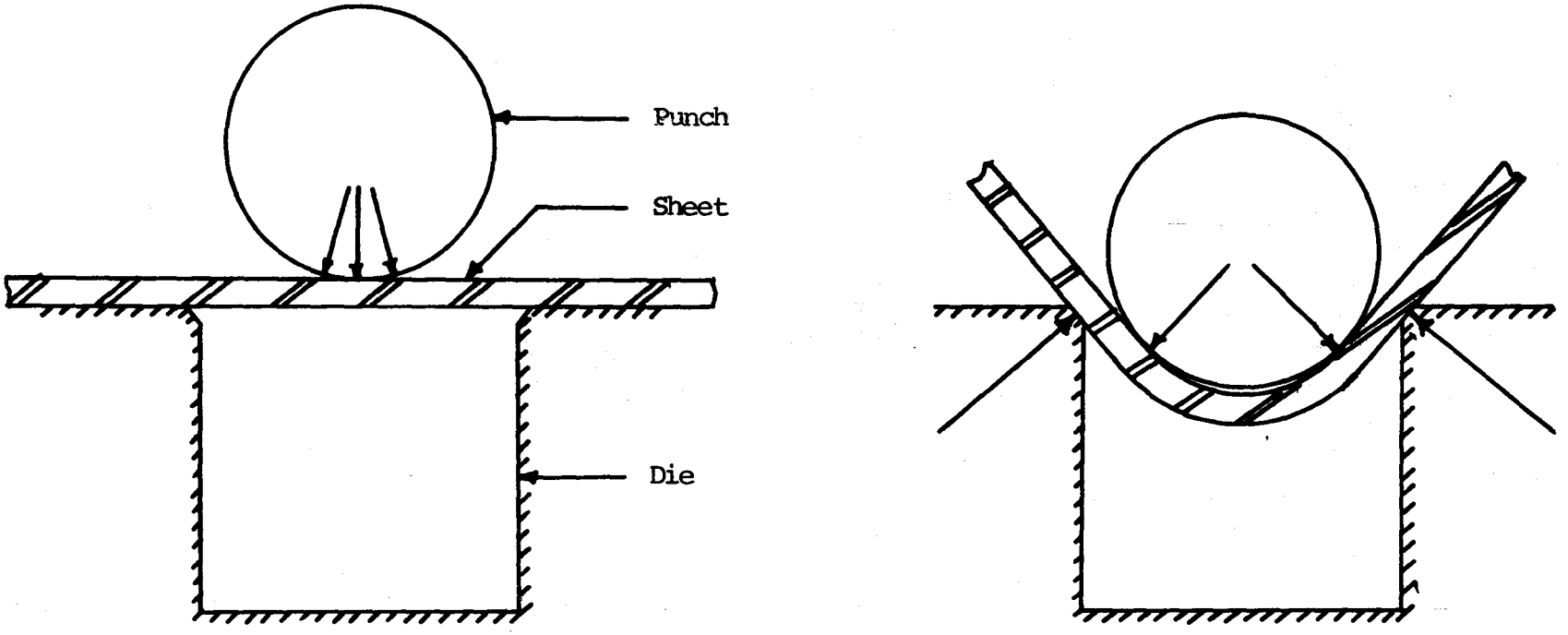

FIG. 1.1 AIR-PRESS-BRAKING

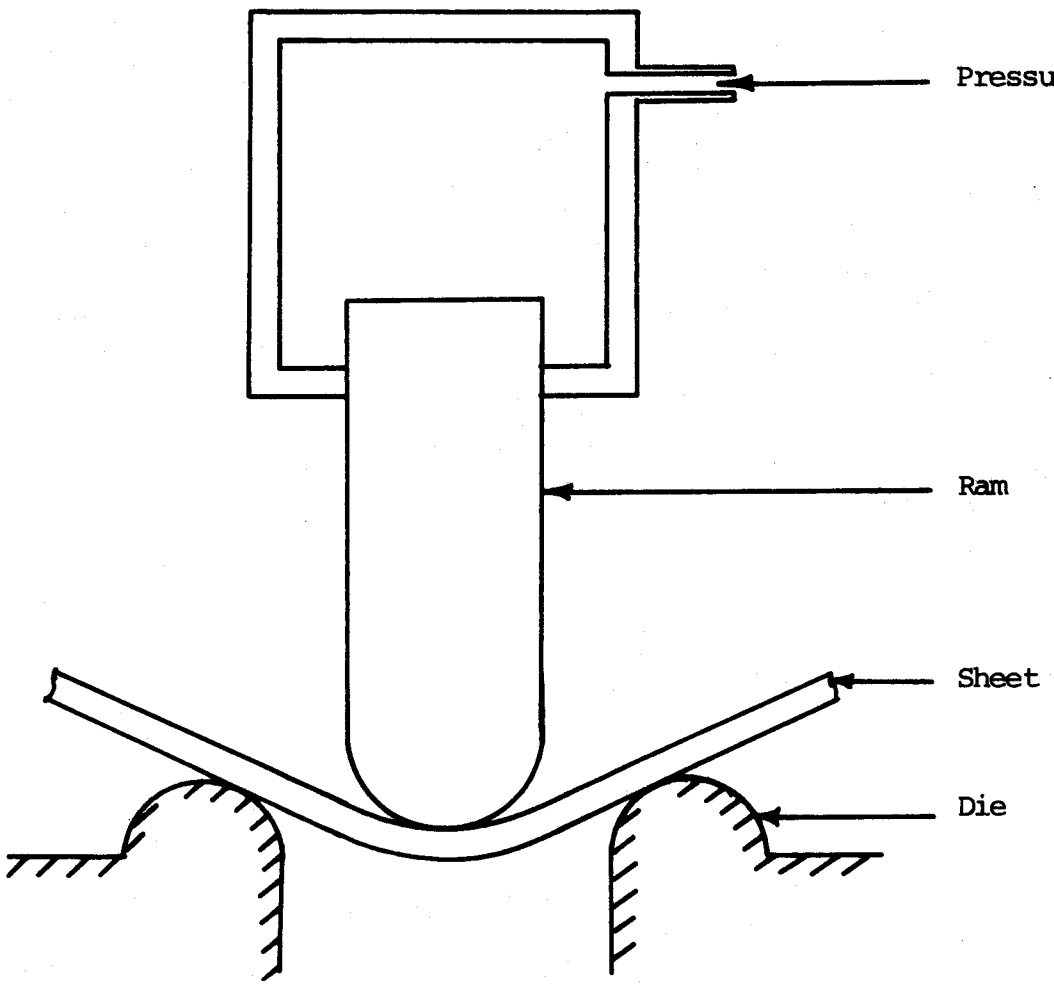

FIG. 1.2 SCHEMATIC DIAGRAM OF A TYPICAL SHEET BENDING PRESS

inside surface at the point of bending. However, this radial pressure is smaller than that developed in the case of either roll-forming or coin-press braking. Fig. 1.1 shows a simple air press application.

1.3 Literature Survey

Although the art of sheet bending and cold forming of structural sections is fully developed, the mathematical analysis of predicting residual stresses and strains is fairly complex and tedious. A number of investigators[2,6,19,20,25,26,35,38,39] have studied the behaviour of sheet metals bent to a circular profile by end couples however. In actual cold-working processes the loading system required to bend the sheet to the required shape is complex. In 1943, Schroeder[19] investigated the basic mechanical phenomenon occuring during the bending and spring back of sheet metals. Schroeder[19] and Gardiner[39], in their analysis of spring back assumed the neutral axis to coincide with the centroidal axis of the sheet and they took only circumferential stresses into consideration. Junker[26], in 1965, studied the surface strains developed in the bending of thick steel plates. In 1950, Lubahn and Sachs[35] and Hill[6] analysed the stresses and strains in plastically bent parts under conditions of plane strain as well as plane stress. In their analysis

they assumed "ideal plastic metal" i.e. metal with no strain-hardening. Their solutions show the movement of the neutral plane towards the compression side with curvature. Alexander[38], in 1959, studied the plain strain bending of wide plates. His analysis, true for moderate bending, neglects the stresses in the radial direction. He also investigated a geometric solution of the problem as described by Hill also. These computations are based on the classical theories of Prandtl-Reuss, Tresca and Von Mises.

Shaffer and House[36,37] gave the solution to the problem of the elastic-plastic bending of a wide curved bar of incompressible, perfectly plastic material under conditions of plane-strain. The corresponding problem under the conditions of plane-stress was investigated by Eason[33], who obtained solutions both for Tresca and Von Mises yield criteria and the associated flow rules. These investigations reported the shift of the neutral axis, in the elastic-plastic range of bending.

Karren[2,3], in 1967 and others[1,3,4], in their study of cold-forming of the structural steel shapes reported that a certain amount of radial pressure exists in die bending in addition to bending moment. The metal in a corner is even more highly compressed in the radial direction if it is coin pressed or roll-formed.

Sangdahl, Aul and Sachs[5] discovered that the ductility (defined as the maximum circumferential strain at fracture) is dependent upon the rectangular dimensions of the sheet. It decreases with increased lateral dimension to thickness ratio and vice-versa. Ductility was reported to decrease with an increasing ratio of longitudinal to circumferential stress i.e. if the stress-state changes from uniaxial tension to biaxial tension, until the plane strain state is reached.

The maximum-shearing-stress yield criterion derived by Tresca (1864) and the energy-distortion yield criterion by Von Mises (1913), are the two most commonly accepted conditions of yielding. Eason[32] gives an account of the different problems which have been solved by using Tresca and/or Von Mises criteria. He concludes that the distribution of stress for any given problem is relatively insensitive to the yield condition.

Rolfe[8] and Rolfe, Haak and Gross[30] reported that specimens taken from locations of high plastic deformation in HY-80 (United States Navy specification for all 80,000 psi minimum yield strength quenched and tempered alloy steel) steel plates cold-formed to different radii exhibited no Bauschinger effect (a phenomenon that results in an increase in the proportional limit and yield strength by reloading a plastically deformed specimen in the same direction, but in a decrease by reloading in the opposite direction) when

tested in the longitudinal direction. An increase in both tensile and compressive yield strength was observed as a result of strain hardening. In the structural components, which are usually cold-formed under plane-strain conditions the results of tests showed that regardless of the direction of cold-deformation (tension or compression) both the tensile and compressive yield strengths of specimens cut in the direction transverse to the direction of cold deformation were increased. Similar conclusions were drawn by Karren[2].

Cold forming of structural components may reduce the yield strength of a component if it is loaded in a direction opposite to that of cold forming. This reduction in yield strength is greatest for small amounts of cold deformation and is progressively decreased by strain hardening at large amounts. The Bauschinger effect is affected by the state-of-stress during forming (plane stress or plane strain) - more for plane stress axial deformation than for plane-strain bending deformation. The increase in tensile yield strength in the longitudinal direction from a compressive plastic strain in the tangential direction is offset by the reduction from the equal tensile plastic strain in the radial direction*

* *The condition that the volume remains constant during the plastic flow, can mathematically be expressed as:*

$$\varepsilon_\theta + \varepsilon_r + \varepsilon_z = 0$$

where ε_θ, ε_r, ε_z are normal strains in the circumferential, radial and lateral directions. For plane strain bending, $\varepsilon_z = 0$, hence, $\varepsilon_\theta = -\varepsilon_r$.

The significance of these results to cold-formed structural members is that, the apparent loss in yield strength in most structural members due to the Bauschinger effect should not be as great as the loss indicated by tests of uniaxially prestrained material.

Hill[6] showed that the neutral surface (i.e. the surface where the sign of circumferential stress reverses) and the fibre of zero strain are not the same. The neutral surface moves towards the centre of curvature and an area that was under compression, thus becomes stretched. Due to this shift of neutral axis tensile surface strains are greater than the compressive surface strains. Measurements by Rolfe, Haak and Gross[30] showed that the strain varies linearly through the thickness of the plate.

1.4 Current Work

The literature survey indicates that considerable work has been done to determine residual stresses in cold forming processes, but few investigators have computed the residual stress and strain components for a general

case. The residual stresses in the lateral direction (i.e. along the axis of bending) in a cold-formed structural section should be evaluated to determine the load carrying capacity of such a structural member. Since the radial stresses in the sharp bent sheets reach significant levels and also the position of the neutral axis does not, at all times, coincide with the centroidal axis, it is proposed to reinvestigate and extend the problem to improve understanding of behaviour of some cold formed structural shapes.

The first part of this research is devoted to the analysis of circumferential, radial and lateral (longitudinal) stresses in a wide sheet bent to such an extent that the elastic core is negligible in comparison with the thickness. Because of the condition of plane strain it was assumed that the Bauschinger effect is not significant in the lateral direction of a plastically bent sheet.

In the theory of plasticity there are two commonly accepted conditions of yielding--those due to Tresca and Von Mises. Mathematically, the Tresca yield condition is more tractable, and as a result has received more attention in recent years than the more mathematically acceptable Von Mises yield condition. Few problems have been solved for both the Tresca and Von Mises yield criteria and as a result there is little evidence of the effect of choosing one yield criterion rather than the other in a particular

problem for which the solutions differ. However, the analysis and calculations based on both criteria are presented in this work.

The next part of the thesis consists of a"spring-back" analysis of the bent sheet and an analysis of the "spring-back" or unloading stresses in the circumferential, radial and lateral directions. At first it is assumed that the spring-back is completely elastic and that the elastic unloading stress components are evaluated using the Airy stress function. The results of the two analyses are superimposed to obtain the residual stresses. However, the assumption that unloading is completely elastic is violated within a thin core of sheet below the neutral axis and plastic flow occurs in this zone. The thickness of this plastic core increases as the radius of curvature decreases.

An analysis is presented to evaluate the residual stress components considering the plastic core. For this purpose the thickness of sheet is divided into three zones—two zones near the concave and convex boundaries where spring back is elastic and separated by a plastic core. Equations are developed to evaluate elastic spring back stresses and subsequently the equations of residual stress components for the three zones are worked out. Unfortunately, the equations for spring back stresses are in incremental form and quite complicated, however, the stress distribution can be calculated

for any numerical problem.

Computer programs have been developed to calculate the bending, spring back, residual and deviatoric stress components in radial, circumferential and lateral directions both by an approximate analysis (neglecting plastic core) as well as by an exact analysis (considering plastic core). In these programs one needs to change only one parameter (ratio of inner fibre radius to sheet thickness, a/t) to get the stress components associated with a given radius of bend.

The calculations have been done for a/t = 1.5, 2, 3, 4, 5, 6 and 25 and a sheet thickness t of 1/4". The residual stresses are plotted and a comparison is made between the values given by the approximate and exact analyses. Except for one calculation in which Poisson's ratio ν is taken to be 0.5 a value of 0.3 has been assumed throughout this work. Comparison is also made between the stress components for a/t = 25 (a case of moderate bending i.e. an outer fibre strain of 2 per cent maximum) and those for the case of severe bending, a/t = 1.5.

The fourth part of the work is the geometric representation of the stress path and residual stress distribution on the plane of deviatoric states of stress (a plane passing through the origin and normal to the line which is inclined at equal angles with the axes). The stress paths are plotted

during bending and spring back. In addition the effect of subsequent uniaxial tensile loading is studied.

Primary tests were carried out on the 1/16" thick Alcan 2S-H14 aluminum sheets to determine its basic material properties. The yield point and the value for Young's modulus of elasticity were determined by A.S.T.M. standard tension tests. A few approximate calculations have been done to verify the validity of some of the assumptions made in the analysis. 7" x 7" x 1/16" thick aluminum sheets were bent to 1/16" internal radius i.e. a/t = 1 and the lateral strains were measured. A calculation based on these readings proved the existence of plane-strain conditions during the bending of wide sheets. Furthermore, the assumption of virtual constancy of physical dimensions of the sheet during spring-back was verified.

CHAPTER II

SHEET BENDING ANALYSIS

The analysis outlined in this chapter shows a method of calculating the stresses in the circumferential, radial and lateral directions in a wide metal sheet, plastically bent, by cold-forming in one direction.

To attempt an analysis of stresses in bent sheet, caused by cold work it is helpful to choose a model with a somewhat simpler force system acting than actually exists in any of the common methods of cold-forming. Despite the complex force system existing in actual cold-working processes, it is instructive and worthwhile to begin by investigating the simplified model[6,10]. Such a model in which the application of a pure bending moment to a wide flat sheet produces a uniform curvature and uniform tangential (circumferential) strain, is shown in Fig. 2.1.

The following set of assumptions is made to simplify the mathematical treatment of the problem.

(1) The metal is assumed to be "elastic-perfectly plastic" i.e. an ideal plastic metal which means that the metal obeys Hooke's law up to the yield point, and does not work-harden within the plastic range. For an actual metal with a specific stress-strain curve, the solution would be but little more complex than that presented here.

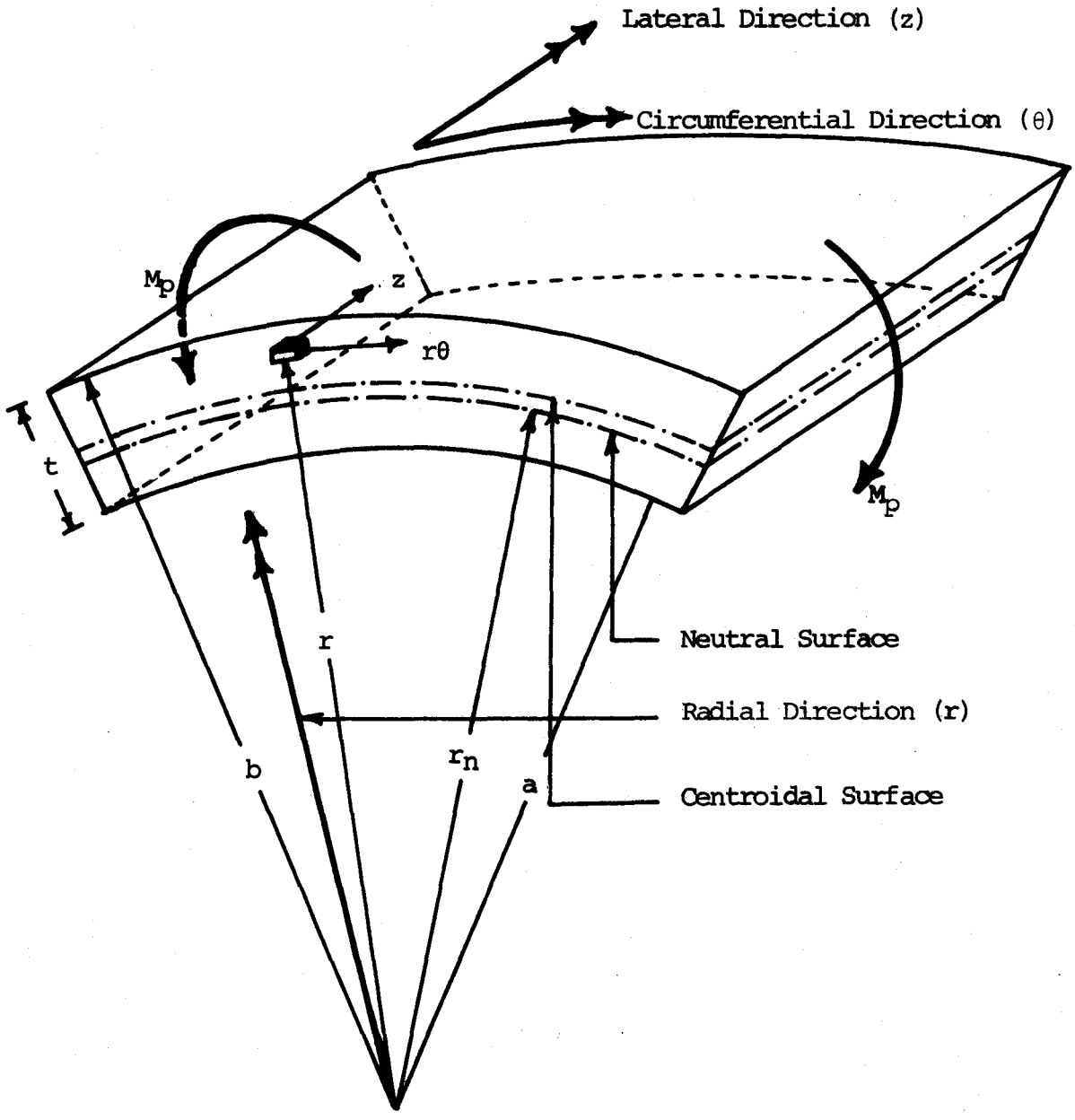

FIG. 2.1 GEOMETRY OF THE BENT SHEET SHOWING THE SYSTEM OF AXES USED

(2) The sheet is externally loaded by end moments only, which ensures that except at the ends of the bent sheet, there exists no pressure against inner or outer surfaces of the sheet. The bend is assumed to be sufficiently long in the circumferential direction so that the end effects do not interfere with the behaviour of the central portion.
(3) It is furthermore assumed that the bending moment applied to the edges of the sheet is sufficiently intense to cause the elastic core to virtually disappear so that the sheet is entirely plastic. During initial bending of a metal sheet behaviour is purely elastic; further bending causes yielding of outer fibres resulting in permanent strains. At subsequent stages of bending the centre core of the cross section remains elastic, and the outer fibres are plastic. As bending continues, the thickness of this elastic core diminishes. The complete elimination of this elastic core is, theoretically possible only with infinitely large displacements[36]. Practically, however, real materials exhibit a certain amount of strain-hardening so that the so-called fully plastic moment is attained with finite displacements, and the assumption of complete plastification during severe bending seems to be a reasonable one.
(4) Transverse planes are assumed to remain plane and Bauschinger effect is considered negligible.

(5) Further it is assumed that the sheet is wide enough so that except near the ends, the anticlastic curvature is negligible and the sheet may be analysed as a problem of plane-strain.

If a long narrow rectangular plate is loaded by end couples with axes parallel to long sides, the anticlastic curvature develops and the surface of the plate no longer remains cylinderical[11]. On the other hand, if a wide plate is bent, anticlastic curvature is prevented by membrane stresses which are developed at the ends where a so-called boundary layer effect is created[40]. The result is that the lateral strain ε_z is zero at every section except at the very ends of the sheet.

(6) It may be shown that the thickness of the sheet does not change during the plastic deformation[6,10]. This does not mean that the thickness of an elementary volume inside the bent sheet does not change however. It simply means that the overall thickness t=b-a remains constant.

2.1 Mathematical Formulation of the Problem

It can be readily seen that there exists no shear on the circumferential, radial and lateral planes, due to symmetry and hence these define the three principal stress directions.

During plastic flow the behaviour of the metal is supposed to be governed by the following "law of plastic flow" which is equivalent to an expression of incompressibility.

(i) $$\varepsilon^P_{max} + \varepsilon^P_{int} + \varepsilon^P_{min} = 0 \qquad [2.1.1]$$

or $$d\varepsilon^P_{max} + d\varepsilon^P_{int} + d\varepsilon^P_{min} = 0 \qquad [2.1.2]$$

where ε^P_{max}, ε^P_{min}, ε^P_{int} denote the maximum, minimum and intermediate principal strains respectively and $d\varepsilon$ is the increment in ε.

(ii) The stresses and strains in the plastic range are related by the Prandtl-Reuss equations

$$d\varepsilon^P_{ij} = d\lambda\ \sigma'_{ij}$$

where $d\varepsilon^P_{ij}$ = Plastic strain increment tensor

$d\lambda$ = A nonnegative scalar factor of proportionality (it may vary throughout the loading history)

σ'_{ij} = Deviatoric stress tensor

The above equation is equivalent to saying that the plastic strain increment (and not the total strain) is at any stage of loading history proportional to the instantaneous stress deviation. It also implies that the principal axes of stress and of plastic strain increment tensors coincide and that the increments of plastic strain depend on the current values of the deviatoric stress state (and not on the stress

increment required to reach this state).

In principal directions, the equations assume the form

$$d\varepsilon^P_{max} = d\lambda\sigma'_{max}; \quad d\varepsilon^P_{int} = d\lambda\sigma'_{int}; \quad d\varepsilon^P_{min} = d\lambda\sigma'_{min}$$

where

$d\varepsilon^P_{max}$, $d\varepsilon^P_{int}$, $d\varepsilon^P_{min}$ are the increments in the maximum, intermediate and minimum principal strains (plastic) respectively.

and σ'_{max}, σ'_{int}, σ'_{min} are the deviatoric components of maximum, intermediate and minimum principal stresses.

The equations can now be written as

$$\frac{\sigma'_{max}}{d\varepsilon^P_{max}} = \frac{\sigma'_{int}}{d\varepsilon^P_{int}} = \frac{\sigma'_{min}}{d\varepsilon^P_{min}} = \frac{1}{d\lambda}$$

or

$$\frac{\sigma'_{max} - \sigma'_{int}}{d\varepsilon^P_{max} - d\varepsilon^P_{int}} = \frac{\sigma'_{int} - \sigma'_{min}}{d\varepsilon^P_{int} - d\varepsilon^P_{min}} = \frac{\sigma'_{min} - \sigma'_{max}}{d\varepsilon^P_{min} - d\varepsilon^P_{max}} = \frac{1}{d\lambda}$$

Substituting

$$\sigma'_{max} = \sigma_{max} - \bar{\sigma}$$

$$\sigma'_{int} = \sigma_{int} - \bar{\sigma}$$

$$\sigma'_{min} = \sigma_{min} - \bar{\sigma}$$

where $\bar{\sigma}$ = Mean or hydrostatic stress component

$$= \frac{1}{3}(\sigma_{max} + \sigma_{int} + \sigma_{min})$$

Therefore

$$\frac{\sigma_{max} - \sigma_{int}}{d\varepsilon^P_{max} - d\varepsilon^P_{int}} = \frac{\sigma_{int} - \sigma_{min}}{d\varepsilon^P_{int} - d\varepsilon^P_{min}} = \frac{\sigma_{min} - \sigma_{max}}{d\varepsilon^P_{min} - d\varepsilon^P_{max}} = \frac{1}{d\lambda} \qquad [2.2]$$

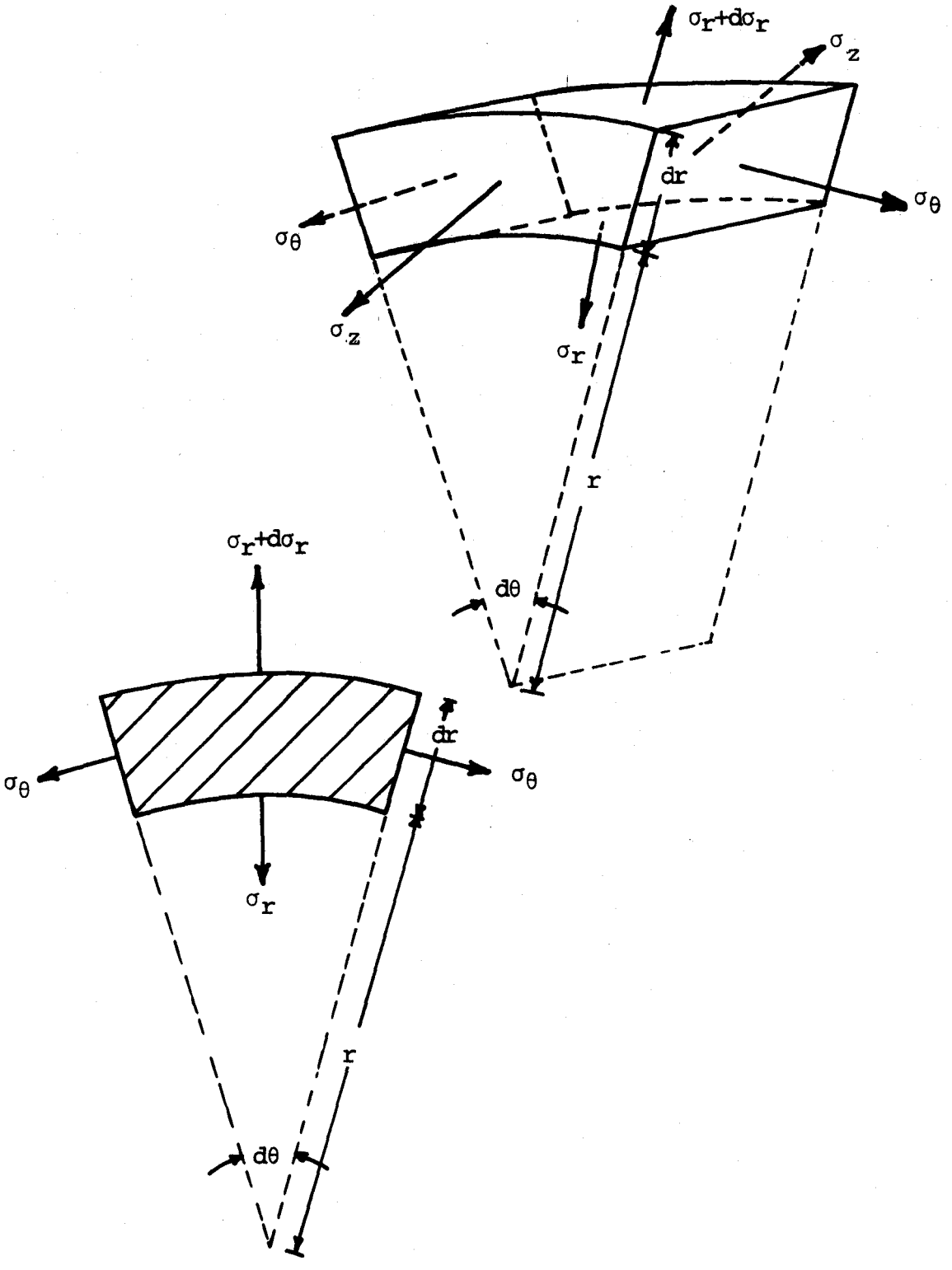

FIG. 2.2 STRESSES ON A TYPICAL VOLUME ELEMENT

(iii) As afore-said, both Tresca and Von Mises yield criteria will be used in the analysis. They mathematically, are represented as:

$$\text{Tresca: } \sigma_{max} - \sigma_{min} = \sigma_y \qquad [2.3.1]$$

$$\text{Von Mises: } (\sigma_{max}-\sigma_{int})^2+(\sigma_{int}-\sigma_{min})^2+(\sigma_{min}-\sigma_{max})^2=2\sigma_y^2 \qquad [2.3.2]$$

where σ_y = Uniaxial stress necessary to cause plastic flow.

(iv) The equilibrium condition requires that there be no radial stress at concave and convex surfaces as they are free from external loading

i.e. $\sigma_r = 0$ when $r=a$ [2.4.1]

$\sigma_r = 0$ when $r=b$ [2.4.2]

where σ_r = Normal stress in radial direction

and a and b are the radii of inner (concave) and outer (convex) boundaries respectively.

(v) Equilibrium of forces, on a volume element such as shown in Fig. 2.2, in the radial direction, gives:

$$\frac{d\sigma_r}{dr} = \frac{\sigma_\theta-\sigma_r}{r} \qquad [2.5]$$

where σ_θ = Circumferential stress component

(vi) Lateral strain ε_z being zero at all points, the constant volume condition requires, this to be the intermediate principal strain ε^P_{int} and lateral stress will be intermediate principal stress.

i.e. $$\varepsilon_z = \varepsilon^P_{int} = 0 \qquad [2.6.1]$$

or $$d\varepsilon_z = d\varepsilon^P_{int} = 0 \qquad [2.6.2]$$

(vii) In the bent sheet under load, σ_θ is the tensile stress and σ_r is zero, at the convex surface and σ_θ is compressive while σ_r is zero, at the concave surface. Hence, at the convex surface, $\sigma_\theta = \sigma_{max}$ and $\sigma_r = \sigma_{min}$ [2.7.1]

and at the concave surface $\sigma_\theta = \sigma_{min}$ and $\sigma_r = \sigma_{max}$ [2.7.2]

Substituting equation [2.6.2] in [2.1.2] and then substituting the results in equation [2.2] yields

$$\sigma_{int} = \frac{\sigma_{max} + \sigma_{min}}{2} \qquad [2.8]$$

2.2 Von Mises Criterion

Substituting [2.8] in [2.3.2] gives

$$\sigma_{max} - \sigma_{min} = \frac{2}{\sqrt{3}}\sigma_y \qquad [2.9]$$

Using [2.7.1] at the convex surface, equation [2.9] becomes

$$\sigma_\theta - \sigma_r = \frac{2}{\sqrt{3}}\sigma_y$$

Substituting in [2.5]

$$\frac{d\sigma_r}{dr} = \frac{2}{\sqrt{3}}\frac{\sigma_y}{r}$$

i.e. $$\int_o^{\sigma_r} \frac{d\sigma_r}{\sigma_y} = \frac{2}{\sqrt{3}} \int_b^r \frac{dr}{r}$$

or $$\frac{\sigma_r}{\sigma_y} = \frac{2}{\sqrt{3}} \ln \frac{r}{b} \qquad [2.10.1]$$

Using [2.7.2] at the concave surface, equation [2.9] becomes

$$\sigma_r - \sigma_\theta = \frac{2}{\sqrt{3}}\sigma_y$$

Substituting in [2.5]

$$\frac{d\sigma_r}{dr} = -\frac{2}{\sqrt{3}}\frac{\sigma_y}{r}$$

Integrating as before,

$$\frac{\sigma_r}{\sigma_y} = -\frac{2}{\sqrt{3}} \ln \frac{r}{a} \qquad [2.10.2]$$

Equation [2.10.1] shows that σ_r is negative for $r<b$ and equation [2.10.2] shows that σ_r is negative for $r>a$.

As r becomes greater than a or smaller than b equations [2.10.2] and [2.10.1] respectively, are applicable, iff, σ_r and σ_θ are continuous. Both these equations will yield the same solution at a particular value of r, where the tangential stress σ_θ changes its sign and this point lies on the neutral plane.

Equation [2.10.1] is applicable for $r_n \leq r \leq b$ and equation [2.10.2] is applicable for $r_n \geq r \geq a$

where r_n = Radius to neutral surface.

Equating the two equations

$$\ln \frac{r_n}{b} = -\ln \frac{r_n}{a}$$

$$\text{i.e.} \qquad r_n = \sqrt{ab} \qquad [2.11]$$

Now, for $r_n \leq r \leq b$, equation [2.9] gives

$$\sigma_\theta - \sigma_r = \frac{2}{\sqrt{3}}\sigma_y$$

$$\text{i.e.} \quad \frac{\sigma_\theta}{\sigma_y} = \frac{2}{\sqrt{3}} + \frac{\sigma_r}{\sigma_y}$$

$$\text{i.e.} \quad \frac{\sigma_\theta}{\sigma_y} = \frac{2}{\sqrt{3}} \left(1+\ln\frac{r}{b}\right) \quad \text{for } r_n \leq r \leq b \qquad [2.12.1]$$

Similarily,

$$\frac{\sigma_\theta}{\sigma_y} = -\frac{2}{\sqrt{3}} \left(1+\ln\frac{r}{a}\right) \quad \text{for } r_n \geq r \geq a \qquad [2.12.2]$$

Equation [2.8] yields the value of σ_z at any value of r and the resulting expression is

$$\sigma_z = \frac{\sigma_\theta+\sigma_r}{2} \qquad [2.13]$$

$$\text{i.e.} \quad \frac{\sigma_z}{\sigma_y} = \frac{2}{\sqrt{3}}\left(\frac{1}{2}+\ln\frac{r}{b}\right) \quad \text{for } r_n \leq r \leq b \qquad [2.13.1]$$

and

$$\frac{\sigma_z}{\sigma_y} = -\frac{2}{\sqrt{3}}\left(\frac{1}{2}+\ln\frac{r}{a}\right) \quad \text{for } r_n \geq r \geq a \qquad [2.13.2]$$

Thus using Von Mises yield condition equations [2.10.1], [2.12.1] and [2.13.1] give the values of radial, circumferential and lateral stresses respectively for $r_n \leq r \leq b$. The values of radial, circumferential and lateral stresses for the region $r_n \geq r \geq a$, are given by the equations [2.10.2], [2.12.2] and [2.13.2]. The position of the neutral surface is given by equation [2.11].

2.3 Tresca Criterion

Equations [2.7.1] and [2.3.1] yield,

$$\sigma_\theta - \sigma_r = \sigma_y$$

Equation [2.5] now yields

$$\frac{d\sigma_r}{dr} = \frac{\sigma_y}{r}$$

Integrating as in the Von Mises case

for $r_n \leq r \leq b$ $$\frac{\sigma_r}{\sigma_y} = \ln\frac{r}{b} \qquad [2.14.1]$$

Similarily for $r_n \geq r \geq a$

$$\frac{\sigma_r}{\sigma_y} = -\ln\frac{r}{a} \qquad [2.14.2]$$

A similar approach as before gives for Tresca material

$$r_n = \sqrt{ab} \qquad [2.11]$$

$$\frac{\sigma_\theta}{\sigma_y} = (1+\ln\frac{r}{b}) \quad \text{for } r_n \leq r \leq b \qquad [2.15.1]$$

$$\frac{\sigma_\theta}{\sigma_y} = -(1+\ln\frac{r}{a}) \quad \text{for } r_n \geq r \geq a \qquad [2.15.2]$$

$$\frac{\sigma_z}{\sigma_y} = (\frac{1}{2} + \ln\frac{r}{b}) \quad \text{for } r_n \leq r \leq b \qquad [2.16.1]$$

and $$\frac{\sigma_z}{\sigma_y} = -(\frac{1}{2}+\ln\frac{r}{a}) \quad \text{for } r_n \geq r \geq a \qquad [2.16.2]$$

The expressions deduced show that all the stresses based on Von Mises yield criterion are $\frac{2}{\sqrt{3}}$ times the stresses computed by using Tresca's yield criterion. However, the position of the neutral surface is independent of the choice of yield criterion and the external loading and is purely a function of the geometry of the problem.

2.4 Moment Required to Bend the Sheet

The bending moment per unit width required to produce the foregoing stress distribution, in the plastically bent sheet is calculated by taking the moment of circumferential stress distribution about the centre of curvature.

$$M_p = \int_a^b r\,\sigma_\theta dr$$

Using stress distribution of equations [2.12.1] and [2.12.2]

or

$$M_p = \int_{r_n}^{b} \frac{2}{\sqrt{3}}\,\sigma_y\left(1+\ln\frac{r}{b}\right) r\,dr - \int_{a}^{r_n} \frac{2}{\sqrt{3}}\,\sigma_y\left(1+\ln\frac{r}{a}\right) r\,dr$$

$$\text{i.e. } \frac{\sqrt{3}}{2}\frac{M_p}{\sigma_y} = \int_{r_n}^{b} r\,dr - \int_{a}^{r_n} r\,dr + \int_{r_n}^{b} r\ln\frac{r}{b}\,dr - \int_{a}^{r_n} r\ln\frac{r}{a}\,dr$$

$$= \frac{b^2+a^2-2r_n^2}{2} - \frac{b^2+a^2-2r_n^2}{4} - \frac{r_n^2}{2}\ln\frac{r_n^2}{ab} \qquad [2.17.1]$$

Substitution for $r_n = \sqrt{ab}$ into [2.17.1] yields

$$\frac{M_p}{(\sqrt{3}/2)\sigma_y} = \frac{t^2}{4}$$

Hence the moment expression based upon Von Mises yield condition is

$$M_p = \frac{2}{\sqrt{3}}\,\frac{t^2}{4}\,\sigma_y \qquad [2.18.1]$$

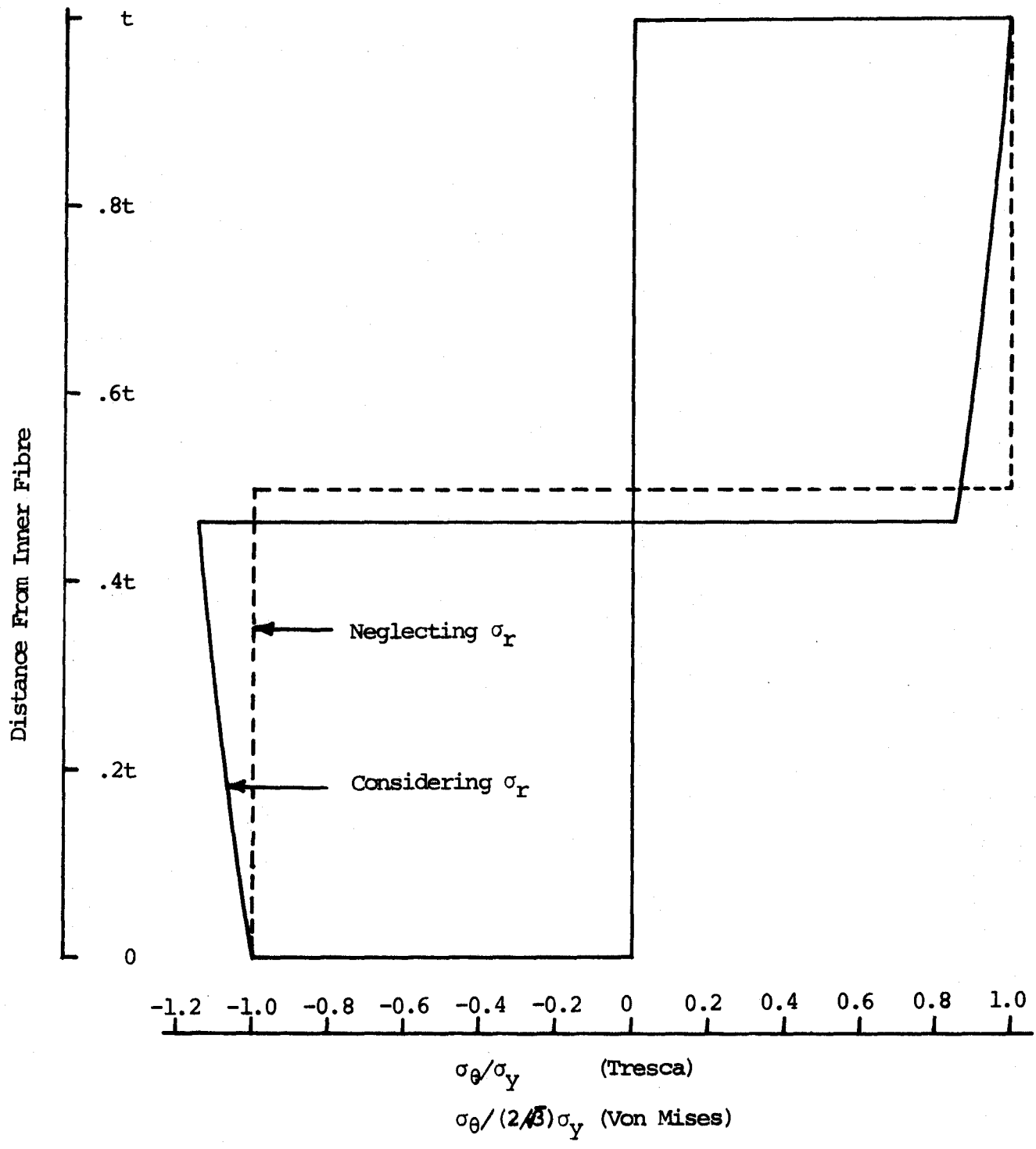

FIG. 2.3 CIRCUMFERENTIAL STRESS (σ_θ) DISTRIBUTION FOR a/t=3.0, ν=.3

The corresponding relation for Tresca's yield criterion is found to be

$$M_p = \frac{t^2}{4}\sigma_y \qquad [2.18.2]$$

Hence fully plastic moment M_p is constant for a particular material and sheet thickness. It does not depend upon the curvature of the bend.

Expression [2.17.1] may be re-written for Tresca's yield criterion

$$\frac{M_p}{\sigma_y} = \frac{b^2+a^2-2r_n^2}{2} - \frac{b^2+a^2-2r_n^2}{4} - \frac{r_n^2}{2}\ln\frac{r_n^2}{ab} \qquad [2.17.2]$$

If radial stress is neglected (true in moderate bending cases), the circumferential stress distribution consists of two rectangular blocks of width σ_y and height $\frac{t}{2}$ (Fig. 2.3). One of which represents tensile stress and the other compressive stress. The moment expression for this case is

$$M_p = -\int_a^{r_n} \sigma_y\, r\, dr + \int_{r_n}^{b} \sigma_y\, r\, dr$$

$$= \sigma_y \frac{b^2-a^2-2r_n^2}{2}$$

i.e.
$$\frac{M_p}{\sigma_y} = \frac{b^2-a^2-2r_n^2}{2} \qquad [2.19]$$

Equilibrium of forces requires that

$$r_n = a + \frac{t}{2}$$

$$= a + \frac{b-a}{2}$$

$$= \frac{b+a}{2}$$

Equation [2.19] yields

$$\frac{M_p}{\sigma_y} = \frac{b^2+a^2-2\left(\frac{b+a}{2}\right)^2}{2}$$

or

$$M_p = \frac{t^2}{4}\sigma_y$$

This expression is the same as [2.18.2] and yet both have been derived under different assumptions. Expression [2.18.2] has been derived under more general conditions of bending.

The first term in [2.17.2] is a contribution due to the rectangular hoop stress blocks. Whereas the second and third terms in the same moment expression are the contributions of σ_r distribution. Furthermore the first term is similar to the right-hand side of [2.19] and yet both are not the same. The shift of neutral-axis, necessary to satisfy equilibrium in the first case, changes the value of r_n from $r_n=\frac{b+a}{2}$ in [2.19] to $r_n=\sqrt{ab}$ in [2.17.2] and yet the end result of the two different approaches lead to the same expression for moment.

The neutral surface initially coincides with the centroidal surface. As bending progresses it moves towards the inner fibres thus causing an extension in the fibres situated between the centroidal plane and the neutral plane (these

fibres were under compression before the shift). It can, therefore, be concluded that at each stage of bending there exists one fibre which has been compressed and then stretched by equal amounts such that the net change in length is zero.

CHAPTER III

SPRING-BACK ANALYSIS

This chapter deals with the analysis of stresses produced by spring back and the resulting residual stresses in a wide metal sheet subjected to cold bending in one direction. To start with the assumption is made that spring back is completely elastic and as a result the analysis is based upon the use of Airy's stress function[36,37,39]. Subsequently it is demonstrated that the resulting residual stresses calculated by assuming spring-back completely elastic violate yield and plastic flow is shown to occur in a thin core of sheet, just below the neutral axis. However this analysis serves as an approximate method to calculate residual stress components.

An exact analysis is then performed considering the plastic core and a method to calculate residual stresses is demonstrated.

It was noted in Chapter II that the neutral axis shifts towards the concave or inner fibres during bending of sheet. Its position was found to be at the geometric mean of the inner and outer fibres radii when the sheet is completely plastic. During elastic spring-back (approximate analysis) the neutral axis shifts towards the convex or outer fibres but remains below the centroidal axis of the sheet.

The moment M_p required to bend the wide sheet to its fully plastic stage was evaluated in Chapter II. The spring-back of the sheet, after the bending moment M_p has been removed, can analytically be treated by a simple model in which an initially curved sheet is subjected to the unloading edge couples M^s, which are equal in magnitude but opposite in sign to the fully plastic moments M_p.

3.1 Approximate Analysis — Completely Elastic

The simple model discussed above makes it possible to use the classical theory of 'Wide Curved Bar Bending'[36,37,39] in analysing spring-back. In addition to the assumptions of Chapter II, the following are made:

(1) Spring-back (unloading) is caused by uniform edge moments, M^s, (equal but opposite to M_p) per unit width.

(2) The physical dimensions of the sheet are assumed to remain constant during spring-back . The validity of this assumption is discussed in Chapter IV.

(3) Spring-back is completely elastic for bends of quite sharp radius. Beyond a certain cruvature this assumption no longer holds and is considered more fully in section 3.3.

Although the total deformations of the fibres in the curved sheet are proportional to the distances of the fibres from the neutral surface, the strains (deformations per unit length) of the fibres are not proportional to these distances

because the fibres are not of equal length. But for bending stresses that do not exceed the elastic strength of the material the stress on any fibre in the sheet is proportional to the strain of the fibre, and hence the elastic stresses in the fibres of a curved sheet are not proportional to the distances of the fibres from the neutral surface.

For unloading by end moments only, i.e. no external radial forces in the region considered, the equilibrium-of-force condition applied at the concave and convex surfaces of the bent part requires that the radial stresses at these surfaces be zero.

Fig. 3.1 shows the geometry of the sheet bent to inner and outer radii, a and b respectively. An elementary volume element taken from the sheet and the forces acting on this element are shown in Fig. 3.2.

The stress distribution is symmetrical with respect to any radial section because bending moment is the same in all radial cross sections. Therefore, it is concluded that the stress components do not depend on θ and are functions of r only.

From symmetry it follows also that the shearing stresses must vanish on the planes determined by the radial, lateral and circumferential directions, and consequently these are the principal directions.

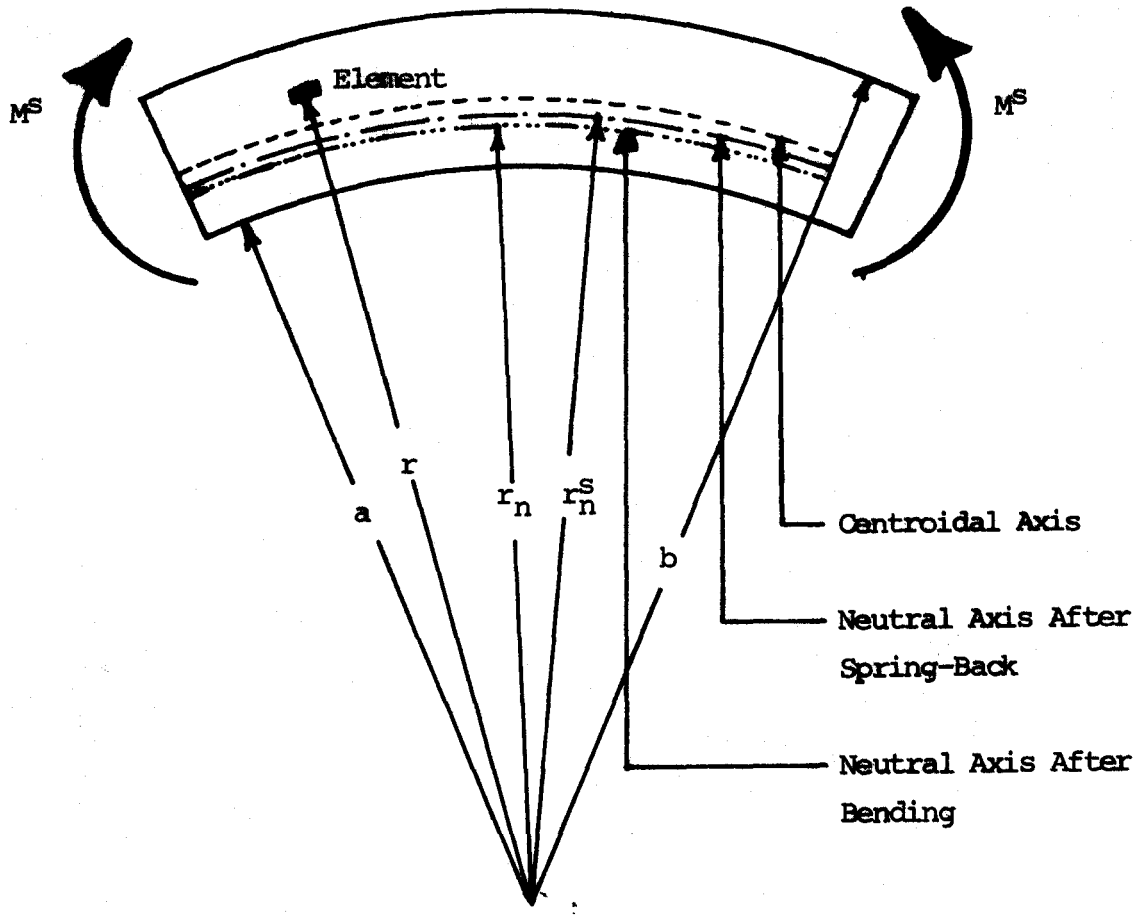

FIG. 3.1 GEOMETRY OF THE CURVED SHEET

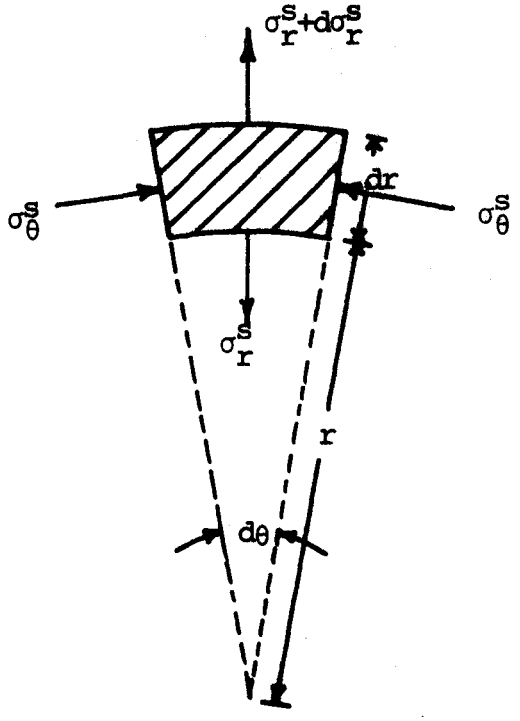

FIG. 3.2 STRESSES ON A TYPICAL ELEMENT

Under such circumstances, the only non-trivial equation of equilibrium which the stress components must satisfy is

$$\frac{d\sigma_r^s}{dr} = \frac{\sigma_\theta^s - \sigma_r^s}{r} \qquad [3.1]$$

where σ_r^s and σ_θ^s = Radial and hoop spring-back stresses.

The above equation of equilibrium is satisfied by substituting

$$\sigma_r^s = \frac{1}{r}\frac{d\phi}{dr} \qquad [3.2]$$

and

$$\sigma_\theta^s = \frac{d^2\phi}{dr^2} \qquad [3.3]$$

where ϕ is the Airy stress function as a function of r only.

When ϕ depends only on r, the equation of compatibility[39], which must be satisfied by the stress components defined by equations [3.2] and [3.3], becomes

$$\left(\frac{d^2}{dr^2} + \frac{1}{r}\frac{d}{dr}\right)\left(\frac{d^2\phi}{dr^2} + \frac{1}{r}\frac{d\phi}{dr}\right) = \frac{d^4\phi}{dr^4} + \frac{2}{r}\frac{d^3\phi}{dr^3} - \frac{1}{r^2}\frac{d^2\phi}{dr^2} + \frac{1}{r^3}\frac{d\phi}{dr} = 0 \qquad [3.4]$$

The above differential equation can be reduced to a linear differential equation with constant coefficients, by a substitution such as $r=e^w$, where w is a variable. The general solution of equation [3.4] is

$$\phi = A \ln r + Br^2 \ln r + Cr^2 + D \qquad [3.5]$$

where A,B,C and D are the constants of integration,

which can be determined from the boundary conditions. This solution can, of course, be checked by direct substitution.

The stress components from equations [3.2] and [3.3], now, become

$$\sigma_r^s = \frac{1}{r}\frac{d\phi}{dr} = \frac{A}{r^2} + B(1+2\ \ln\ r) + 2C \qquad [3.6]$$

$$\sigma_\theta^s = \frac{d^2\phi}{dr^2} = -\frac{A}{r^2} + B(3+2\ \ln\ r) + 2C \qquad [3.7]$$

The boundary conditions, for the problem under consideration, are

(1) The concave and convex boundaries of the sheet are free from normal forces

$$\text{i.e., } \sigma_r^s = 0 \quad \text{for } r=a \text{ and } r=b$$

(2) The normal stresses at the end of the sheet, give rise to the unloading moment M^s only.

$$\text{i.e. } \int_a^b \sigma_\theta^s\, dr = 0 \text{ and } \int_a^b \sigma_\theta^s\, r\, dr = -M^s$$

Under these boundary conditions, it can be shown[39] that the constants A, B and C in equations [3.6] and [3.7] assume the values

$$A = -\frac{4M^s}{N}\, a^2b^2\ \ln\frac{b}{a}$$

$$B = -\frac{2M^s}{N}\,(b^2 - a^2)$$

and,
$$C = \frac{M^s}{N}[b^2-a^2+2(b^2\ \ln\ b - a^2\ \ln\ a)]$$

where, $$N = (b^2-a^2)^2 - 4a^2b^2(\ln\frac{b}{a})^2 \qquad [3.10]$$

Substituting the values of these constants into

equations [3.6] and [3.7], the expressions for stress components σ_θ^s and σ_r^s become

$$\sigma_r^s = -\frac{4M^s}{N}\left(\frac{a^2b^2}{r^2}\ln\frac{b}{a} + b^2\ln\frac{r}{b} + a^2\ln\frac{a}{r}\right) \qquad [3.8]$$

$$\sigma_\theta^s = -\frac{4M^s}{N}\left(-\frac{a^2b^2}{r^2}\ln\frac{b}{a} + b^2\ln\frac{r}{b} + a^2\ln\frac{a}{r} + b^2-a^2\right) \qquad [3.9]$$

where N, as expressed before, is given by

$$N = (b^2-a^2)^2-4a^2b^2(\ln\frac{b}{a})^2 \qquad [3.10]$$

and the magnitude of M^s is given by equations [2.18.1] and [2.18.2].

From equations [3.8] and [3.9] it can be shown that for the direction of bending as indicated in Fig. 3.1, the radial stress σ_r^s is always positive (tensile) whereas the circumferential stress σ_θ^s is compressive near the convex boundary but tensile near the concave boundary.

The position of the neutral surface (or axis) r_n^s may be calculated by equating the circumferential stress component to zero and it can be seen from expression [3.9] that the position of the neutral axis, again, depends only on the geometry of the sheet, not on the unloading moment, M^s. It has been shown[39] that the point of maximum released stress σ_r^s is somewhat displaced from the neutral axis in the direction of the center of curvature.

To obtain an expression for the stress component σ_z^s, in the lateral direction, the condition that the released

strain ε_z^s is zero for the present case of plane strain unloading, is substituted in the stress-strain relation in the elastic case

$$\text{i.e.} \quad \varepsilon_z^s = \frac{\sigma_z^s}{E} - \frac{\nu}{E}(\sigma_r^s + \sigma_\theta^s) = 0$$

$$\text{i.e.} \quad \sigma_z^s = \nu(\sigma_r^s + \sigma_\theta^s) \qquad [3.10.1]$$

$$\text{i.e.} \quad \sigma_z^s = -\nu\frac{4M^s}{N}(2b^2 \ln\frac{r}{b} + 2a^2 \ln\frac{a}{r} + b^2-a^2) \qquad [3.10.2]$$

3.1.1 Residual Stresses

The expressions for the residual stresses σ_r^R, σ_θ^R and σ_z^R are obtained by superimposing (adding algebrically) bending stresses σ_r, σ_θ and σ_z and unloading or spring-back stresses σ_r^s, σ_θ^s and σ_z^s. They are given below for the appropriate regions indicated.

Von Mises Material

$$\sigma_r^R = \sigma_r + \sigma_r^s$$

$$= \frac{2}{\sqrt{3}}\sigma_y[\ln\frac{r}{b} - \frac{t^2}{N}(\frac{a^2b^2}{r^2}\ln\frac{b}{a} + b^2 \ln\frac{r}{b} + a^2 \ln\frac{a}{r})] \quad \text{for } r_n \leq r \leq b \qquad [3.11.1]$$

$$\sigma_r^R = \frac{2}{\sqrt{3}}\sigma_y[-\ln\frac{r}{a} - \frac{t^2}{N}(\frac{a^2b^2}{r^2}\ln\frac{b}{a} + b^2 \ln\frac{r}{b} + a^2 \ln\frac{a}{r})] \quad \text{for } r_n \geq r \geq a \qquad [3.11.2]$$

$$\sigma_\theta^R = \sigma_\theta + \sigma_\theta^s = \frac{2}{\sqrt{3}}\sigma_y[1 + \ln\frac{r}{b} - \frac{t^2}{N}(-\frac{a^2b^2}{r^2}\ln\frac{b}{a} + b^2 \ln\frac{r}{b} + a^2 \ln\frac{a}{r} + b^2-a^2)] \quad \text{for } r_n \leq r \leq b \qquad [3.12.1]$$

$$\sigma_\theta^R = \frac{2}{\sqrt{3}}\sigma_y[-1-\ln\frac{r}{a} - \frac{t^2}{N}(-\frac{a^2b^2}{r^2}\ln\frac{b}{a} + b^2\ln\frac{r}{b} + a^2\ln\frac{a}{r} + b^2-a^2)] \quad \text{for } r_n \geq r \geq a \qquad [3.12.2]$$

$$\sigma_z^R = \sigma_z + \sigma_z^s = \frac{2}{\sqrt{3}}\sigma_y[\frac{1}{2} + \ln\frac{r}{b} - \frac{\nu t^2}{N}(2b^2\ln\frac{r}{b} + 2a^2\ln\frac{a}{r} + b^2-a^2)] \quad \text{for } r_n \leq r \leq b \qquad [3.13.1]$$

$$\sigma_z^R = \frac{2}{\sqrt{3}}\sigma_y[-\frac{1}{2}-\ln\frac{r}{a} - \frac{\nu t^2}{N}(2b^2\ln\frac{r}{b} + 2a^2\ln\frac{a}{r} + b^2-a^2)] \quad \text{for } r_n \geq r \geq a \qquad [3.13.2]$$

where N and r_n are given by equations [3.10] and [2.11] respectively.

Tresca Material

It can be readily seen that the above expressions for the residual stresses are true for the Tresca criteria also, if the factor $\frac{2}{\sqrt{3}}$ is omitted. It can, therefore, be concluded that the residual stresses based on Von Mises yield criterion are $\frac{2}{\sqrt{3}}$ times the stresses based on Tresca's yield criterion and as such the general distribution of the stress components σ_θ, σ_r, σ_z, σ_θ^s, σ_r^s, σ_z^s, σ_θ^R, σ_r^R, and σ_z^R is the same for either criterion of yielding.

A computer program has been developed to compute residual stress components for any given problem and is presented in Appendix A.

3.2 Validity of the Assumption of Elastic Spring-Back

Equations [3.11.1], [3.11.2], [3.12.1], [3.12.2], [3.13.1] and [3.13.2] give the residual stress components if

the spring back is completely elastic. However, as will be shown, this assumption is violated within a thin core of sheet below the neutral axis of bending (r_n)

The unloading is elastic if the residual stresses (σ_θ^R and σ_r^R) satisfy the yield criterion

$$\sigma_{max} - \sigma_{min} \leq \frac{2}{\sqrt{3}}\sigma_y \text{ (Von Mises)} \qquad [2.9]$$

where σ_{max} = Maximum principal stress

σ_{min} = Minimum principal stress

Now,

$$\sigma_\theta^R - \sigma_r^R = \frac{2}{\sqrt{3}}\sigma_y\left[1-\frac{t^2}{N}\left(-\frac{2a^2b^2}{r^2}\ln\frac{b}{a} + b^2-a^2\right)\right]$$

$$\text{for } r_n \leq r \leq b \qquad [3.14.1]$$

and,

$$\sigma_\theta^R - \sigma_r^R = \frac{2}{\sqrt{3}}\sigma_y\left[-1-\frac{t^2}{N}\left(-\frac{2a^2b^2}{r^2}\ln\frac{b}{a} + b^2-a^2\right)\right]$$

$$\text{for } r_n \geq r \geq a \qquad [3.14.2]$$

Comparing equations [3.14.1] and [3.14.2] with equation [2.9], it is evident that the unloading is elastic if

$$V = \frac{t^2}{N}\left(-\frac{2a^2b^2}{r^2}\ln\frac{b}{a} + b^2-a^2\right) \text{ is positive}$$

in the domain $r_n \leq r \leq b$ and negative in the domain $r_n \geq r \geq a$.

N is positive for any value of a and b and t^2 is always positive, hence, the expression V increases as r increases from a negative value at r=a to a positive value at r=b and becomes zero at r=ρ such that

$$-\frac{2a^2b^2}{\rho^2}\ln\frac{b}{a} = -(b^2-a^2)$$

or

$$\rho^2 = \frac{2a^2b^2}{(b^2-a^2)}\ln\frac{b}{a} \qquad [3.14.3]$$

This value is less than $r_n^2 = ab$ for any value of a and b (as long as b>a)

i.e. $\rho < r_n$

Therefore V is postive in the domain $r_n \geq r \geq \rho$ and therefore this is the region in which equation [3.14.2] violates the yield criterion of equation [2.9]. Obviously, the assumption that unloading is entirely elastic is not valid and plastic flow occurs in the region $r_n \geq r \geq \rho$.

For the cases of moderate bending ρ approaches r_n and the region of plastic flow diminishes. In such cases, the residual stresses given in section 3.1.1 will not be far from the actual stress components. This, however, is not true for sharp bends and as will be shown later(Chapter V) a significant difference in stress components is obtained if the zone of plastic flow is considered.

3.3 Exact Analysis — Plastic Core

As discussed in the previous section, the entire thickness of the sheet could be divided into three zones—two elastic zones near the concave and convex boundaries separated by a plastic core. The residual stresses in the elastic zones

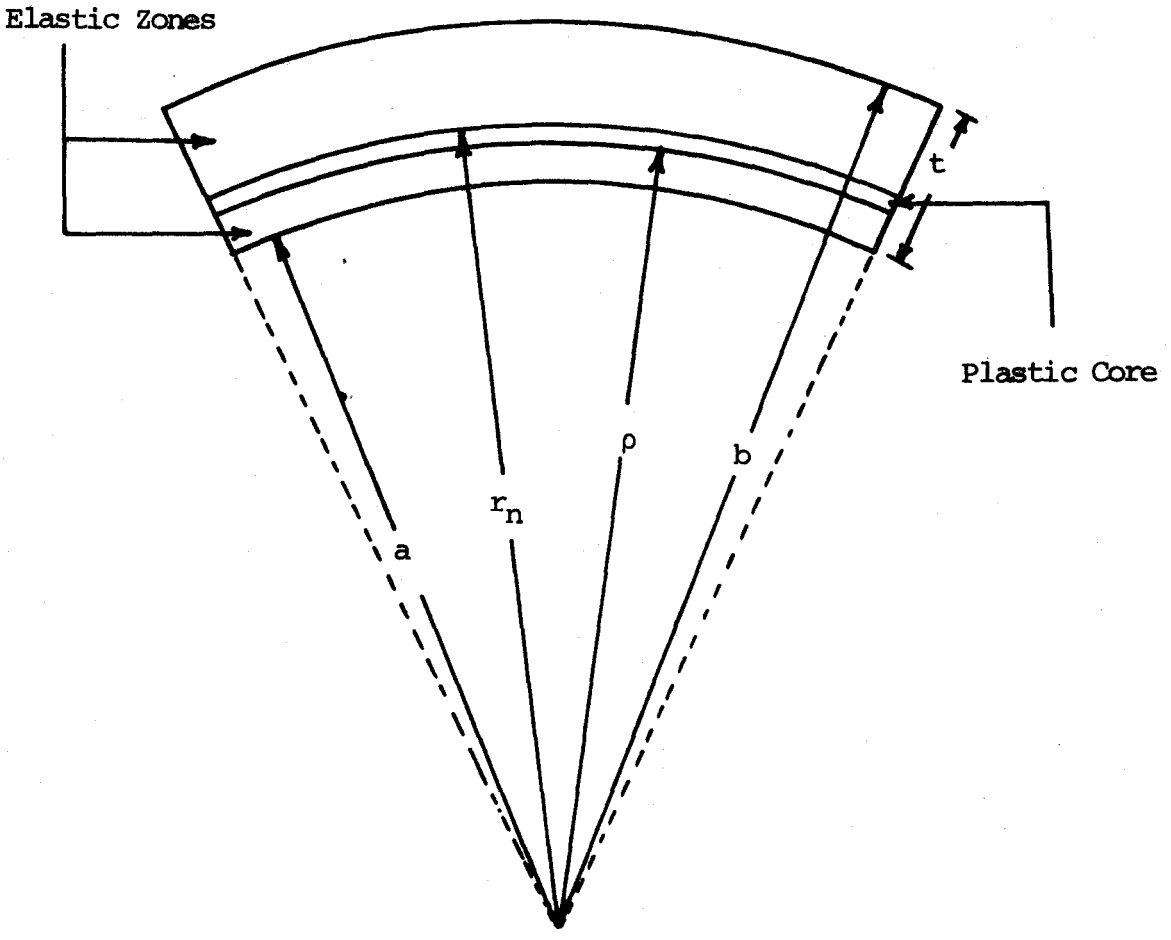

FIG. 3.3 ELASTIC AND PLASTIC RESIDUAL STRESS ZONES AFTER SPRING-BACK

are not determined by simply superimposing the bending stresses (given in Chapter II) on the elastic unloading stresses (found in section 3.1) since adjustments in the stresses of the plastic core and its thickness reflect in the elastic core regions through the equations of equilibrium and compatibility. This adjustment in the elastic stresses is considered in section 3.3.2. The stresses in the plastic core are found by using appropriate plastic flow laws and the equation of equilibrium. Fig. 3.3 shows the elastic and plastic zones of residual stresses. The outer elastic-plastic boundary is at a known radius $r=r_n=\sqrt{ab}$, whereas, the inner elastic-plastic boundary is at a yet unknown radius $r=\rho$.

3.3.1 Stresses in Plastic Zone

The residual stress components σ_θ^R, σ_r^R and σ_z^R, in this zone must satisfy the yield criterion

$$\sigma_r^R - \sigma_\theta^R = \sigma_y \quad \text{(Tresca)}^{**} \qquad [3.15]$$

and the equation of equilibrium

$$\frac{d\sigma_r^R}{dr} = \frac{\sigma_\theta^R - \sigma_r^R}{r} \qquad [3.16]$$

Substituting equation [3.15] in [3.16] and rearranging

$$\frac{d\sigma_r^R}{\sigma_y} = -\frac{dr}{r}$$

** *For convenience Tresca yield criterion has been considered*

Integrating

$$\frac{\sigma_r^R}{\sigma_y} = - \ln(rk)$$

where $\ln(k)$ is the constant of integration.

Therefore,

$$\sigma_\theta^R = \sigma_r^R - \sigma_y$$

$$= - \sigma_y \ln(rk) - \sigma_y$$

$$= - \sigma_y [1 + \ln(rk)]$$

Hence, for the plastic region $\rho \leq r \leq r_n$

$$\sigma_r^R = - \sigma_y \ln(rk) \qquad [3.17]$$

and

$$\sigma_\theta^R = - \sigma_y [1 + \ln(rk)] \qquad [3.18]$$

where ρ and k are unknowns.

3.3.2 Unloading Stresses in Elastic Zones

Fig. 3.4 shows the curved sheet subjected to unloading edge couples, M_p. The assumption is made that there is one fibre in the sheet which does not change in length. The position of such a fibre will be different at different stages of unloading but at each stage of unloading there is only one fibre where circumferential displacement is zero. The position of this surface, when the sheet has been completely unloaded, is shown by NN. Total deformations of the fibres between two normal sections such as AB and A_1B_1 are assumed to vary directly with the distances of the fibres from NN, shortening above NN and stretching below it; i.e.

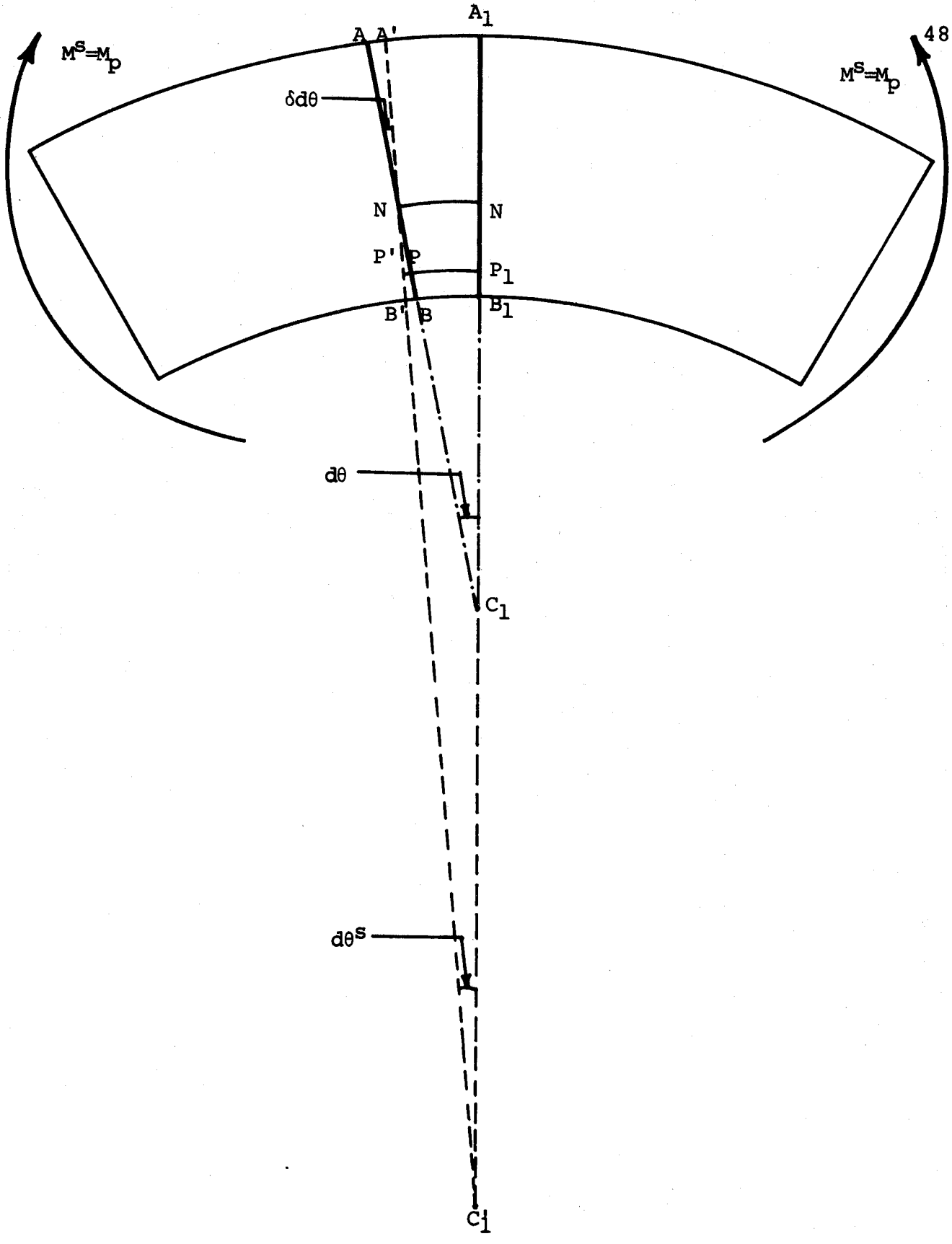

FIG. 3.4 UNLOADING STRAINS IN SHEET

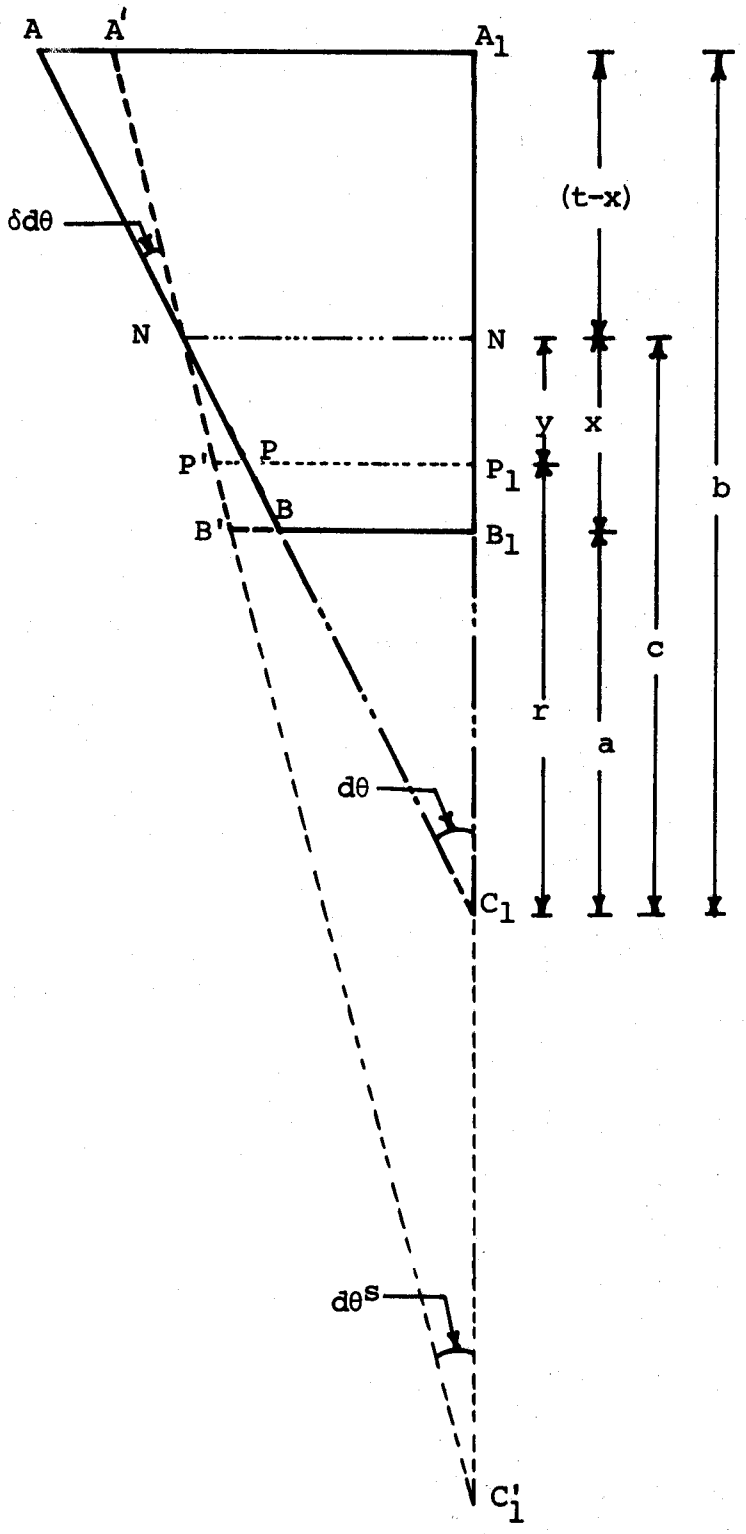

FIG. 3.5 ENLARGED VIEW OF FIG. 3.4

plane sections are assumed to remain plane during and after unloading. In Fig. 3,4 A_1B_1 is a section of symmetry which remains vertical. After the sheet is completely unloaded section AB rotates by an angle $\delta d\theta$ and occupies a new position represented by A'B'. The centre of curvature changes from C_1 to C_1'.

Fig. 3.5 shows the enlarged part A_1ABB_1 of the sheet. The initial lengths of the fibres of a curved sheet are not equal; hence the strains of the fibres are not proportional to the distances of the fibres from NN, eventhough the total deformations of the fibres are proportional to these distances. Hence, the elastic stresses in the fibres of a curved sheet are not proportional to distance from NN (the fibre, where circumferential strain, ε_θ^s, is zero). It is found convenient to express the spring-back circumferential strain, ε_θ^s, of any fibre such as P_1P in terms of the spring back circumferential strain $\varepsilon_{\theta_i}^s$ of the innermost fibre B_1B, radius r of the fibre (or distance y from NN) and the distance x from the innermost fibre which defines its position.

The strain of any fibre P_1P is given by

$$\varepsilon_\theta^s = \frac{PP'}{P_1P}$$

$$= \frac{(\frac{BB'}{x})y}{r \quad d\theta}$$

$$= \frac{(BB')y}{x \; r \; d\theta}$$

Now, the strain at the inner fibre B_1B is

$$\varepsilon^s_{\theta_i} = \frac{BB'}{B_1B}$$

$$= \frac{BB'}{a\ d\theta}$$

i.e. $$\frac{BB'}{d\theta} = a\ \varepsilon^s_{\theta_i}$$

Therefore,

$$\varepsilon^s_\theta = \frac{a\varepsilon^s_{\theta_i}\ y}{x\ r}$$

Substituting

$$y = a+x-r$$

$$\varepsilon^s_\theta = \frac{a\varepsilon^s_{\theta_i}\ (a+x-r)}{x\ r} \qquad [3.19]$$

For the direction of moment as shown in Fig. 3.4 ε^s_θ is positive (tensile) if $r<(a+x)$ and negative if $r>(a+x)$

The relations between the components of elastic stress and the components of strains are given by Hooke's law

$$\varepsilon^s_\theta = \frac{\sigma^s_\theta}{E} - \frac{\nu}{E}\ (\sigma^s_r + \sigma^s_z)$$

$$\varepsilon^s_r = \frac{\sigma^s_r}{E} - \frac{\nu}{E}\ (\sigma^s_z + \sigma^s_\theta)$$

$$\varepsilon^s_z = \frac{\sigma^s_z}{E} - \frac{\nu}{E}\ (\sigma^s_\theta + \sigma^s_r)$$

Under the conditions of plane strain, $\varepsilon^s_z = 0$ gives

$$\sigma^s_z = \nu(\sigma^s_\theta + \sigma^s_r)$$

Therefore,

$$\varepsilon^s_\theta = \frac{\sigma^s_\theta}{E} - \frac{\nu}{E}\ [\sigma^s_r + \nu(\sigma^s_\theta + \sigma^s_r)]$$

$$= \left(\frac{1+\nu}{E}\right)\left[(1-\nu)\sigma_\theta^s - \nu\sigma_r^s\right]$$

or,

$$\sigma_\theta^s = \left(\frac{E}{1-\nu^2}\right)\varepsilon_\theta^s + \left(\frac{\nu}{1-\nu}\right)\sigma_r^s$$

Subtracting σ_r^s from both sides

$$\sigma_\theta^s - \sigma_r^s = \left(\frac{E}{1-\nu^2}\right)\varepsilon_\theta^s + \left(\frac{2\nu-1}{1-\nu}\right)\sigma_r^s$$

or

$$\sigma_\theta^s - \sigma_r^s = \alpha\varepsilon_\theta^s + \beta\sigma_r^s \qquad [3.21]$$

where α and β are constants for a metal and are given by

$$\alpha = \frac{E}{1-\nu^2} \qquad [3.21.1]$$

$$\beta = \frac{2\nu-1}{1-\nu} \qquad [3.21.2]$$

Now, the stress components σ_θ^s and σ_r^s must satisfy the equilibrium condition

$$\frac{d\sigma_r^s}{dr} = \frac{\sigma_\theta^s - \sigma_r^s}{r}$$

Substituting the value of $(\sigma_\theta^s - \sigma_r^s)$ from equation [3.21]

$$\frac{d\sigma_r^s}{dr} = \frac{\alpha\varepsilon_\theta^s + \beta\sigma_r^s}{r}$$

or $$\Delta\sigma_r^s = \left[\alpha\varepsilon_\theta^s + \beta\sigma_r^s\right]\frac{\Delta r}{r}$$

in incremental form.

The value of ε_θ^s is substituted from equation [3.19]

$$\Delta\sigma_r^s = \left[\alpha\,\frac{a\varepsilon_{\theta_i}^s}{x}\,\frac{(a+x-r)}{r} + \beta\sigma_r^s\right]\frac{\Delta r}{r}$$

$$= \left[\left(\frac{\alpha a\varepsilon_{\theta_i}^s}{x}\right)\left(\frac{a+x-r}{r^2}\right) + \beta\frac{\sigma_r^s}{r}\right]\Delta r$$

Putting $$\gamma = \left(\frac{\alpha a\, \varepsilon^s_{\theta_i}}{x}\right) \qquad [3.21.3]$$

and $$c = (a+x) \qquad (=\text{radius to NN}) \qquad [3.21.4]$$

$$\Delta\sigma^s_r = \left[\gamma\left(\frac{c-r}{r^2}\right) + \beta\frac{\sigma^s_r}{r}\right]\Delta r \qquad [3.22]$$

Now, from equation [3.21]

$$\sigma^s_\theta = \alpha\varepsilon^s_\theta + (\beta+1)\sigma^s_r;$$

substituting the value of ε^s_θ from equation [3.19]

$$\sigma^s_\theta = \alpha\frac{a\varepsilon^s_{\theta_i}(a+x-r)}{x\, r} + (\beta+1)\,\sigma^s_r$$

$$= \gamma\left(\frac{c-r}{r}\right) + (\beta+1)\,\sigma^s_r \qquad [3.23]$$

where γ and c are defined in [3.21.3] and [3.21.4].

Equations [3.22] and [3.23] contain two unknowns, namely, γ and c, which can be found by using the boundary conditions described below.

3.3.3 Residual Stresses

Residual stress components in the two elastic zones are found by superimposing the bending stresses given by equations [2.14.1], [2.14.2], [2.15.1] and [2.15.2] with the elastic unloading stresses given by equations [3.22] and [3.23]. In the plastic zone these components are given by equations [3.17] and [3.18].

Boundary Conditions

Equilibrium demands that

(1) $\sigma_r^R = 0$ at r=a (σ_r^s is also zero as σ_r=0)

(2) $\sigma_r^R = 0$ at r=b (σ_r^s is also zero as σ_r=0)

and (3) σ_r^R should be continuous at the elastic-plastic boundaries $r=\rho$ and $r=r_n$.

(4) To satisfy the yield criterion at the elastic-plastic boundary $r=\rho$, σ_θ^R should be continuous at $r=\rho$.

(5) When all the moment has been released

$$\int_a^b \sigma_\theta^R \, r \, dr = 0$$

(6) Equilibrium of residual stress system demands that the resultant circumferential force (area of stress distribution across the thickness) should be zero, i.e.

$$\int_a^b \sigma_\theta^R \, dr = 0$$

Apparently there are only four unknowns, namely γ, c, ρ and k, involved in the expressions for residual stress components, however, since equation [3.22] is in incremental form, another unknown becomes involved making the total number of unknowns five. Conditions (1) to (5) are sufficient to determine all the constants and it is found that the sixth condition is identically satisfied by the stress distribution found from the earlier boundary conditions.

Using earlier equations condition (4) gives

$$\sigma^R_{\theta_\rho} = -\sigma_y(1+\ln\frac{\rho}{a}) + \sigma^s_{\theta_\rho} = -\sigma_y[1+\ln(\rho k)]$$

i.e. $$\sigma^s_{\theta_\rho} = -\sigma_y[1+\ln(\rho k) - 1 - \ln\frac{\rho}{a}]$$

$$= -\sigma_y \ln(ak) \qquad [3.24]$$

where the second subscript refers to circumferential stress at r=ρ.Condition (3) gives

$$\sigma^R_{r_\rho} = -\sigma_y \ln\frac{\rho}{a} + \sigma^s_{r_\rho} = -\sigma_y \ln(\rho k)$$

$$\text{i.e.} \quad \sigma^s_{r_\rho} = -\sigma_y \ln(ak) \qquad [3.25]$$

where the second subscript refers to radial stress at r=ρ. Also,

$$\sigma^R_{r_{r_n}} = -\sigma_y \ln(r_n k) = \sigma_y \ln\frac{r_n}{b} + \sigma^s_{r_{r_n}}$$

$$\text{i.e.} \quad \sigma^s_{r_{r_n}} = -\sigma_y \ln(\frac{r_n^2 k}{b})$$

substituting $r_n = \sqrt{ab}$ [2.11]

$$\sigma^s_{r_{r_n}} = -\sigma_y \ln(ak) \qquad [3.26]$$

where the second subscript refers to radial stress at $r=r_n$. At r=ρ equation [3.23] becomes

$$\sigma^s_{\theta_\rho} = \gamma(\frac{c-\rho}{\rho}) + (\beta+1)\sigma^s_{r_\rho}$$

Substituting values of $\sigma^s_{\theta_\rho}$ and $\sigma^s_{r_\rho}$ from equations [3.24] and [3.25] respectively

$$-\sigma_y \ln(ak) = \gamma\left(\frac{c-\rho}{\rho}\right) + (\beta+1)\left[-\sigma_y \ln(ak)\right]$$

or
$$0 = \gamma\left(\frac{c-\rho}{\rho}\right) - \beta\sigma_y \ln(ak) \qquad [3.27]$$

Substituting from equation [3.26]

$$0 = \gamma\left(\frac{c-\rho}{\rho}\right) + \beta\sigma^s_{r_{r_n}}$$

$$\rho = \frac{c\gamma}{\gamma-\beta\sigma^s_{r_{r_n}}}$$

or
$$\rho = \frac{c}{1-\beta\left(\frac{\sigma^s_{r_{r_n}}}{\gamma}\right)} \qquad [3.28]$$

Rearranging
$$-\left(\frac{\sigma^s_{r_{r_n}}}{\gamma}\right) = \frac{1}{\beta}\left(\frac{c-\rho}{\rho}\right) \qquad [3.29]$$

Condition (6) gives

$$\int_a^b \sigma^R_\theta \, dr = 0$$

or
$$\int_a^\rho \sigma^R_\theta \, dr + \int_\rho^{r_n} \sigma^R_\theta \, dr + \int_{r_n}^b \sigma^R_\theta \, dr = 0$$

Putting the values of σ^R_θ from earlier equations for the appropriate zones

$$\int_a^\rho -\sigma_y\left(1+\ln\frac{r}{a}\right)dr + \int_a^\rho \sigma^s_\theta dr + \int_\rho^{r_n} -\sigma_y[1+\ln(rk)]dr$$

$$+ \int_{r_n}^b \sigma_y\left(1+\ln\frac{r}{b}\right)dr + \int_{r_n}^b \sigma^s_\theta \, dr = 0$$

Putting $\int \ln(rk)\,dr = r\ln(rk) - r$ + Constant, etc.

$$- \sigma_y(\rho \ln\frac{\rho}{a}) + \int_a^{\rho} \sigma_\theta^s \, dr + - \sigma_y[r_n \ln(r_n k) - \rho \ln(\rho k)]$$

$$+ \sigma_y(-r_n \ln\frac{r_n}{b}) + \int_{r_n}^{b} \sigma_\theta^s \, dr = 0$$

or $$\int_a^{\rho} \sigma_\theta^s \, dr + \int_{r_n}^{b} \sigma_\theta^s \, dr - \sigma_y[-\rho \ln(ak) + r_n \ln(\frac{r_n^2 k}{b})] = 0$$

substituting for r_n

$$\int_a^{\rho} \sigma_\theta^s \, dr + \int_{r_n}^{b} \sigma_\theta^s \, dr - \sigma_y[-\rho \ln(ak) + r_n \ln(ak)] = 0$$

or $$\int_a^{\rho} \sigma_\theta^s \, dr + \int_{r_n}^{b} \sigma_\theta^s \, dr - \sigma_y \ln(ak)(r_n - \rho) = 0$$

or $$\Sigma F = F_1 + F_2 + F_3 = 0 \qquad [3.30]$$

where

$$F_1 = \int_a^{\rho} \sigma_\theta^s \, dr \qquad [3.31]$$

$$F_2 = \int_{r_n}^{b} \sigma_\theta^s \, dr \qquad [3.32]$$

$$F_3 = - \sigma_y \ln(ak)(r_n - \rho) \qquad [3.32.1]$$

As afore-said equation [3.30] is not needed in calculating the constants. It however provides a check and it is seen that the stress components found by using other boundary conditions satisfy [3.30] identically.

Condition (5) gives

$$\int_a^{\rho} \sigma_\theta^R \, r \, dr + \int_{\rho}^{r_n} \sigma_\theta^R \, r \, dr + \int_{r_n}^{b} \sigma_\theta^R \, r \, dr = 0$$

or $$\int_a^{\rho} -\sigma_y(1+\ln\frac{r}{a}) r \, dr + \int_a^{\rho} \sigma_\theta^s \, r \, dr + \int_{\rho}^{r_n} -\sigma_y[1+\ln(rk)]dr$$

$$+ \int_{r_n}^{b} \sigma_y(1+\ln\frac{r}{b}) r \, dr + \int_{r_n}^{b} \sigma_\theta^s \, r \, dr = 0$$

Putting

$$M_1 = \int_a^{\rho} \sigma_\theta^s \, r \, dr \qquad [3.33]$$

$$M_2 = \int_{r_n}^{b} \sigma_\theta^s \, r \, dr \qquad [3.34]$$

and $$\int r \ln(rk)dr = \frac{r^2}{2} \ln(rk) - \frac{r^2}{4} + \text{Constant etc.}$$

and simplifying.

$$M_1 + M_2 - \sigma_y(\frac{\rho^2}{4} + \frac{\rho^2}{2} \ln\frac{\rho}{a} - \frac{a^2}{4})$$
$$- \sigma_y[\frac{r_n^2}{4} + \frac{r_n^2}{2} \ln(r_n k) - \frac{\rho^2}{4} - \frac{\rho^2}{2} \ln(\rho k)]$$
$$+ \sigma_y(\frac{b^2}{4} - \frac{r_n^2}{4} - \frac{r_n^2}{2} \ln\frac{r_n}{b}) = 0$$

or

$$M_1 + M_2 - \sigma_y[-\frac{b^2+a^2-2r_n^2}{4} - \frac{\rho^2}{2} \ln(ak) + \frac{r_n^2}{2} \ln(\frac{r_n^2 k}{b})] = 0$$

or $$M_1 + M_2 - \sigma_y[-\frac{t^2}{4} + \frac{1}{2}(r_n^2 - \rho^2)\ln(ak)] = 0$$

or $$\Sigma M = M_1 + M_2 + M_3 = 0 \qquad [3.35]$$

where $$M_3 = -\sigma_y[-\frac{t^2}{4} + \frac{1}{2}(r_n^2-\rho^2)\ln(ak)] \qquad [3.34.1]$$

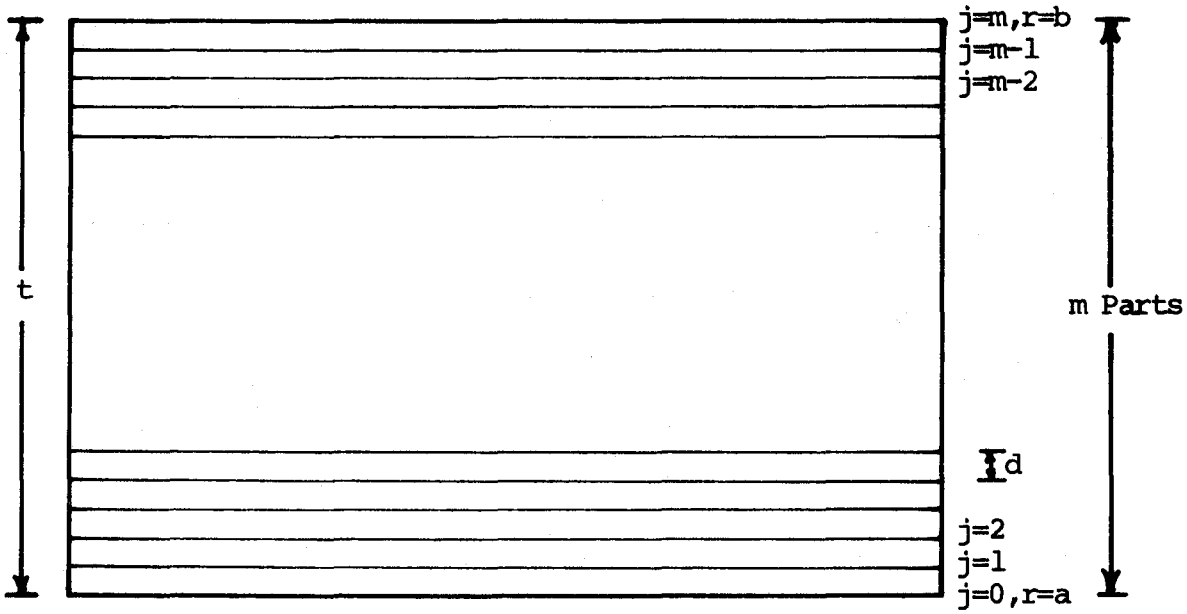

FIG. 3.6 SHEET THICKNESS DIVIDED IN m PARTS

3.3.4 Determination of Unknowns-c, ρ, γ and k

Because the problem is set up in incremental form, the total sheet thickness t is divided into m parts, each of thickness $d(=\frac{t}{m})$.

Equation [3.22] can be written as

$$\Delta\sigma^s_{r_j} = \left[\gamma\left\{\frac{c-(a+jd)}{(a+jd)^2}\right\} + \beta\frac{\sigma^s_{r_j}}{a+jd}\right]d$$

where,

j = Boundary of any general division such that $j=0$ at $r=a$ and $j=m$ at $r=b$ (Fig. 3.6).

$r = a+jd$ at j^{th} boundary

$\Delta r = d$

$\Delta\sigma^s_{r_j}$ = Differential increment in unloading radial stress at j^{th} boundary

and $\sigma^s_{r_j}$ = Unloading radial stress at j^{th} boundary

Now $\sigma^s_{r_o} = 0$ at $r=a$, $j=0$

$$\sigma^s_{r_1} = \Delta\sigma^s_{r_o} + \sigma^s_{r_o} \quad \text{at } r=a+d,\ j=1$$

$$\sigma^s_{r_2} = \Delta\sigma^s_{r_1} + \sigma^s_{r_1} \quad \text{at } r=a+2d,\ j=2 \text{ etc}$$

Similarily

$$\sigma^s_{r_j} = \Delta\sigma^s_{r_{j-1}} + \sigma^s_{r_{j-1}}$$

and $$\Delta\sigma^s_{r_{j-1}} = \left[\gamma\left(\frac{c-\{a+(j-1)d\}}{\{a+(j-1)d\}^2}\right) + \beta\frac{\sigma^s_{r_{j-1}}}{a+(j-1)d}\right]d$$

Therefore:

$$\sigma^s_{r_j} = \gamma d\left(\frac{c-\{a+(j-1)d\}}{\{a+(j-1)d\}^2}\right) + \frac{a+\{j-1+\beta\}d}{a+(j-1)d}\,\sigma^s_{r_{j-1}}$$

Similarily, the expression for $\sigma^s_{r_{j-1}}$ shall contain a term with $\sigma^s_{r_{j-2}}$; and the expression for $\sigma^s_{r_{j-2}}$ will contain a term with $\sigma^s_{r_{j-3}}$ and so on, till the term $\sigma^s_{r_1}$ will contain $\sigma^s_{r_o}$ which is zero. Substituting this series of values

$$\sigma^s_{r_j} = \gamma d\left(\frac{c-\{a+(j-1)d\}}{\{a+(j-1)d\}^2}\right) + \frac{a+(j-1+\beta)d}{a+(j-1)d}\Bigg\{\gamma d\left(\frac{c-\{a+(j-2)d\}}{\{a+(j-2)d\}^2}\right)$$
$$+ \frac{a+(j-2+\beta)d}{a+(j-2)d}\Bigg\{\gamma d\left(\frac{c-\{a+(j-3)d\}}{\{a+(j-3)d\}^2}\right) + \frac{a+(j-3+\beta)d}{a+(j-3)d}\Bigg\{\cdots\cdots$$
$$\cdot\cdot\Bigg\{\cdots\cdots\cdots\cdots\cdots\cdots + \frac{a+(3+\beta)d}{a+3d}\Bigg[\gamma d\left(\frac{c-(a+2d)}{(a+2d)^2}\right)$$
$$+ \frac{a+(2+\beta)d}{a+2d}\Bigg\{\gamma d\left(\frac{c-(a+d)}{(a+d)^2}\right) + \frac{a+(1+\beta)d}{a+d}\Bigg[\gamma d\left(\frac{c-a}{a^2}\right)$$
$$+ \frac{a+\beta d}{a}[\sigma^s_{r_o}]\Bigg]\Bigg\}\Bigg]\cdots\cdots\Bigg\}\cdots\cdots\Bigg\}\Bigg\}.$$

$\sigma^s_{r_o}$ being zero (boundary condition (1)), γd can be taken out as a common factor and $\sigma^s_{r_j}$ can be expressed as

$$\sigma^s_{r_j} = \gamma d\left[\frac{c-\{a+(j-1)d\}}{\{a+(j-1)d\}^2} + \frac{\{a+(j-1+\beta)d\}\{c-[a+(j-2)d]\}}{\{a+(j-1)d\}\{a+(j-2)d\}^2}\right.$$

$$+\frac{\{a+(j-1+\beta)d\}\ \{a+(j-2+\beta)d\}\ \{c-[a+(j-3)d]\}}{\{a+(j-1)d\}\ \{a+(j-2)d\}\ \{a+(j-3)d\}^2}+\ .....$$

$$.....+.....$$

$$....+\frac{\{a+(j-1+\beta)d\}\ \{a+(j-2+\beta)d\}.....}{\{a+(j-1)d\}\ \{a+(j-2)d\}.....}$$

$$\frac{...\{a+(2+\beta)d\}\ \{a+(1+\beta)d\}\ (c-a)}{...(a+2d)\ (a+d)\ a^2}]$$

$$\text{or } \left(\frac{\sigma^s_{r_j}}{\gamma}\right) = d\left[c\left(\frac{1}{\{a+(j-1)d\}^2}+\frac{\{a+(j-1+\beta)d\}}{\{a+(j-1)d\}\ \{a+(j-2)d\}^2}\right.\right.$$

$$+\frac{\{a+(j-1+\beta)d\}\ \{a+(j-2+\beta)d\}}{\{a+(j-1)d\}\ \{a+(j-2)d\}\ \{a+(j-3)d\}^2}+\ .....$$

$$.....+\left.\frac{\{a+(j-1+\beta)d\}.....\ a+(1+\beta)d}{\{a+(j-1)d\}.....\{a+d\}a^2}\right)$$

$$-\left(\frac{1}{\{a+(j-1)d\}}+\frac{\{a+(j-1+\beta)d\}}{\{a+(j-1)d\}\{a+(j-2)d\}}+\ .....\right.$$

$$....+\left.\left.\frac{\{a+(j-1+\beta)d\}.....\{a+(1+\beta)d\}}{\{a+(j-1)d\}.....(a+d)a}\right)\right]$$

[3.36]

At r=b, j=m and the radial stress, $\sigma^s_{r_m}$, which should be zero according to boundary condition number (2), is given by

$$\sigma^s_{r_m} = \gamma d\left[c\left(\frac{1}{\{a+(m-1)d\}^2} + \frac{\{a+(m-1+\beta)d\}}{\{a+(m-1)d\}\{a+(m-2)d\}^2}\right.\right.$$

$$+ \frac{\{a+(m-1+\beta)d\}\{a+(m-2+\beta)d\}}{\{a+(m-1)d\}\{a+(m-2)d\}\{a+(m-3)d\}^2} + \cdots\cdots\cdots$$

$$\left.\cdots\cdots + \frac{\{a+(m-1+\beta)d\}\cdots\cdots\cdots\{a+(1+\beta)d\}}{\{a+(m-1)d\}\cdots\cdots\cdots\cdots(a+d)a^2}\right)$$

$$-\left(\frac{1}{\{a+(m-1)d\}} + \frac{\{a+(m-1+\beta)d\}}{\{a+(m-1)d\}\{a+(m-2)d\}} + \cdots\cdots\cdots\right.$$

$$\left.\left.\cdots\cdots + \frac{\{a+(m-1+\beta)d\}\cdots\cdots\cdots\{a+(1+\beta)d\}}{\{a+(m-1)d\}\cdots\cdots\cdots\cdots(a+d)a}\right)\right]$$

$\gamma d \neq 0$, hence the coefficient of γd must be equal to zero. This gives an expression for the value of the constant c.

$$c = \left[\frac{1}{\{a+(m-1)d\}} + \frac{\{a+(m-1+\beta)d\}}{\{a+(m-1)d\}(a+(m-2)d\}} + \cdots\cdots\cdots\right.$$

$$\left.\cdots\cdots + \frac{\{a+(m-1+\beta)d\}\cdots\cdots\cdots\{a+(1+\beta)d\}}{\{a+(m-1)d\}\cdots\cdots\cdots\cdots(a+d)a}\right] \Big/$$

$$\left[\frac{1}{\{a+(m-1)d\}^2} + \frac{\{a+(m-1+\beta)d\}}{\{a+(m-1)d\}(a+(m-2)d\}^2} + \cdots\cdots\cdots\right.$$

$$\left.\cdots\cdots\cdots + \frac{\{a+(m-1+\beta)d\}\cdots\cdots\cdots\{a+(1+\beta)d\}}{\{a+(m-1)d\}\cdots\cdots\cdots\{a+d\}a^2}\right] \qquad [3.37]$$

Now,

$$\sigma^s_\theta = \gamma\left(\frac{c-r}{r}\right) + (\beta+1)\sigma^s_r \qquad [3.23]$$

Therefore,

$$\sigma^s_{\theta_j} = \gamma\left\{\frac{c-(a+jd)}{(a+jd)}\right\} + (\beta+1)\ \sigma^s_{r_j}$$

i.e.
$$\left(\frac{\sigma^s_{\theta_j}}{\gamma}\right) = \left\{\frac{c-(a+jd)}{(a+jd)}\right\} + (\beta+1)\left(\frac{\sigma^s_{r_j}}{\gamma}\right) \qquad [3.38]$$

where $\sigma^s_{\theta_j}$ = Unloading circumferential stress at the j^{th} boundary.

$\left(\frac{\sigma^s_{r_j}}{\gamma}\right)$ is given by equation [3.36]

c is given by equation [3.37]

and β is given by equation [3.21.2]

Now from [3.28]

$$\rho = \frac{c}{1-\beta\left(\frac{\sigma^s_{r_{r_n}}}{\gamma}\right)}$$

while at $r=r_n$, $j = \frac{(r_n-a)}{d}$

therefore, $\left(\frac{\sigma^s_{r_{r_n}}}{\gamma}\right)$ can be found by using equation [3.36]. When this value is put into equation [3.28] along with the values of c and β from equations [3.37] and [3.12.2] respectively, the value of ρ is found. As will be shown in Chapter V, even for a/t=1.5, this value of ρ does not differ very much from that given by equation [3.14.3].

Furthermore, putting values of M_1 and M_2 from equations [3.33] and [3.34] respectively into equation [3.35] results in

$$\int_a^{\rho} \sigma_\theta^s \, r \, dr + \int_{r_n}^{b} \sigma_\theta^s \, r \, dr + \sigma_y \frac{t^2}{4} - \frac{1}{2}(r_n^2 - \rho^2)$$

$$\sigma_y \ln(ak) = 0$$

$$\text{or} \quad [4 \int_a^{\rho} \frac{\sigma_\theta^s}{\gamma} r \, dr + 4 \int_{r_n}^{b} \frac{\sigma_\theta^s}{\gamma} r \, dr - 2(r_n^2 - \rho^2) \frac{\sigma_y \ln(ak)}{\gamma}] \gamma$$

$$= -\sigma_y t^2$$

Therefore, rearranging and using equation [3.26]

$$(\frac{\gamma}{\sigma_y}) = - \frac{t^2}{2(r_n^2-\rho^2)(\frac{\sigma_{r_{r_n}}^s}{\gamma})+4[\int_a^{\rho} (\frac{\sigma_\theta^s}{\gamma}) \, r \, dr + \int_{r_n}^{b} (\frac{\sigma_\theta^s}{\gamma}) \, r \, dr]} \qquad [3.39]$$

where $(\frac{\sigma_{r_{r_n}}^s}{\gamma})$ is found by using equation [3.36] at $j=\frac{(r_n-a)}{d}$

Integrals $\int_a^{\rho} (\frac{\sigma_\theta^s}{\gamma}) r \, dr$ and $\int_{r_n}^{b} (\frac{\sigma_\theta^s}{\gamma}) \, r \, dr$

are determined as explained below:

$$j = 0 \qquad \text{at } r = a$$

$$= \frac{\rho-a}{d} \qquad \text{at } r = \rho$$

$$= \frac{r_n-a}{d} \qquad \text{at } r = r_n$$

$$= \frac{b-a}{d} = m \qquad \text{at } r = b$$

Now, the moment caused by stress $(\frac{\sigma_\theta^s}{\gamma})$ over the area bounded by the j^{th} and $(j+1)^{th}$ boundaries

$$= \frac{1}{2}\, d\left\{\left(\frac{\sigma^s_{\theta_j}}{\gamma}\right) + \left(\frac{\sigma^s_{\theta_{j+1}}}{\gamma}\right)\right\}\{a+(j+.5)d\}$$

Therefore

$$\int_a^\rho \left(\frac{\sigma^s_\theta}{\gamma}\right) r\, dr = \sum_{j=0}^{j=\left(\frac{\rho-a}{d}-1\right)} \frac{1}{2}\, d\left\{\left(\frac{\sigma^s_{\theta_j}}{\gamma}\right)+\left(\frac{\sigma^s_{\theta_{j+1}}}{\gamma}\right)\right\}$$

$$\{a+(j+.5)d\}$$

and

$$\int_{r_n}^b \left(\frac{\sigma^s_\theta}{\gamma}\right) r\, dr = \sum_{j=\frac{r_n-a}{d}}^{(m-1)} \frac{1}{2}\, d\left\{\left(\frac{\sigma^s_{\theta_j}}{\gamma}\right)+\left(\frac{\sigma^s_{\theta_{j+1}}}{\gamma}\right)\right\}$$

$$\{a+(j+.5)d\}$$

Now,

$$0 = \gamma\left(\frac{c-\rho}{\rho}\right) - \beta\sigma_y \ln(ak) \qquad [3.29.1]$$

i.e.

$$\ln(ak) = \left(\frac{\gamma}{\sigma_y}\right) \frac{1}{\beta} \left(\frac{c-\rho}{\rho}\right) \qquad [3.40]$$

Therefore, all the unknowns can be computed by using equations [3.37], [3.28], [3.39] and [3.40], in the order they are written. Of course, these equations involve the use of equations [3.36] and [3.38].

Once all the constants are known, the distance, x, Fig. 3.5 and strain $\varepsilon^s_{\theta_i}$ may be determined, if desired.

$$x = c-a \qquad [3.41]$$

$$\gamma = \frac{\alpha a\, \varepsilon^s_{\theta_i}}{x} \qquad [3.21.3]$$

Therefore,

$$\varepsilon^{s}_{\theta_i} = \frac{\gamma x}{\alpha a}$$

$$= \left(\frac{\gamma}{\sigma_y}\right) \frac{\sigma_y x}{\frac{E}{1-\nu^2}\, a}$$

$$= \left(\frac{\gamma}{\sigma_y}\right) \frac{x(1-\nu^2)}{a} \left(\frac{\sigma_y}{E}\right)$$

$$= \left(\frac{\gamma}{\sigma_y}\right) \frac{(1-\nu^2)x}{a} (\varepsilon_y) \qquad [3.42]$$

The quantities $\left(\frac{\sigma^s_{r_j}}{\gamma}\right)$ and $\left(\frac{\sigma^s_{\theta_j}}{\gamma}\right)$ can be found by equations [3.36] and [3.38] at any desired value of r for large m. Since r=a+jd and $\left(\frac{\gamma}{\sigma_y}\right)$ is given by equation [3.39] therefore, $\left(\frac{\sigma^s_r}{\sigma_y}\right)$ and $\left(\frac{\sigma^s_\theta}{\sigma_y}\right)$ can be computed at any specified r. When these values are substituted in the earlier given equations the residual stress components in the circumferential and radial directions can be computed. Stress in the lateral direction is given by

$$\sigma^R_z = \frac{1}{2}(\sigma_\theta + \sigma_r) + \nu(\sigma^s_\theta + \sigma^s_r) \qquad [3.43.1]$$

for $a \leq r < \rho$ and $r_n < r \leq b$

$$\sigma^R_z = \frac{1}{2}(\sigma^R_\theta + \sigma^R_r) \quad \text{for } \rho \leq r \leq r_n \qquad [3.43.2]$$

Unfortunately, the equations involved are so complex that it is not possible to write down explicit relations for the residual stress components. However, it is possible to obtain stress components for any given problem where radius of bend, sheet thickness and material properties

are known. A computer program has been developed for determining the various unknowns and ultimately to determine the stress distribution in all the three principal directions (radial, circumferential and lateral). The program is discussed and presented in Appendix A. This program can be used for any numerical problem. The analysis becomes very much simplified and explicit relations for stress components can be written if ν is taken as 0.5.

It can be readily seen that each stress component gets multiplied by a factor, VM = $(2/\sqrt{3})$, if Von Mises yield criterion is used instead of Tresca.

CHAPTER IV

VALIDITY OF ASSUMPTIONS AND EXPERIMENTAL WORK

The experimental work and the calculations presented in this chapter, are to verify some of the basic assumptions, made in the analysis of stresses during cold-bending of a wide sheet and subsequent spring back. Two types of tests, carried out for this purpose were

(a) Investigation of the stress-strain characteristics of the material used subsequently to determine its yield stress σ_y, and Young's modulus of elasticity E, and the degree of strain hardening.

(b) Bending the sheet material about the z-axis to a known radius and measuring the lateral strain ε_z occuring in the outer fibres (convex boundary) of the sheet during the bending operation.

The results of these tests were, subsequently, used to verify that

(i) the plane strain conditions exist during the bending of wide sheets.

(ii) the dimensions of the bent sheet do not change significantly during spring back.

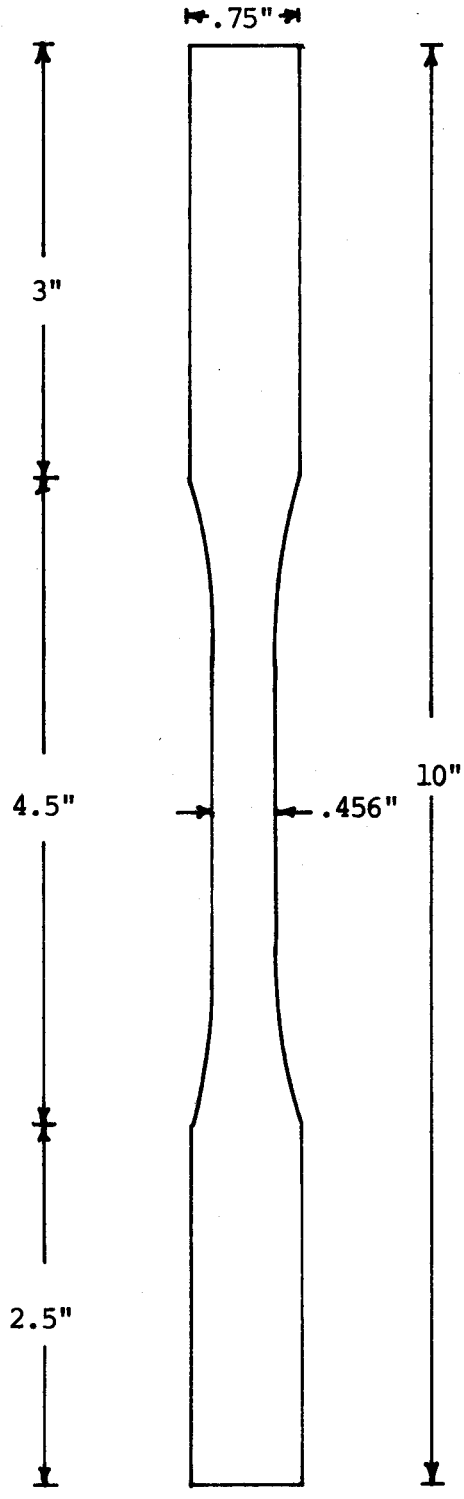

Thickness=1/16"

Area=.0285 sq. in.

FIG. 4.1 DIMENSIONS OF THE TENSION SPECIMEN

Two types of aluminium alloys, Alcon 2S-H14 and 65S-O, were available in the Applied Dynamics Laboratory. Alloy 2S-H14 has less strain hardening as compared to alloy 65S-O and as such that material 1/16 inch in thickness was used in the experiments.

4.1 Stress-Strain Curves

The stress-strain characteristics of the sheet metal were determined by ASTM standard tension tests. Sheet strips of 10" x 3/4" width were taken out in three directions, namely; parallel, at 45° and at 135° to the direction of rolling. These were, then, shaped to a tension test specimen as specified by ASTM on a Tensile Cutter employing a template accessory. Fig. 4.1 shows the final dimensions of the tension specimen .

Budd Foil high elongation strain gauges, type EP-08-500BH, with 120 ohm resistance were used to measure the strains of specimens under tension. To nullify the effect of bending strains which might be present in the test specimens prior to their testing, two strain gauges were mounted along the longitudinal centre-line on each specimen, one being on each face at the centre of the narrow section. The tests were carried out on a "Tinius Olsen" screw type testing machine, and the specimens were all tensioned at a constant strain rate of 0.005 inch/inch/minute. A multiple switching and

Table 4.1

Test Data for Tension Test

(Specimen in the Direction of Rolling)

Load (lbs.)	Stress (ksi)	Strain Face One (μ-in/in)	Strain Face Two (μ-in/in)	Average Strain (μ-in/in)
0	0	0	0	0
50	1.754	593	-201*	196
100	3.508	1126	-242*	442
150	5.263	1536	-208*	664
200	7.017	1994	-116*	939
250	8.772	2380	12	1196
300	10.526	2778	190	1484
350	12.281	3250	422	1836
400	14.035	3810	734	2272
450	15.789	4520	1206	2863
475	16.667	5000	1510	3255
500	17.544	5712	2060	3886
525	18.421	8190	3818	6004
531	18.632	8860	4820	6840

Area = 0.0285 sq. in

*Probably specimen was not perfectly straight and stretching caused compressive strains on the convex surface till the specimen became straight.

Table 4.2

Test Data for Tension Test

(Specimen at 45° to the Direction of Rolling)

Load (lbs)	Stress (ksi)	Strain Face One (μ-in/in)	Strain Face Two (μ-in/in)	Average Strain (μ-in/in)
0	0	0	0	0
50	1.754	166	192	179
100	3.508	344	384	364
150	5.263	532	570	551
200	7.017	718	764	741
250	8.772	926	972	949
300	10.526	1172	1216	1194
350	12.281	1421	1493	1457
375	13.158	1604	1650	1627
400	14.035	1792	1842	1817
425	14.912	2064	2080	2072
450	15.789	2411	2477	2444
475	16.667	2884	2916	2900
500	17.544	3753	4001	3877
517	18.140	5680	6110	5895
520	18.246	6737	7101	6919

Area = 0.0285 sq. in.

Table 4.3

Test Data for Tension Test

(Specimen at 135° to the Direction of Rolling)

Load (lbs)	Stress (ksi)	Strain Face One (μ-in/in)	Strain Face Two (μ-in/in)	Average Strain (μ-in/in)
0	0	0	0	0
50	1.754	252	114	183
100	3.508	474	244	359
150	5.263	695	389	542
200	7.017	912	558	735
250	8.772	1158	746	952
300	10.526	1420	968	1194
350	12.281	1737	1245	1491
375	13.158	1940	1392	1666
400	14.035	2133	1607	1870
450	15.789	2764	2084	2424
475	16.667	3211	2621	2916
500	17.544	4193	3435	3814
510	17.895	4820	4350	4585
518	18.175	5970	5400	5685
520	18.246	6460	5940	6200

Area = 0.0285 sq. in.

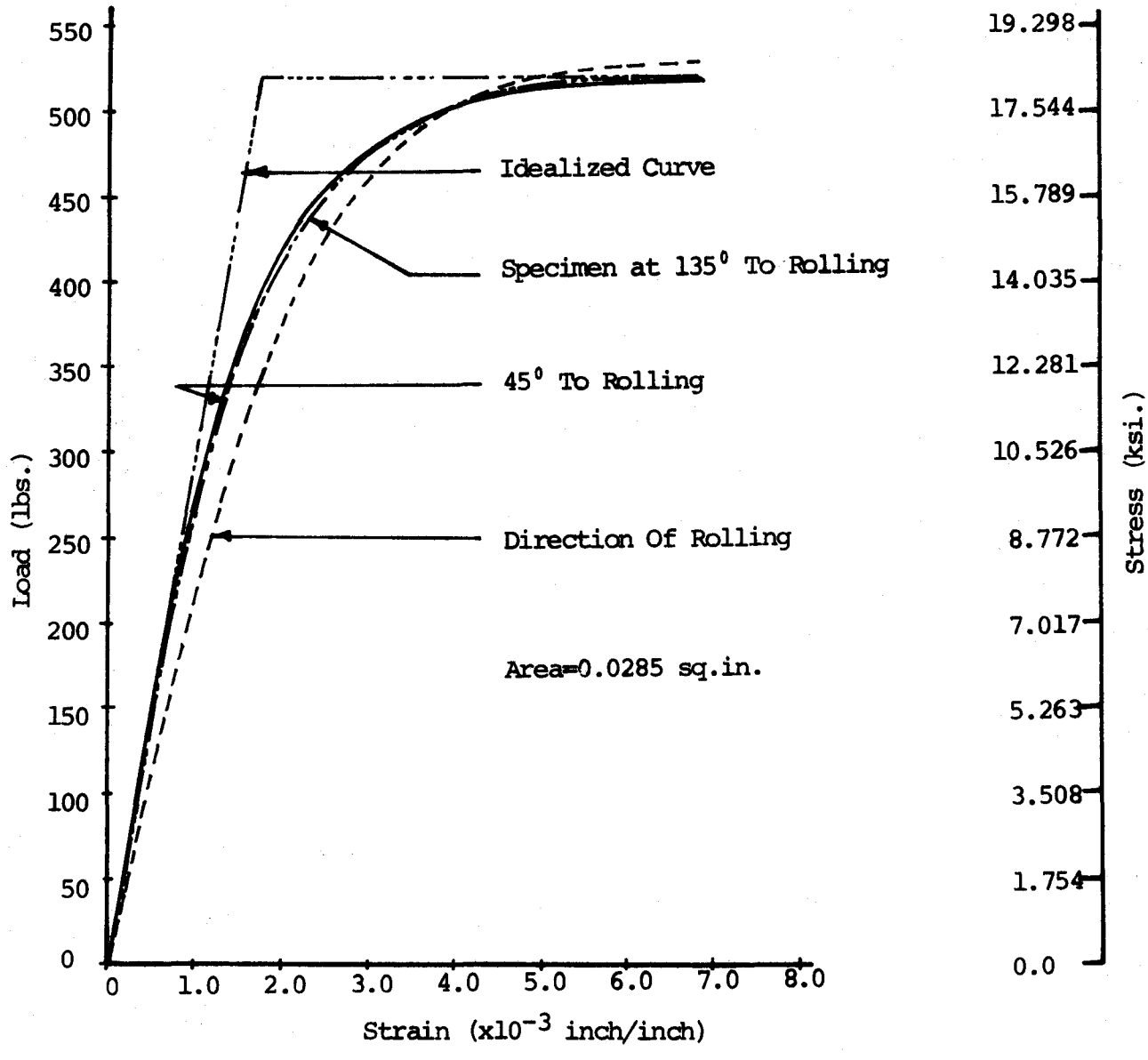

FIG. 4.2 STRESS-STRAIN CURVES FOR ALCON 2S-H14

bridge unit with a galvanometer strain indicator was used to balance the gauges and to measure the strains.

The experimental data for this test are shown in Tables 4.1, 4.2 and 4.3. The stress-strain relationships obtained are as plotted in Fig. 4.2. It was observed that the stress-strain curves for the specimens cut at 45° and 135° to the direction of rolling were practically identical. However, they varied considerably from the stress-strain curve for the specimen cut in a direction parallel to the direction of rolling.

An idealized stress-strain curve is also shown in Fig. 4.2 and the results obtained are shown in Table 4.4.

Table 4.4

Results of Tensile Test

Yield Stress, σ_y	18.245×10^3 psi
Young's Modulus of Elasticity, E	10.136×10^6 psi

4.2 Measurement of Lateral Strains During Bending Operation

The aim of this section of the experimental work was to verify the theoretical prediction that the lateral strains are zero during the bending of a wide metal sheet. This condition of zero lateral strain is called the plane strain

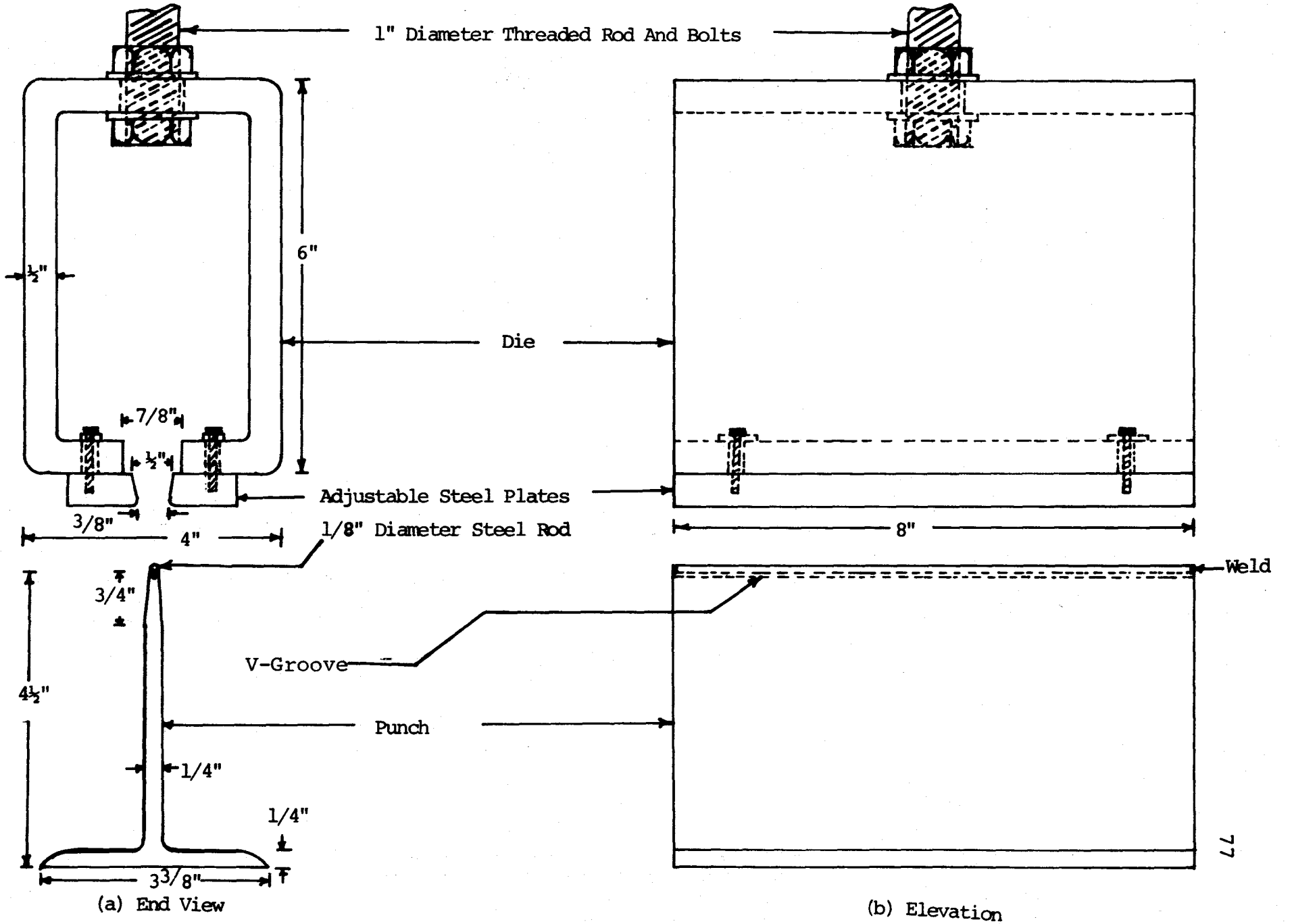

FIG. 4.3 BENDING PRESS

condition and was used in the analysis of the stresses occurring during the bending of a wide sheet. The bending press used is shown in Fig. 4.3, and consisted of a die and a punch. Contrary to usual conventions, the punch was held stationary and the die was forced to move downward over the punch.

The punch was made from an I section available in the Applied Dynamics Laboratory. The top flange was cut to get an inverted tee section and a V-groove was cut in the web of this inverted tee section. The groove was so dimensioned as to accomodate a 1/8" diameter steel bar, at a level just below the horizontal diameter of the bar. This was to ensure that at least half the cross-section of the bar be clear above the inverted tee section. The top 3/4" of the web was tapered as shown in Fig. 4.3. A 1/8" diameter tough steel rod was put in the groove and the ends were welded to ensure full contact of rod with the inverted tee section, at all times.

A 4" x 6" hollow steel beam section, available in the laboratory was selected to make a movable die. A 7/8" wide groove was cut at the centre of one of the short sides (4" side) of the section. Two steel plates, each of 8 x 1 x x 1/2 inch thick were chosen to vary the clearance between the die faces. The plates were rounded along one of their long edges and bolted to the hollow section along the groove, one

plate being on each side of it. The distance between the plates could be changed and adjusted at any desired value between 0 and 7/8". This adjustment was necessary to get the proper radius of curvature. If the clearance were greater the sheet might have resisted bending along and around the steel rod; if the clearance were too small the punch might have sheared through the sheet. A one inch diameter threaded steel rod was fitted at the centre of the face opposite to grooved face, to screw the die with the loading head of the "Tinius Olsen" screw type testing machine.

As aforesaid, the stress-strain curves were practically identical for the specimens cut in the directions at 45° and 135° to the direction of rolling. As the theory assumes that the material is initially isotropic, it was desirable to have the stress-strain characteristics in two perpendicular directions the same. Hence, for this test square pieces, 7" x 7", were cut out from the sheets at 45° to the direction of rolling. The strain gauge was mounted on the sheet as shown in Fig. 4.4, so that the strain could be measured in the lateral (longitudinal) direction on the outside fibres of the bend. As the object of measuring the strain in this direction was to verify the assumed value of zero strain, wire strain gauges of lengths 1 inch, type SR4-A12, with 120 ohm resistance and a gauge factor of 2.05 were used to measure

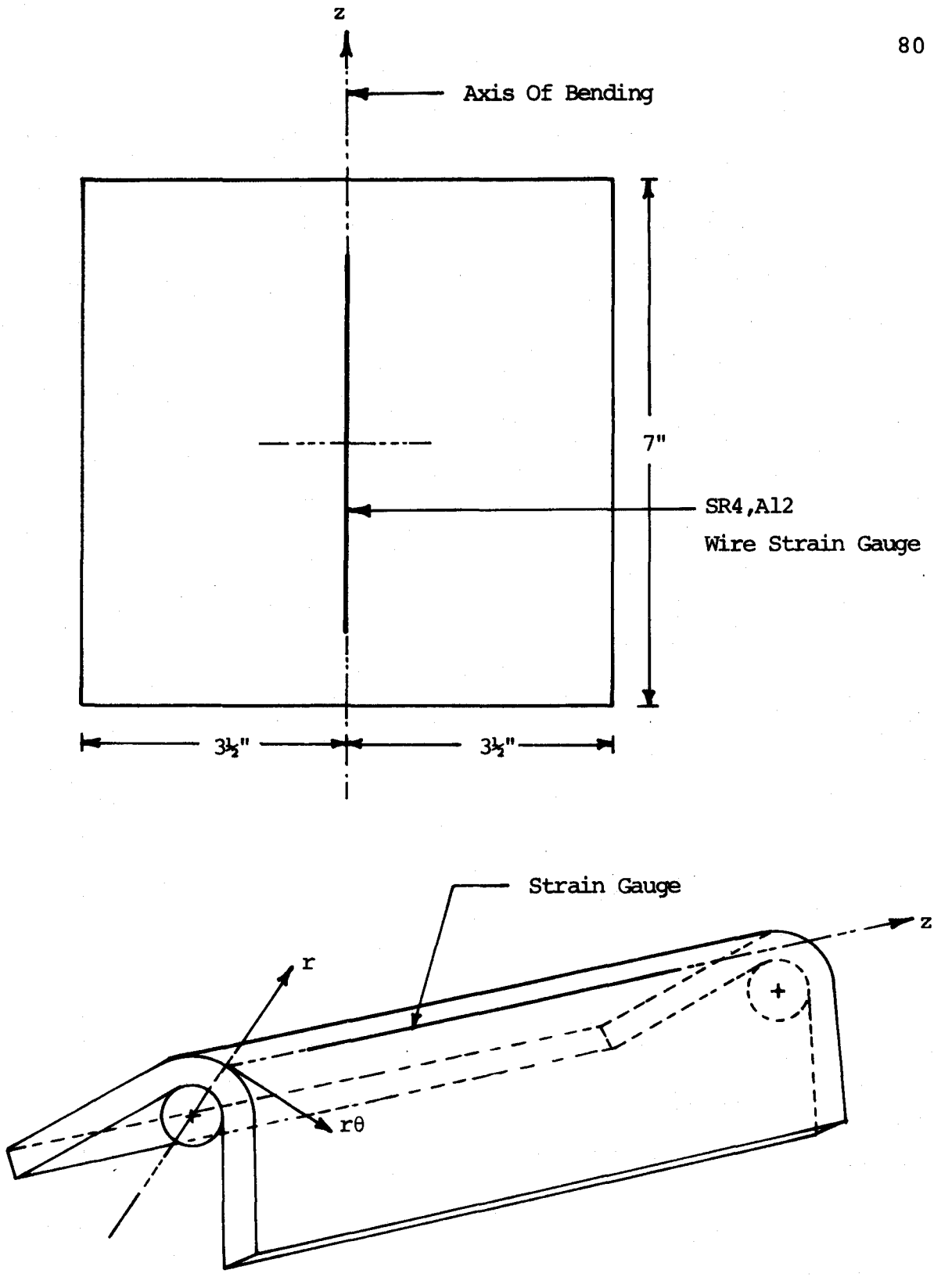

FIG. 4.4 POSITION OF STRAIN GAUGE ON THE SHEET

any small strain in this direction. The strain gauges were mounted exactly at the centre of the sheets, along the z-axis, the axis about which the sheet was bent.

The die was fitted to the loading head of the "Tinius Olsen" screw type testing machine and the sheet was put below it, over the punch in such a way that the centre of the die's goove, wire strain gauge (on the centre of the sheet) and the centroidal axis of the steel rod on the punch were all in one vertical plane. Dial gauges were fixed to measure the travel of the die and the vertical travel of the corners of the sheet. The travel of the die was measured from the instant it just touched the sheet, without bending it, to the final bending position of the sheet. The die was slowly moved down and strains in the lateral direction z were measured using a strain indicator and a multiple switch and balance unit. Unfortunately, the strains after unloading could not be measured as the strain gauges slipped from the sheet surface by the time the bending operation was completed. Nevertheless, the aim of the experiment was to measure the lateral strains during bending so as to verify the assumed zero value of these lateral strains.

4.3 Verification of Plane Strain Condition

The maximum lateral strain ε_z recorded in the outside fibres of the sheet bent in the experiment described above

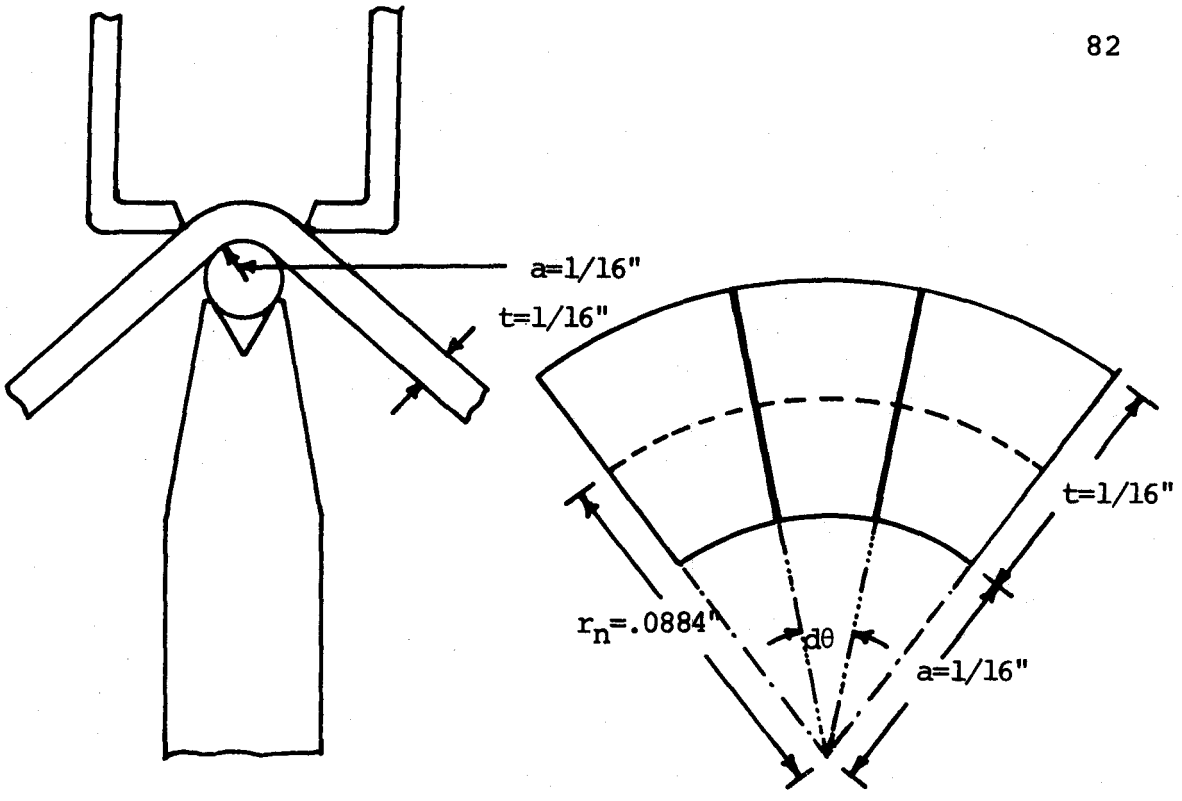

(a) Geometry (b) Element

FIG. 4.5 SHEET BEND AROUND THE ROD

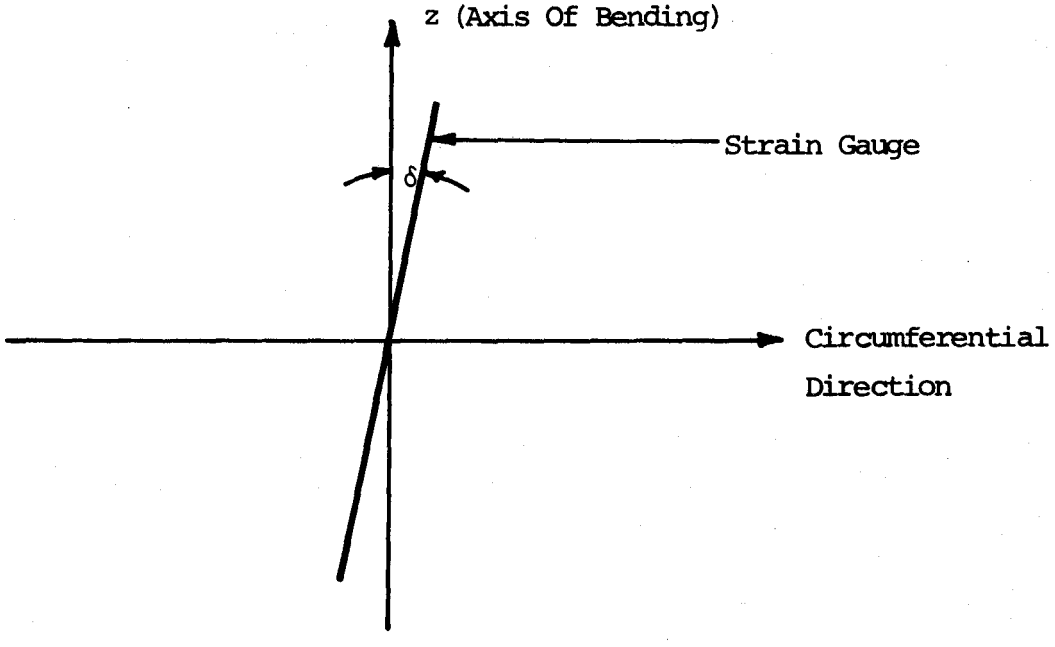

FIG. 4.6 NON-ALIGNMENT OF STRAIN GAUGE

was 1562 micro inch/inch. Since the sheet thickness was 1/16" and it was bent around a 1/8" diameter rod, the radius of curvature of the inside fibres was reduced to a minimum of 1/16". This sharp bending results in an a/t ratio equal to 1, where a is the radius to inside fibres and t, the thickness of the sheet.

Now, the circumferential strain ε_θ can be calculated for this bend simply. Fig. 4.5(a) shows the geometry of the sheet bent around the rod and Fig. 4.5(b) shows an element taken out from the bend.

If r_n is the radius to the neutral axis, then the original length of the outside fibre

= length of fibre at neutral axis

$= r_n \, d\theta$

where $d\theta$ = Angle between two adjacent elements.

The stretched length of the outside fibre

$= b \, d\theta$

Therefore,

$$\varepsilon_\theta = \frac{b \, d\theta - r_n d\theta}{r_n d\theta}$$

$$= \frac{b - r_n}{r_n}$$

For the case under consideration

$t = 1/16$ inch

$r_n = \sqrt{ab}$

$= \sqrt{(1/16)(1/8)}$

$= 0.0884$

Therefore $$\varepsilon_\theta = \frac{0.125 - 0.0884}{0.0884}$$

$$= 0.414 \text{ in/in}$$

$$= 414{,}000 \ \mu\text{-in/in}$$

Now, the maximum lateral strain ε_z recorded in the test was 1562 μ-in/in, which is only 0.377 percent of the circumferential strain ε_θ. Even this small lateral strain seems to be a component of the circumferential strain in the direction of the wire strain gauge, which was not exactly aligned with the axis of bending. It can be shown that even a very small non-alignment of the strain gauge from the axis of bending is enough to give the strain recorded in the lateral direction.

If the angle between the strain gauge and the axis of bending be δ as shown in Fig. 4.6, then the component of the circumferential strain ε_θ in the direction of the strain gauge = $\varepsilon_\theta \sin\delta$. This component of ε_θ is recorded by the strain gauge and the value recorded is 1562 μ-in/in.

Therefore, $$1562 = \varepsilon_\theta \sin\delta$$

i.e., $$\sin\delta = \frac{1562}{414{,}000}$$

or $$\delta = 0.00377 \text{ degrees.}$$

Hence, it is concluded that the lateral strain recorded in the test was due to small non alignment of the strain gauge and the assumption of zero lateral strain (plane strain condition) is valid for the wide sheet bending.

4.4 Verification of Virtual Constancy of Physical Dimensions During Spring-Back.

The calculations performed in this part are somewhat simplified employing the worst bending conditions to verify that the sheet dimensions change negligibly during spring back.

The following data and assumption are used:

(1) $a/t = 1$ (the bending done in actual experiment)

(2) $E = 10.136 \times 10^6$ psi (found by experiment)

(3) $\sigma_y = 18.245 \times 10^3$ psi (found by experiment)

(4) that the neutral axis, at all times, coincides with the centroidal axis of the sheet for simplicity.

Fig. 4.7(a) shows a typical element, taken from the bent sheet and it is assumed that the length of the fibre at the neutral axis is 3 units.

Now, for this element

$$a=t$$

and $$r_n = a + \frac{t}{2}$$

$$= \frac{3}{2} t$$

Therefore, the length of the inner fibre before spring back

$$= a \, d\theta$$

$$= a \frac{3}{r_n}$$

$$= 2 \text{ units.}$$

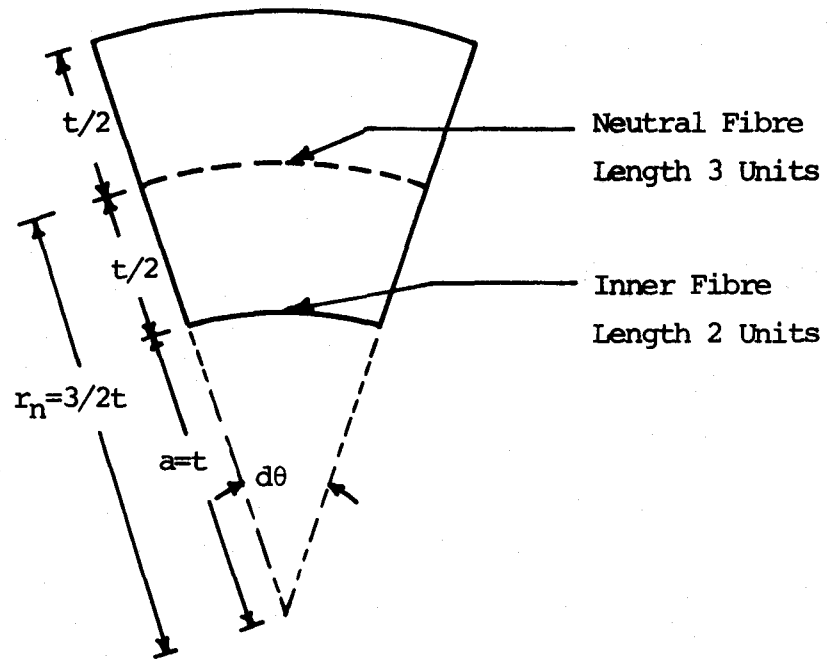

(a) Before Spring-Back

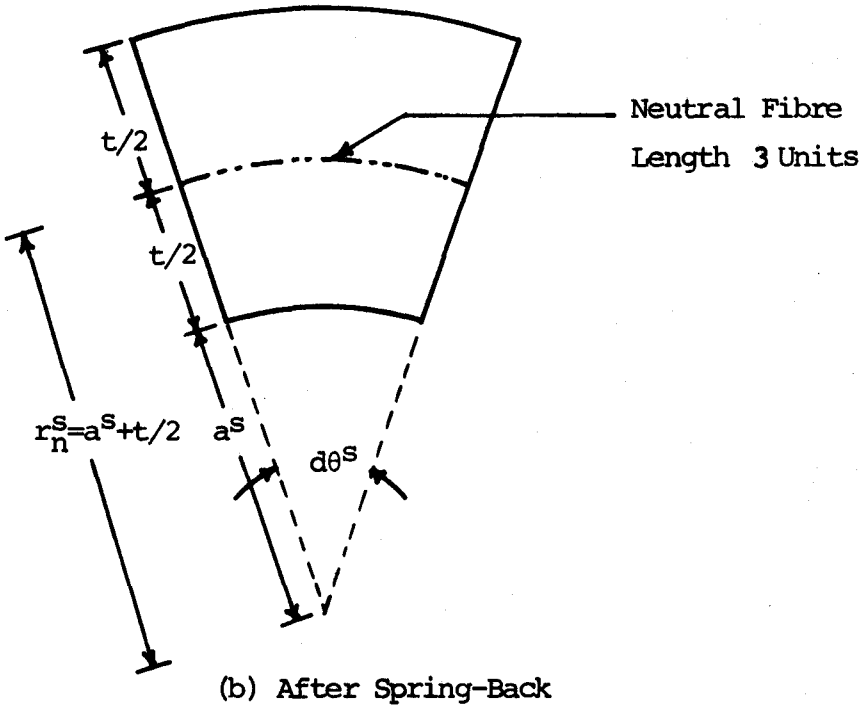

(b) After Spring-Back

FIG. 4.7 GEOMETRY OF ELEMENT FOR a/t=1.0

The same element after spring back is shown in Fig. 4.7 (b). If the radius to neutral axis after spring back is r_n^s and the circumferential strain in the inner fibres, for the worst case, after spring back is assumed to change by 2 ε_y, where

ε_y = yield strain

Then
$$\varepsilon_y = \frac{\sigma_y}{E}$$
$$= \frac{18.245 \times 10^3}{10.136 \times 10^6}$$
$$= 1.8 \times 10^{-3} \text{ in/in}$$

The length of inner fibres, after spring back

$$= 2 + 2 \times (1.8 \times 10^{-3} \times 2)$$
$$= 2.0072 \text{ units}$$

Therefore

$$a^s \, d\theta^s = 2.0072$$

where a^s = Radius of inner fibres after spring back.
and $d\theta^s$ = Angle subtended at the centre of curvature by the element after spring back.

i.e., $$2.0072 = a^s \frac{3}{r_n^s}$$
$$= \frac{3 \, a^s}{a^s + 0.5t}$$

Rearranging
$$\frac{a^s}{t} = \frac{.5 \times 2.0072}{(3-2.0072)}$$
$$= 1.0108.$$

Thus, the spring back altered a/t from an initial value before spring back of 1 to 1.0108, the final value after spring back. The change in a/t ratio is therefore only 1.08%. Hence, it seems quite logical to assume that the physical dimensions of the sheet do not change appreciably during and after spring back in spite of the rather crude assumptions concerning neutral surface location.

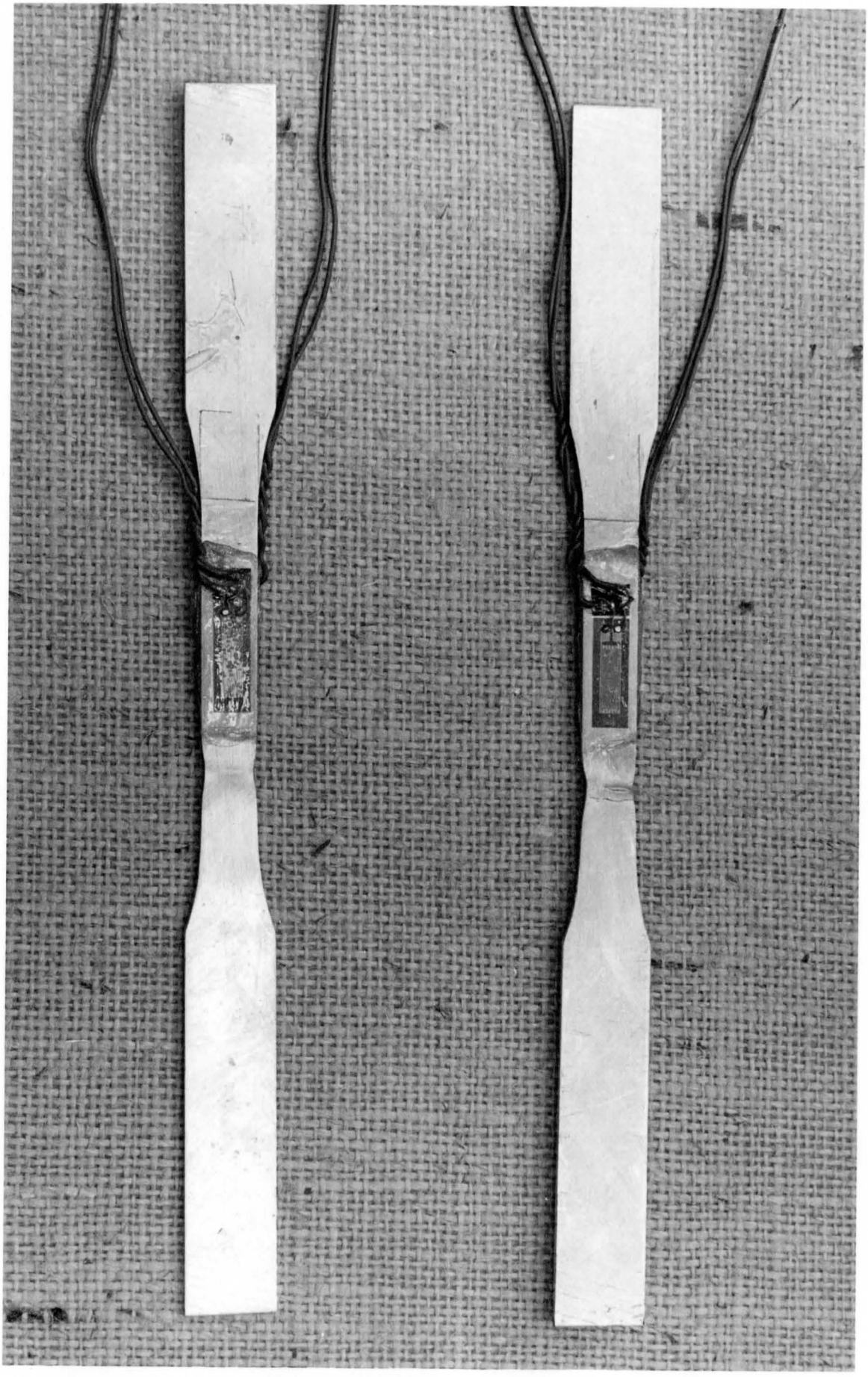

PHOTOGRAPH 4.1 SPECIMENS FOR TENSION TEST

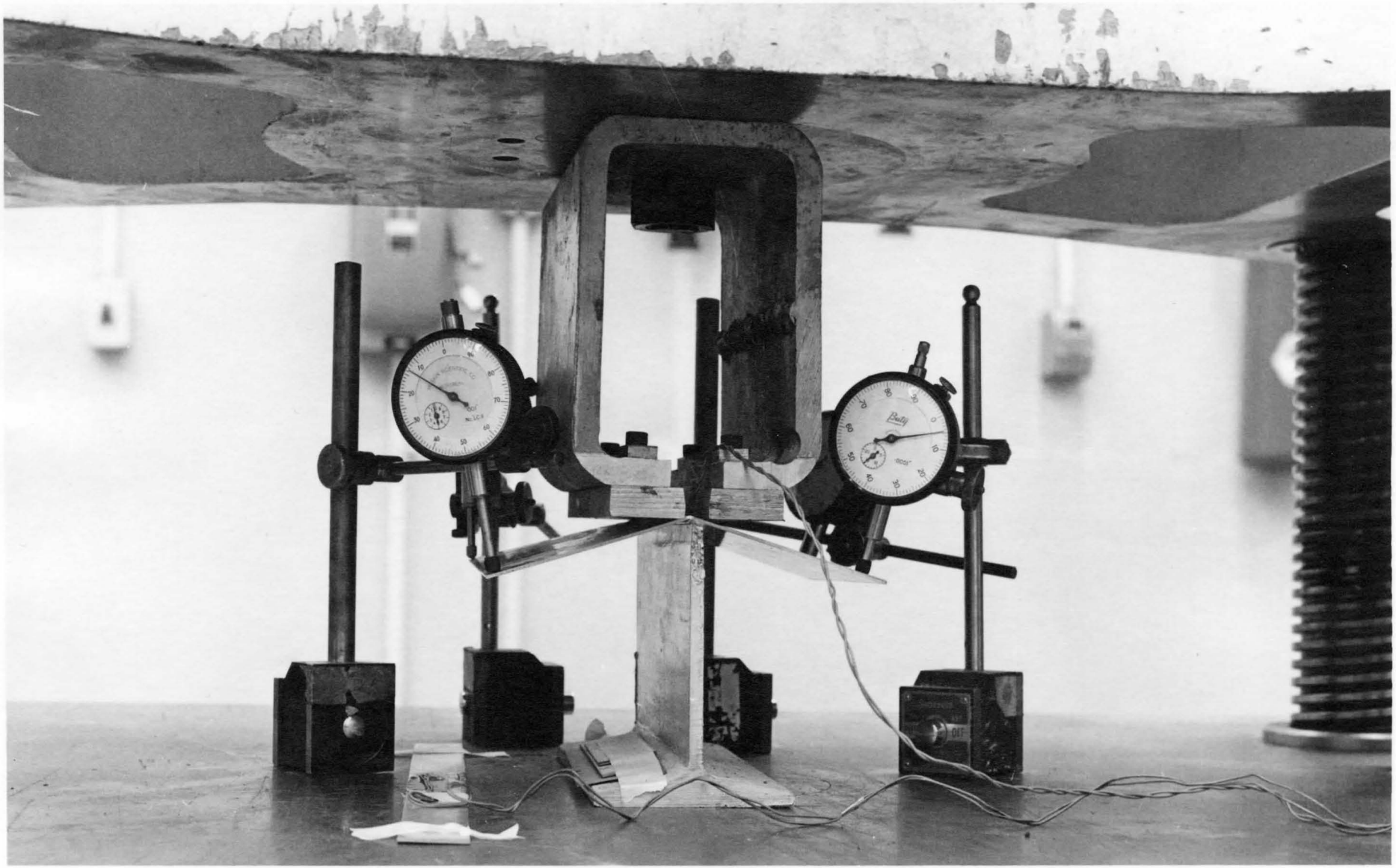

PHOTOGRAPH 4.2 BENDING PRESS

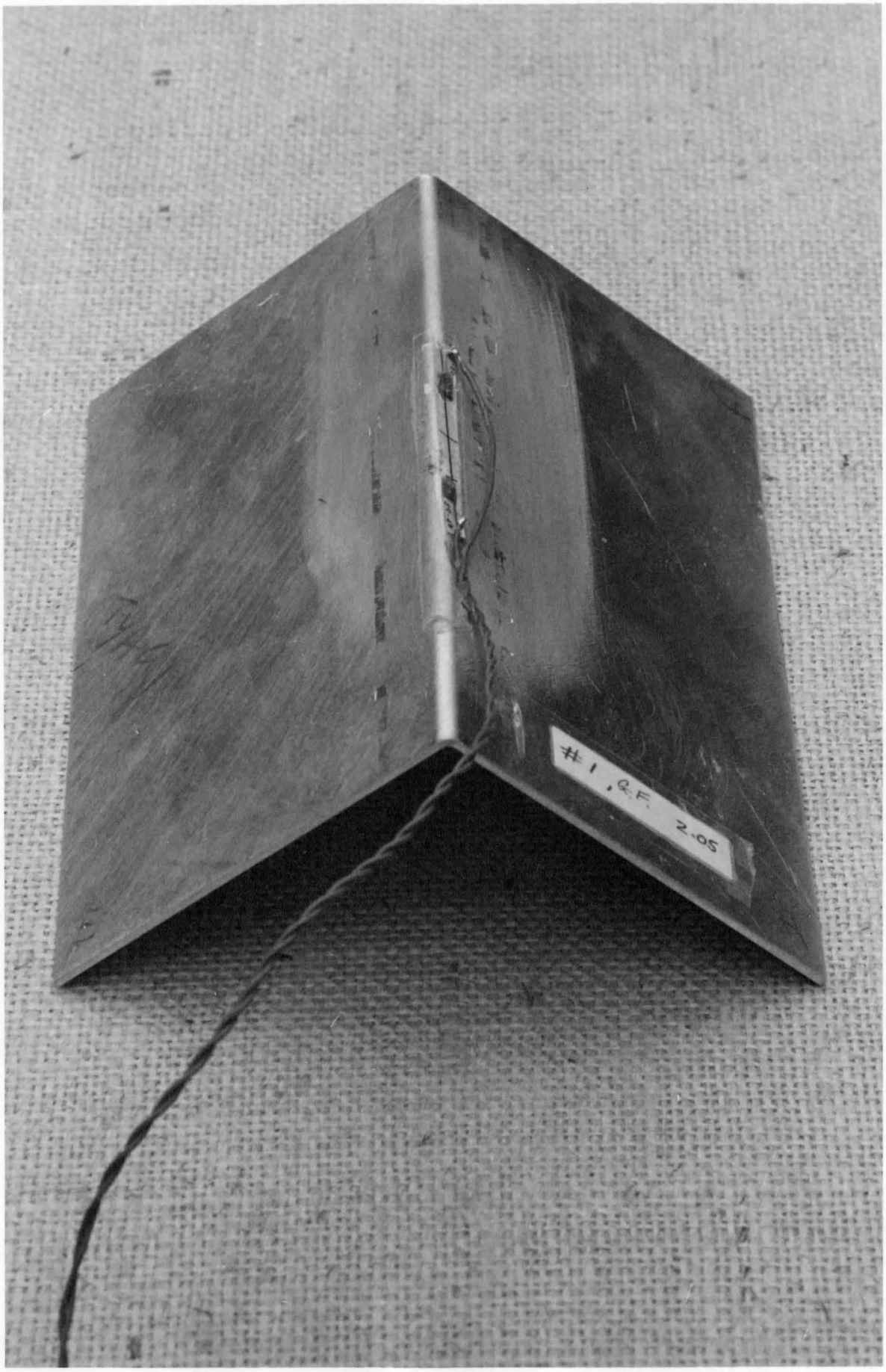

PHOTOGRAPH 4.3 SPECIMEN FOR SHEET BENDING TEST

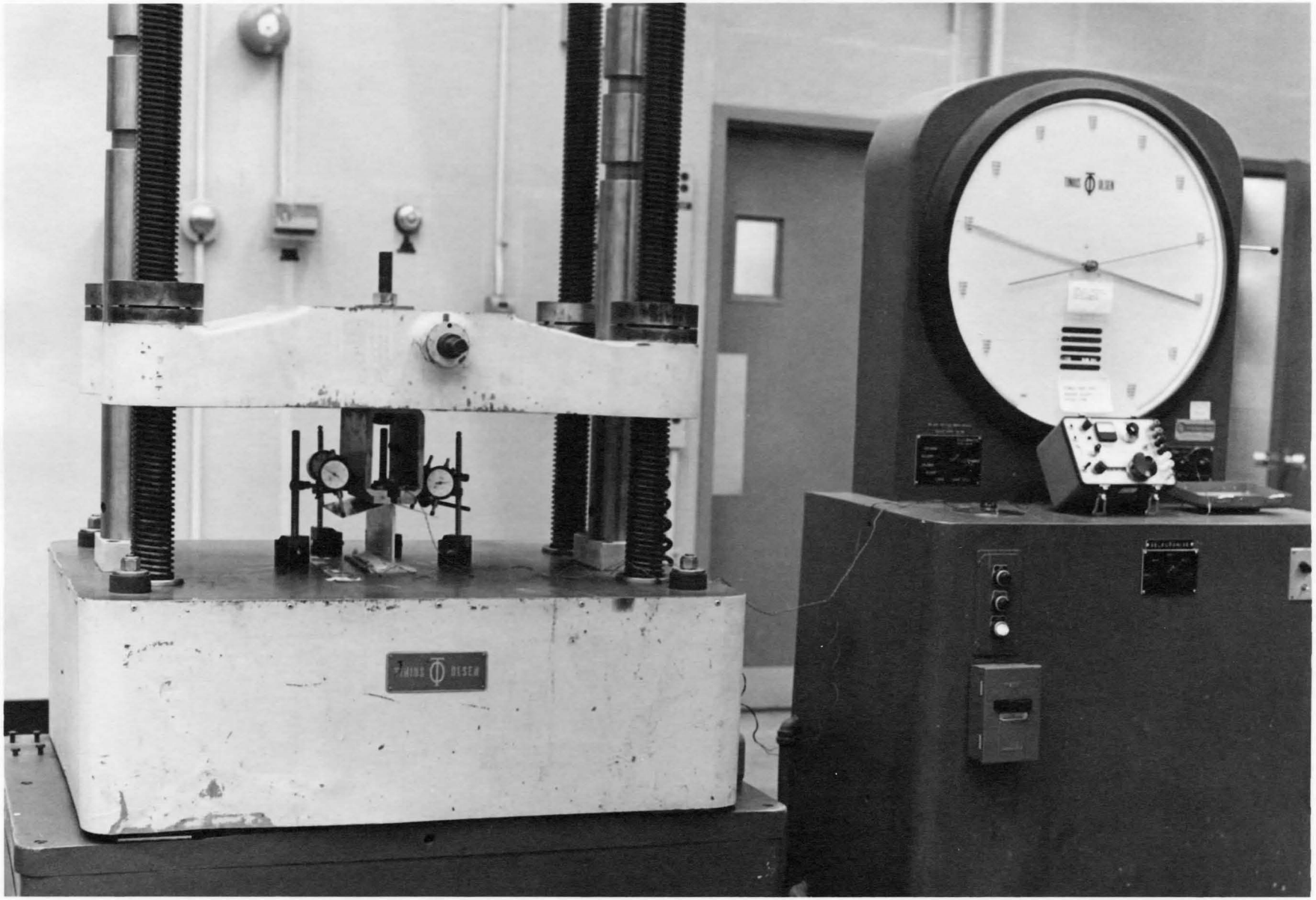

PHOTOGRAPH 4.4 EXPERIMENTAL SET-UP FOR BENDING TEST

CHAPTER V

RESULTS AND DISCUSSIONS

5.1 Plots of Residual Stress Components

Residual stress components in the circumferential, radial and lateral directions have been calculated for a/t = 1.5, 2, 3, 4, 5, 6 and 25. A bending ratio a/t=25 refers to the case of moderate bending* and is included to compare with a simple theory. For computer calculation purposes a sheet thickness t of $\frac{1}{4}$" was assumed. Only the a/t ratio is important however since the results are independent of t. Further, the value of Poisson's ratio ν has been assumed to be 0.3 where compressible material is involved. The results for a value of 0.5 are also examined. The computer programs can be used for any value of t and ν.

The distributions of the residual stress components are shown graphically in Fig. 5.1 to 5.7. The results of the approximate method, as outlined in section 3.1, are also plotted for two extreme cases of a/t=1.5 and 6.

---

*A maximum of 2% outer fibre strain has been assumed for moderate bending

i.e. $\frac{t/2}{a + t/2} = \frac{2}{100}$

or $a/t \simeq 25$

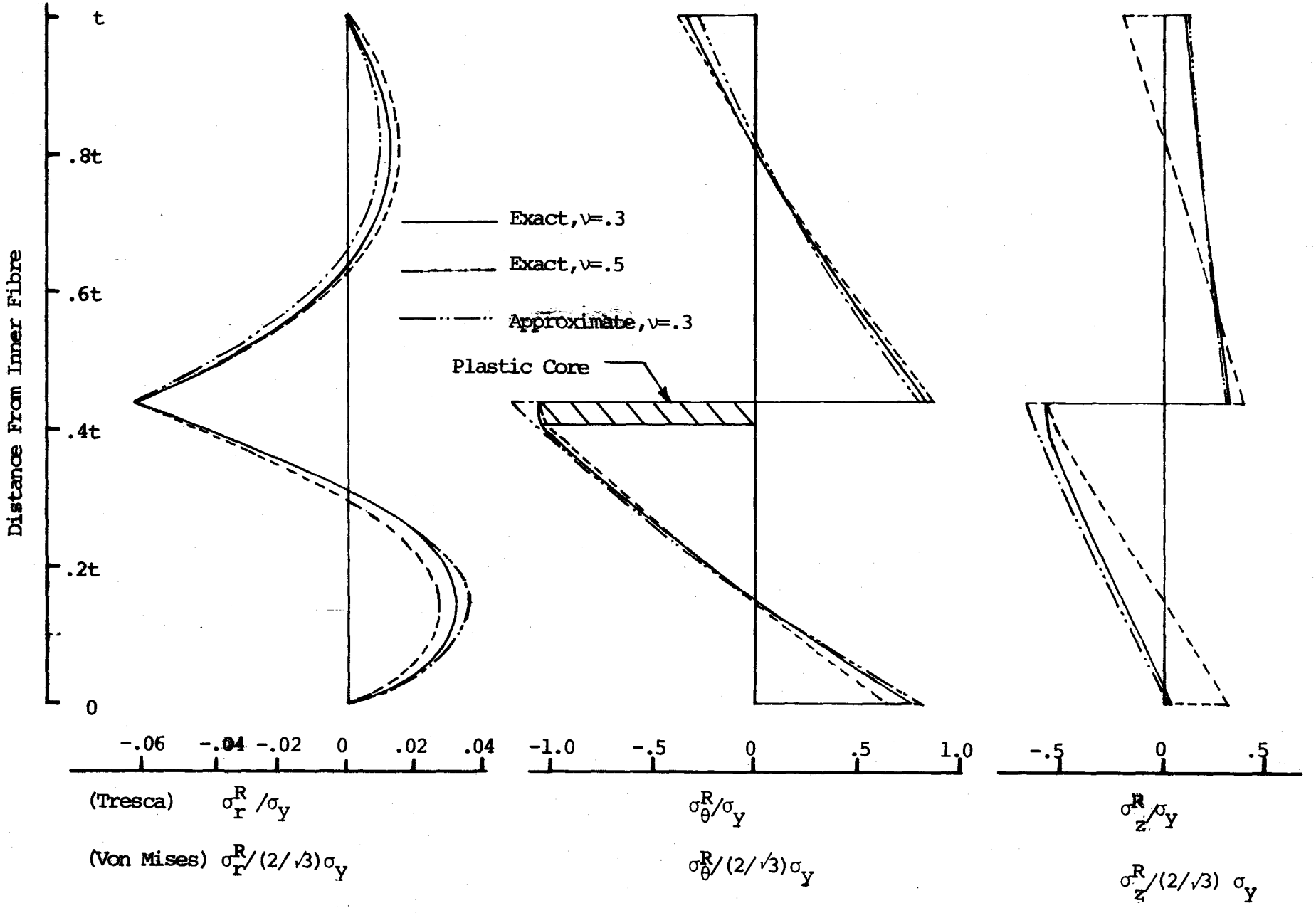

FIG. 5.1 RESIDUAL STRESS DISTRIBUTIONS FOR a/t=1.5

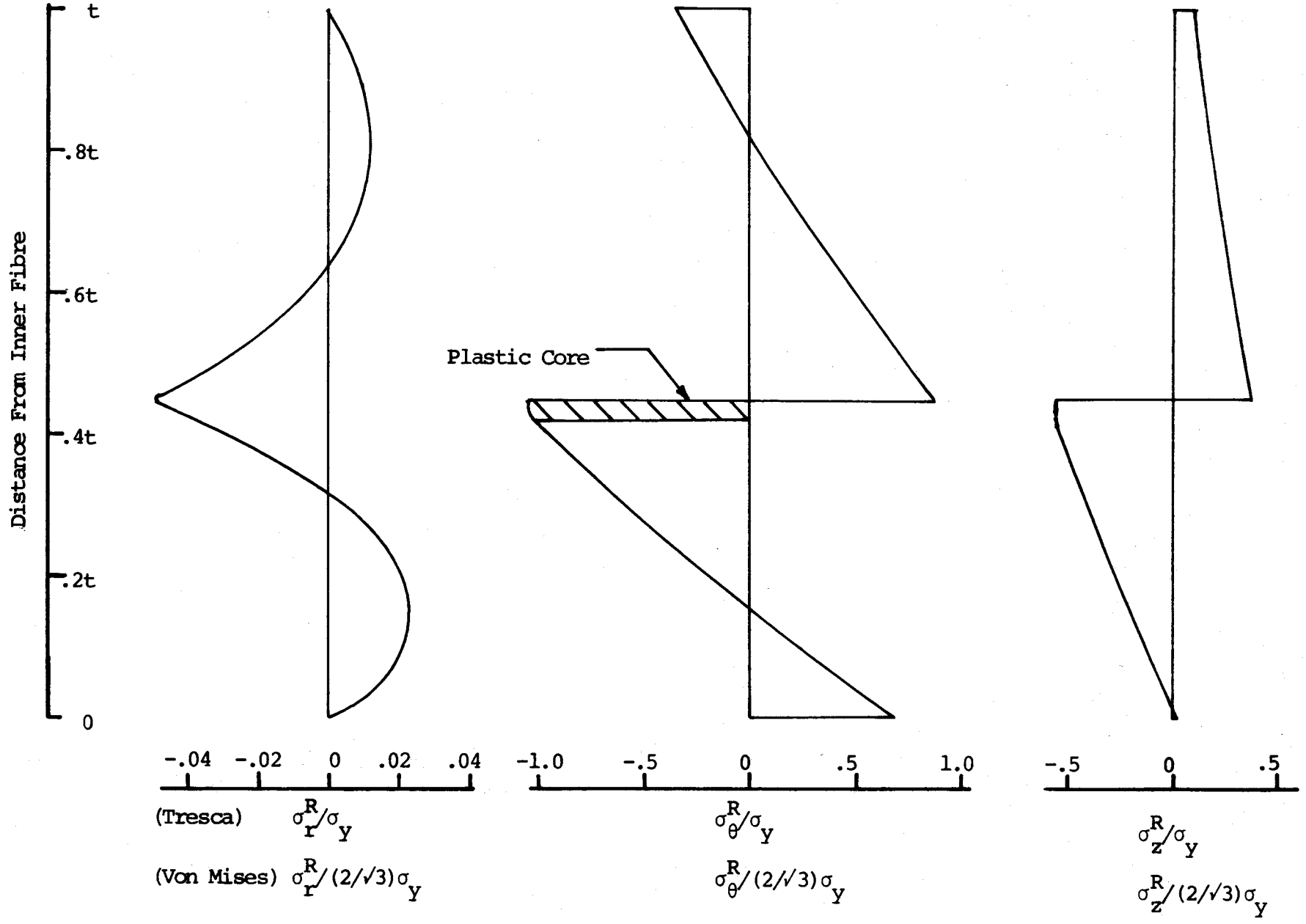

FIG. 5.2 EXACT RESIDUAL STRESS DISTRIBUTIONS FOR a/t=2.0, ν=.3

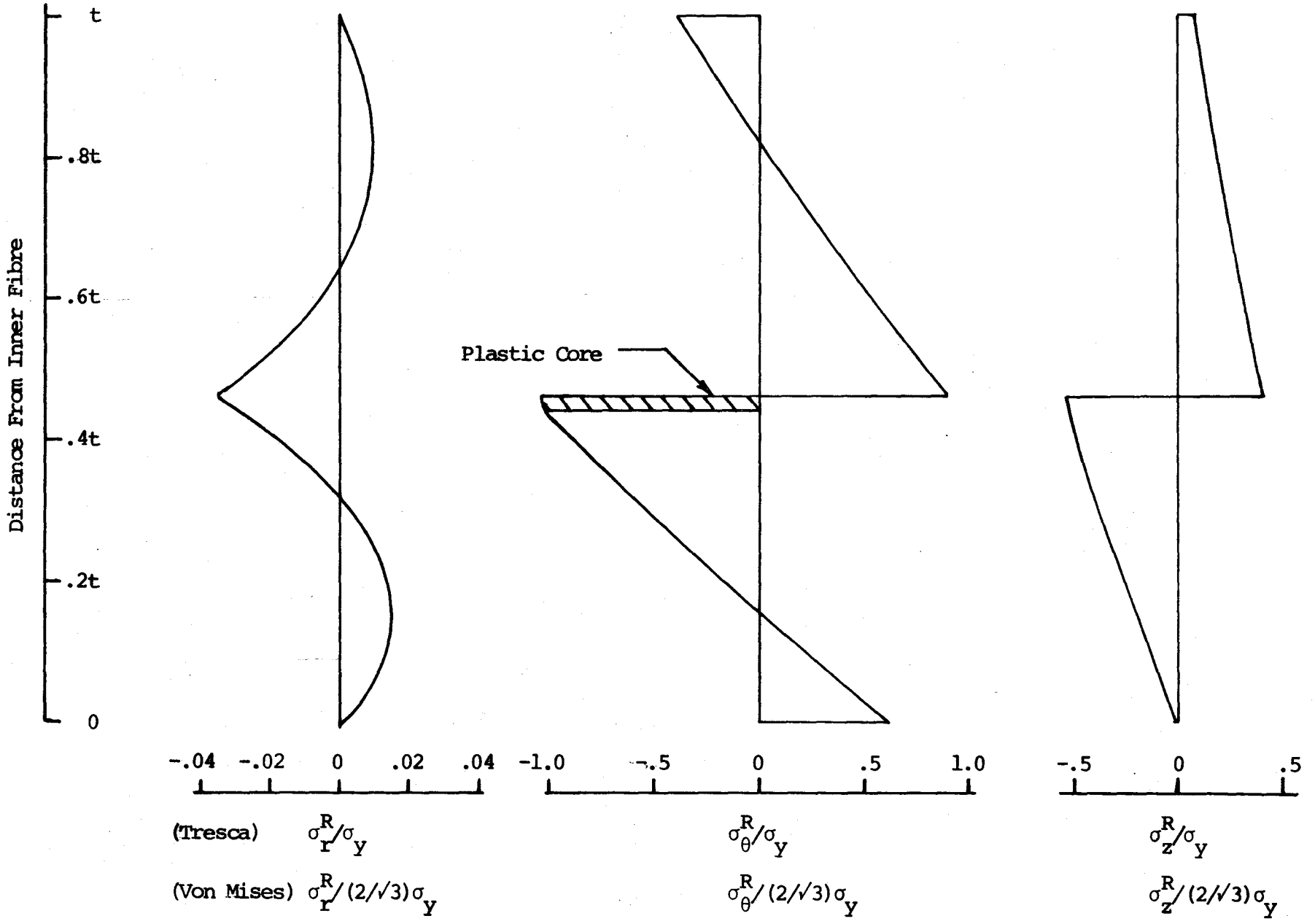

FIG. 5.3 EXACT RESIDUAL STRESS DISTRIBUTIONS FOR a/t=3.0, ν=.3

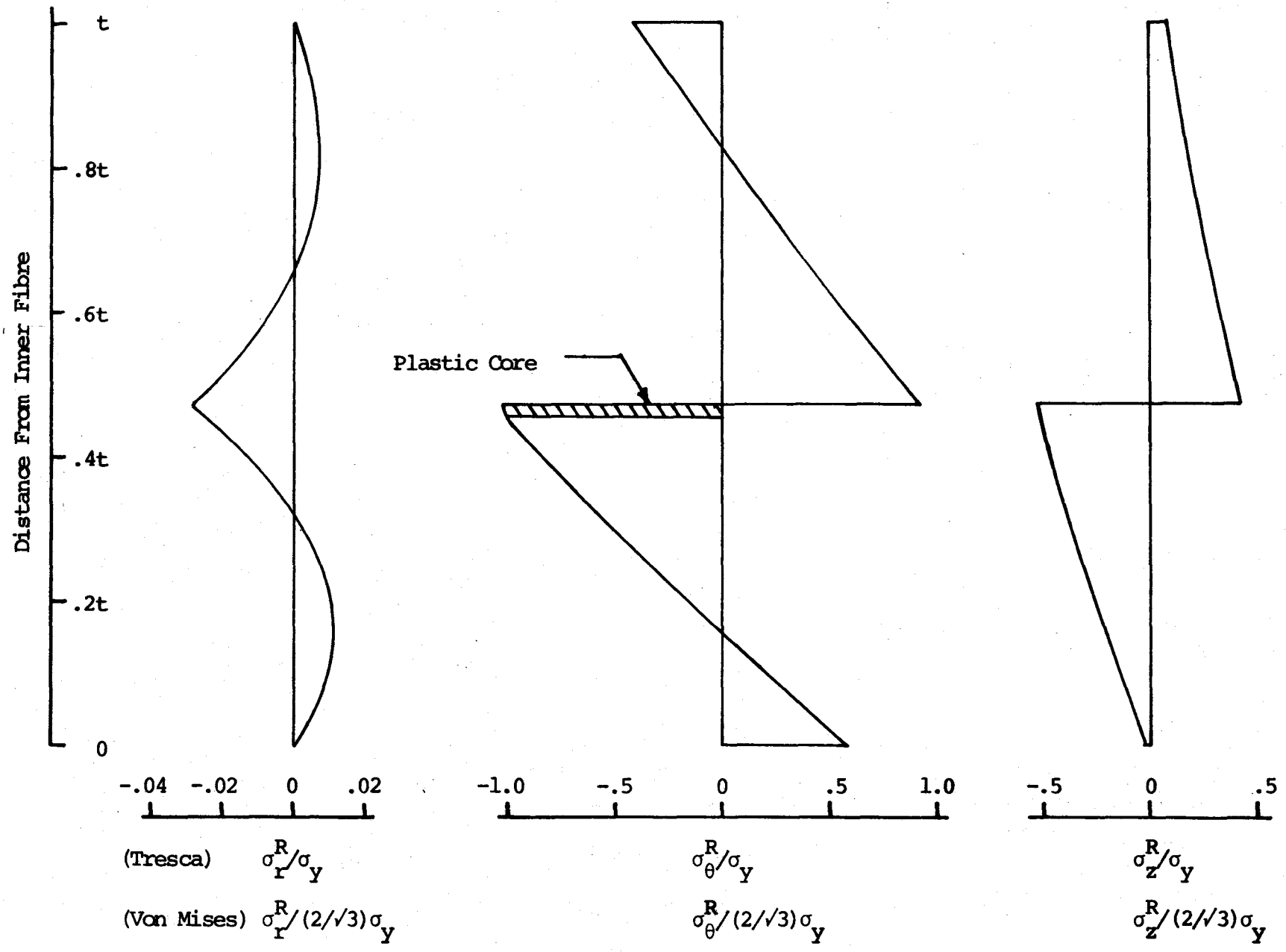

FIG. 5.4 EXACT RESIDUAL STRESS DISTRIBUTIONS FOR a/t=4.0,ν=.3

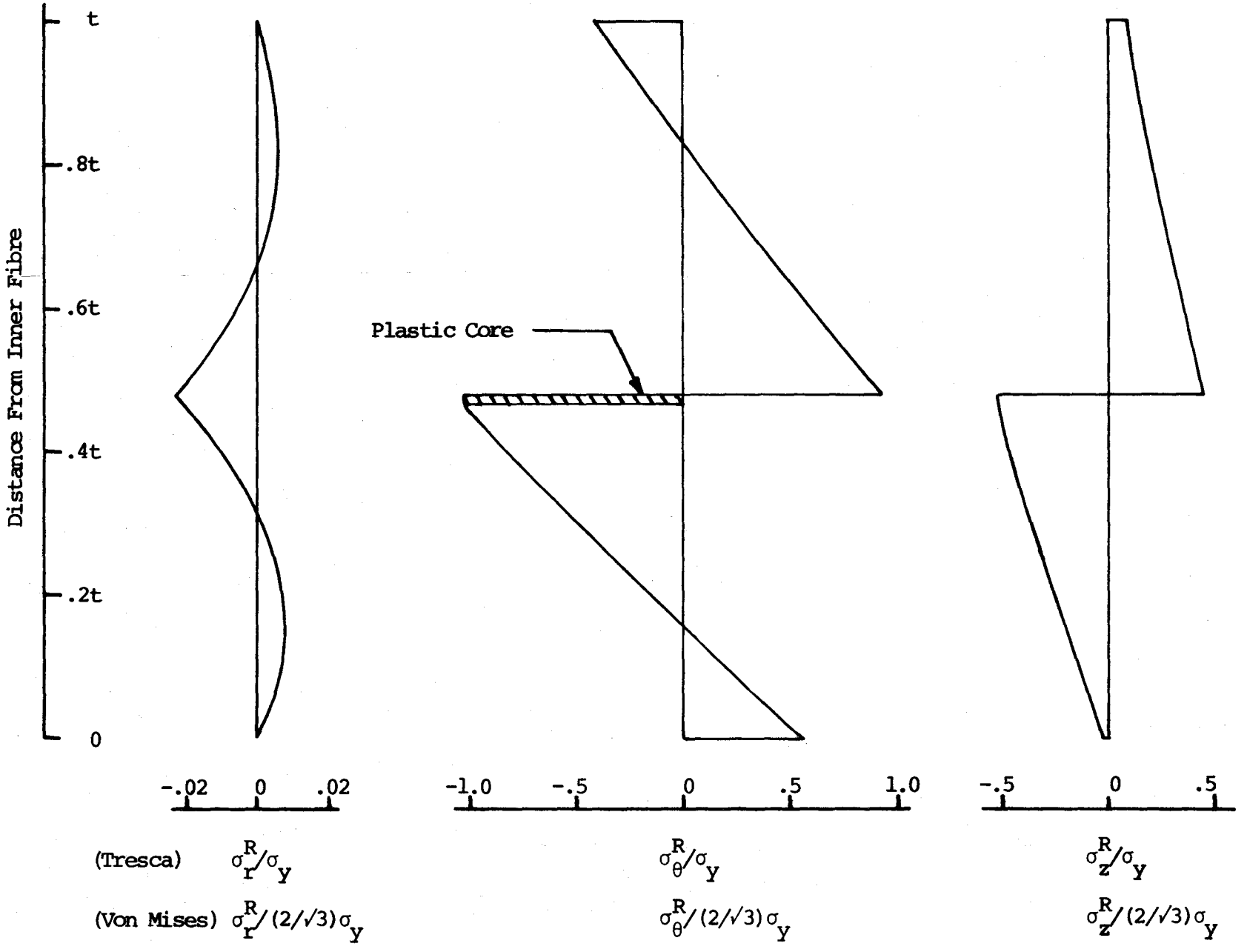

FIG. 5.5 EXACT RESIDUAL STRESS DISTRIBUTIONS FOR a/t=5.0,ν=.3

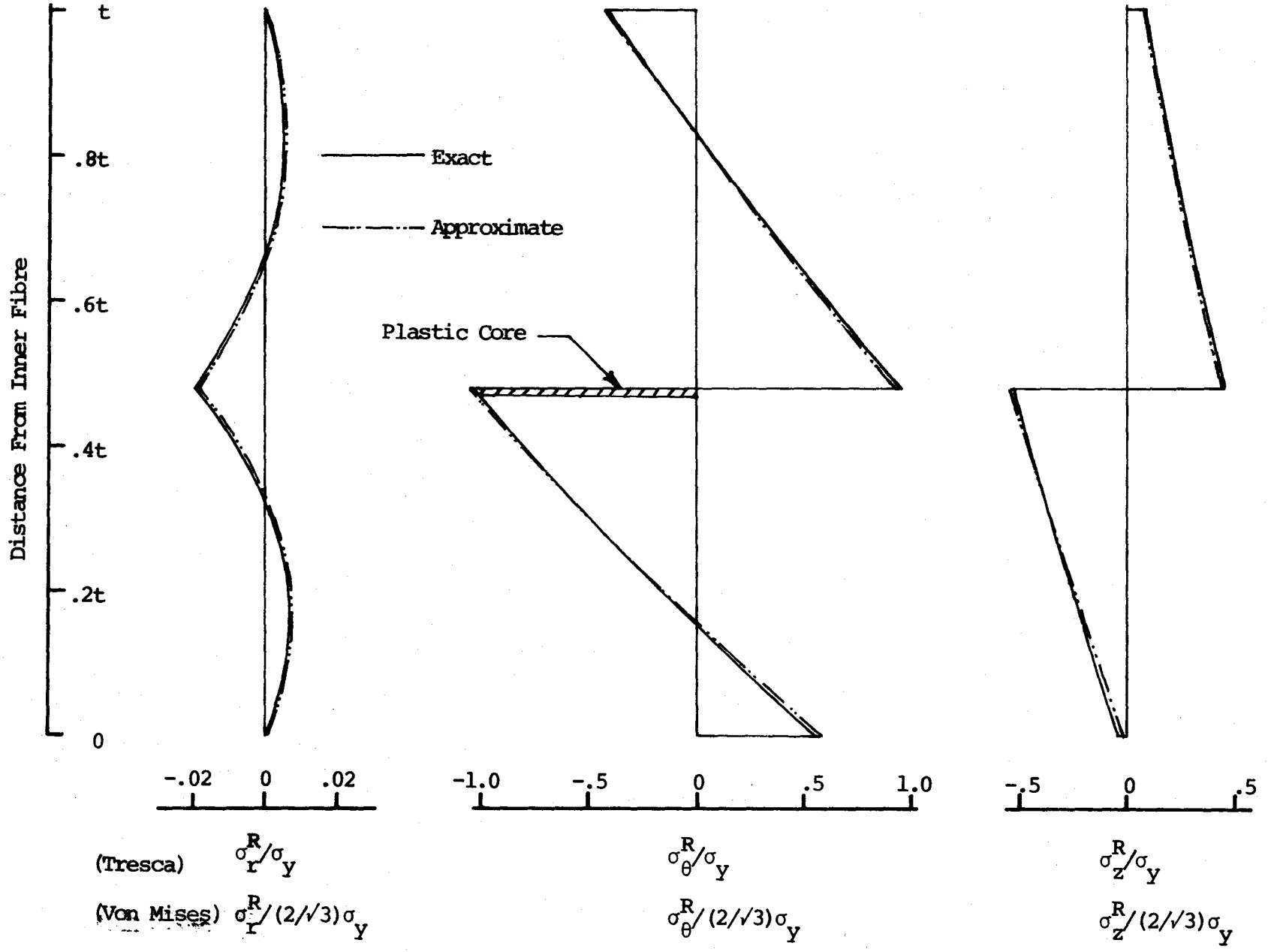

FIG. 5.6 RESIDUAL STRESS DISTRIBUTIONS FOR a/t=6.0,ν=.3

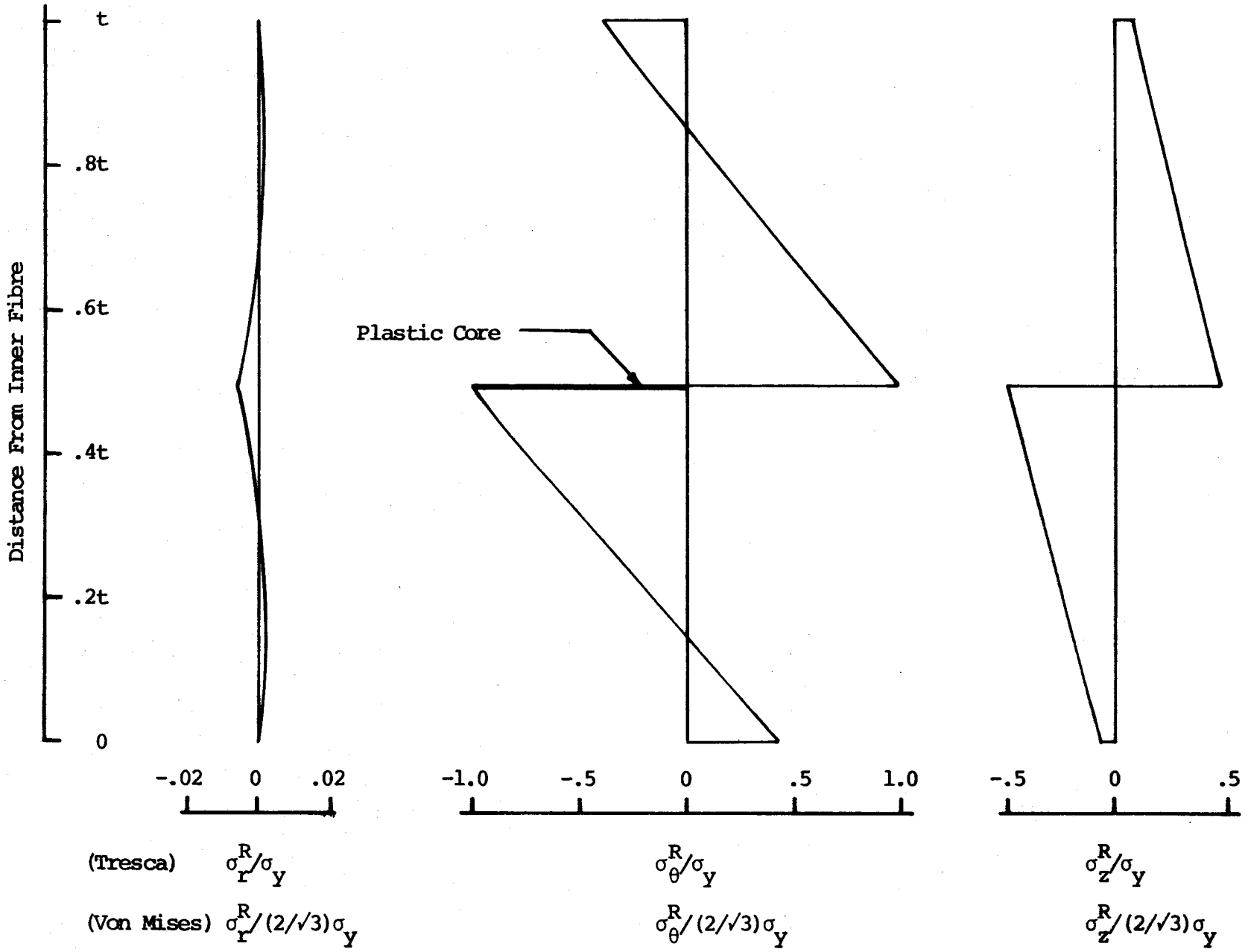

FIG. 5.7 EXACT RESIDUAL STRESS DISTRIBUTIONS FOR a/t=25.0, ν=.3

It may be observed that the discrepancy, in the stress distribution, between the curves based upon the approximate analysis and those upon the exact analysis as described in section 3.3 is considerable for a/t=1.5. For a/t=6 (a case of less severe bending) the two curves are almost identical. Tables 5.1 to 5.3 show the maximum percentage errors in the residual circumferential, radial and lateral stresses if they are calculated by the approximate analysis.

At the inner fibres, σ_θ^R (tensile) increases with decreasing a/t (i.e. as bending becomes more and more severe). At the outer fibres σ_θ^R (compressive) increases in magnitude as the a/t ratio is increased. However, a drop in σ_θ^R is observed at a/t=25 (moderate bending).

It is observed that the maximum positive and maximum negative values of σ_θ^R occur, just above the neutral axis and just below it. The maximum positive value decreases while maximum negative value increases as bending continues. It can be seen that the error in the maximum positive σ_θ^R, if it is calculated by approximate method increases from -.12% at a/t=25 to -3.14% at a/t=1.5. For maximum negative σ_θ^R, the error increases from -.80% at a/t=25 to -12.00% at a/t=1.5. For the case of moderate bending the error may be neglected so far as maximum values of σ_θ^R are concerned.

Table 5.1

Residual Circumferential Stress (σ_θ^R) at Critical Fibres (Exact Method, ν=0.3)

a/t	At Inner Fibre		Maximum Negative (Below N.A.)		Maximum Positive (Above N.A.)		At Outer Fibre	
	*σ_θ^R	*Diff†	*σ_θ^R	*Diff	*σ_θ^R	*Diff	*σ_θ^R	*Diff
1.5	+.74267	+.06170 (8.31%)	-1.06081	-.12733 (12.00%)	+.83681	-.02629 (3.14%)	-.33459	+.04766 (14.24%)
2.0	+.68316	+.05000 (7.32%)	-1.04933	-.09675 (9.22%)	+.87045	-.02091 (2.40%)	-.36218	+.03780 (10.43%)
3.0	+.61970	+.03922 (6.33%)	-1.03576	-.07149 (6.90%)	+.90728	-.01460 (1.61%)	-.39425	+.02420 (6.14%)
4.0	+.58409	+.03647 (6.24%)	-1.02819	-.05494 (5.34%)	+.92790	-.01106 (1.19%)	-.41048	+.01362 (3.32%)
5.0	+.56064	+.03649 (6.51%)	-1.02332	-.04128 (4.03%)	+.94062	-.00886 (.94%)	-.41963	+.00513 (1.22%)
6.0	+.54485	+.03648 (6.69%)	-1.01987	-.03566 (3.49%)	+.95053	-.00733 (.77%)	-.42616	+.00083 (.19%)
25.0	+.42876	+.09112 (21.25%)	-1.00577	-.00803 (.80%)	+.98726	-.00109 (.12%)	-.40082	-.07984 (19.92%)

*Coefficients of σ_y [Tresca] and that of $(2/\sqrt{3})\sigma_y$ [Von Mises]

†Diff = Stress by approximate method - stress by exact method

Table 5.2

Residual Radial Stress (σ_r^R) at Critical Fibres

(Exact Method, ν=0.3)

a/t	Maximum Negative (at Neutral axis)		Maximum Positive		Stress at Maximum Diff	
	*σ_r^R	*Diff†	*σ_r^R	*Diff	*σ_r^R	*Diff
1.5	-.06081	-.00111 (1.82%)	+.03289	+.00221 (6.72%)	+.00660	-.00311 (47.12%)
2.0	-.04933	-.00047 (.95%)	+.02386	+.00158 (6.62%)	+.00848	-.00179 (21.11%)
3.0	-.03576	+.00013 (.36%)	+.01517	+.00101 (6.66%)	+.01387	+.00102 (7.35%)
4.0	-.02819	+.00044 (1.56%)	+.01097	+.00081 (7.38%)	+.00790	+.00088 (11.14%)
5.0	-.02332	+.00062 (2.66%)	+.00852	+.0071 (8.33%)	+.00348	+.00083 (23.85%)
6.0	-.01987	+.00066 (3.32%)	+.00695	+.00063 (9.06%)	-.00016	+.00079 (493.75%)
25.0	-.00577	+.00090 (15.60%)	+.00123	+.00047 (38.21%)	-.00577	+.00090 (15.60%)

*Coefficients of σ_y [Tresca] and that of $(2/\sqrt{3})\sigma_y$ [Von Mises]

†Diff = Stress by approximate method - stress by exact method

Table 5.3

Residual Lateral Stress (σ_z^R) at Critical Fibres (Exact Method, ν=0.3)

a/t	At Inner Fibre		Maximum Negative (Below N.A.)		Maximum Positive (Above N.A.)		At Outer Fibre	
	*σ_z^R	*Diff†	*σ_z^R	*Diff	*σ_z^R	*Diff	*σ_z^R	*Diff
1.5	+.02280	+.01851 (81.18%)	-.56081	-.11627 (20.73%)	+.33059	-.00833 (2.51%)	+.09962	+.01430 (14.35%)
2.0	+.00495	+.01500 (303.03%)	-.54933	-.90910 (16.40%)	+.36516	-.00643 (1.76%)	+.09135	+.01134 (12.41%)
3.0	-.01409	+.01177 (83.53%)	-.53576	-.06463 (12.06%)	+.40389	-.00434 (1.07%)	+.08173	+.00726 (8.88%)
4.0	-.02477	+.01094 (44.16%)	-.52819	-.04970 (9.41%)	+.42526	-.00319 (.75%)	+.07686	+.00408 (5.31%)
5.0	-.03181	+.01095 (34.42%)	-.52332	-.03933 (7.51%)	+.43872	-.00247 (.56%)	+.07411	+.00154 (2.08%)
6.0	-.03655	+.01095 (29.96%)	-.51987	-.03338 (6.42%)	+.44833	-.00201 (.45%)	+.07215	-.00025 (.34%)
25.0	-.07137	+.02733 (38.29%)	-.50577	-.00768 (1.52%)	+.48660	-.00005 (.01%)	+.07975	-.02395 (30.03%)

*Coefficients of σ_y [Tresca] and that of $(2/\sqrt{3})\sigma_y$ [Von Mises]

†Diff = Stress by approximate method - stress by exact method

Table 5.4

Position of Neutral Axis and Thickness of Plastic Core

a/t†	a (Inch)	b (Inch)	Neutral Axis (Inch)		Inner Elastic–Plastic Boundary (inch)			Thickness of Plastic Core			x (Inch)	$\varepsilon_{\theta_i}^s/\varepsilon_y$
			Distance From Inner Fibre	r_n	Distance From Inner Fibre	ρ	ρ††	Inch	%age of total thickness	†† Inch		
1.5	0.375	0.625	0.1091	0.4841	0.1009	0.4759	0.4738	.0082	3.28%	.0103	.1098	1.58
2.0	0.50	0.75	0.1124	0.6124	0.1058	0.6058	0.6041	.0066	2.64%	.0083	.1129	1.53
3.0	.075	1.00	0.1160	0.8660	0.1113	0.8613	0.8601	.0047	1.88%	.0059	.1164	1.47
4.0	1.00	1.25	0.1180	1.1180	0.1143	1.1143	1.1134	.0037	1.48%	.0046	.1183	1.44
5.0	1.25	1.50	0.1193	1.3693	0.1163	1.3663	1.3655	.0030	1.20%	.0038	.1195	1.42
6.0	1.50	1.75	0.1202	1.6202	0.1176	1.6176	1.6170	.0026	1.04%	.0032	.1203	1.40
*25.0	6.25	6.50	0.1238	6.3738	0.1231	6.3731	6.3729	.0007	0.28%	.0009	.1238	1.30

* Moderate bending

†† Using equation [3.14.3]

† t = 1/4"

Table 5.3 shows the residual stresses in the lateral direction σ_z^R at critical fibres. The residual stresses which are of primary importance when considering their effect on the external load carrying capacity of hollow structural sections for example, are those occurring in this direction (lateral). It is seen that the maximum negative σ_z^R increases and maximum positive σ_z^R decreases as the bending ratio (a/t) decreases. The difference between the two methods for the maximum positive σ_z^R varies from -.01% to -2.51% and for the maximum negative σ_z^R from -1.52% to 20.73%.

At the elastic-plastic boundary $r=\rho$, σ_z^R becomes discontinuous, due to the fact that in the elastic zone

$$\sigma_z^R = 0.5(\sigma_\theta + \sigma_r) + \nu(\sigma_\theta^s + \sigma_r^s)$$

when $\nu=0.3$ for example

whereas, in the plastic zone

$$\sigma_z^R = 0.5(\sigma_\theta + \sigma_r) + 0.5(\sigma_\theta^s + \sigma_r^s)$$

$$= 0.5(\sigma_\theta^R + \sigma_r^R).$$

Therefore, an average value of σ_z^R was calculated near the elastic-plastic boundary, so that the distribution is continuous at $r=\rho$. It is seen that σ_z^R comes out to be continuous if ν is assumed as 0.5. The distribution of stress for $\nu=0.5$ is shown in Fig. 5.1.

Fig. 5.7 shows the residual stresses for a/t=25 and it is seen that σ_r^R is negligibly small for this case. This leads to the conclusion that radial stress may be neglected for moderate bending.

Table 5.4 shows that the position of the neutral axis shifts towards the concave (inner) surface as bending continues and so does the elastic-plastic boundary $r=\rho$. The thickness of the plastic core increases as the bending ratio (a/t) decreases. The position of the neutral surface (upper elastic-plastic boundary) $r=r_n$ is independent of the adjustments in stresses due to plastic core. Lower elastic-plastic boundary $r=\rho$ shifts towards the neutral plane (thus decreasing the thickness of the plastic core) due to the adjustments in stress components. It can, however, be seen that even for a/t=1.5 the value of ρ given by equation [3.14.3] does not differ appreciably from that obtained by exact analysis (using equation [3.28]). Furthermore, it is observed that $\varepsilon_{\theta_i}^s$ for a/t=1.5 after spring back changes only by 1.58 ε_y.

5.2 Geometric Representation of Stress Path and Residual Stress Distribution.

The analysis outlined in this section shows a method of geometric representation of stresses on the plane of deviatoric states of stress. A comparison is made between the residual stress distribution for severe bending (a/t=1.5) and that for moderate bending (a/t=25). The stresses are also plotted for a

case where the value of Poisson's ratio ν is assumed to be 0.5 to be compared with the distribution for ν=0.3. In both the above cases the value of a/t is 1.5.

Hill[6], Mendelson[11] and Alexander[38] have described a method of vectorial representation of stress in a rectangular cartesian co-ordinate system. If the principal stresses are plotted in the direction of the axes, the projection of a vector, representing the state of stress at a point in the sheet (or any other body), on the line of hydrostatic states of stress(a line inclined at equal angles with the axes) represents the vectorial sum of the mean or hydrostatic components $(\bar{\sigma},\bar{\sigma},\bar{\sigma})$, where $\bar{\sigma} = (\sigma_\theta + \sigma_r + \sigma_z)/3$. The component perpendicular to the line of hydrostatic states of stress represents the vectorial sum of the deviatoric components $(\sigma'_\theta, \sigma'_r, \sigma'_z)$, where $\sigma' = \sigma_\theta - \bar{\sigma}$, $\sigma'_r = \sigma_r - \bar{\sigma}$, $\sigma'_z = \sigma_z - \bar{\sigma}$. This vector may be regarded as the projection of the total stress vector (vector representing the state of stress at the point under consideration) on a plane passing through the origin and normal to the line of hydrostatic states of stress. This plane represented by $\sigma_\theta + \sigma_r + \sigma_z = 0$ is called the plane of deviatoric states of stress (π plane). The hydrostatic component of the stress is assumed not to influence plastic flow.

Looking in the direction of the line of hydrostatic states of stress, the axes seem to project on the plane of deviatoric states of stress at equal angles of 120° and any

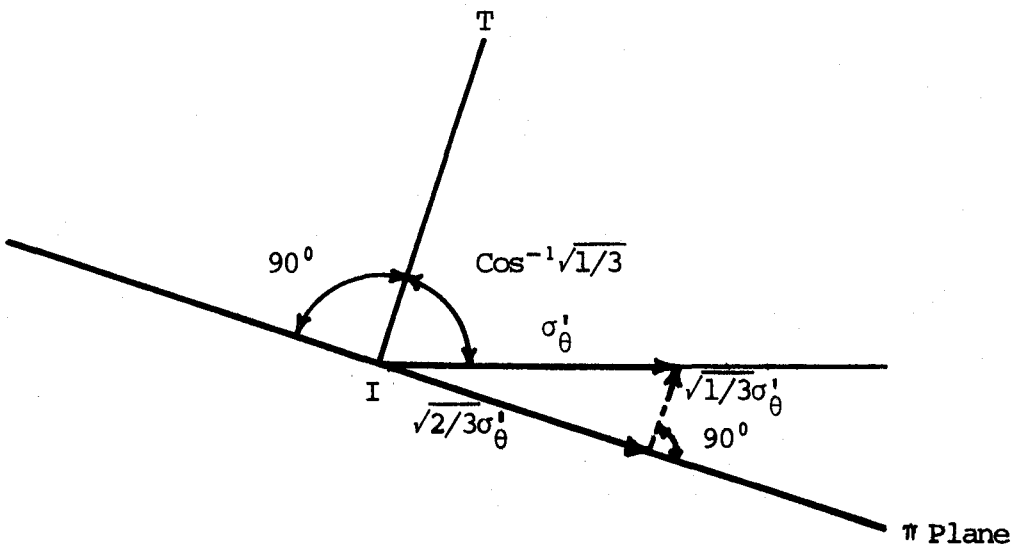

FIG. 5.8(a) PROJECTION OF σ'_θ ON π PLANE

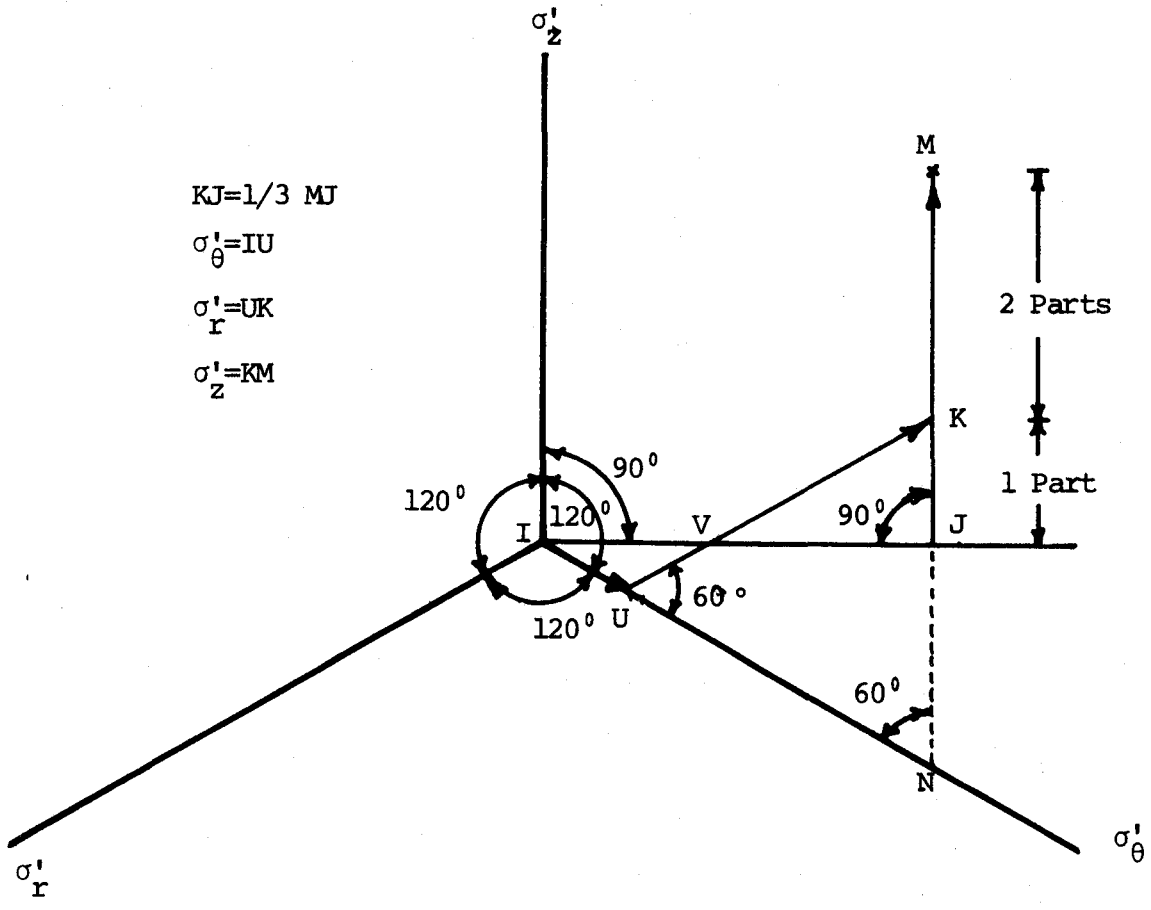

FIG. 5.8(b) REPRESENTATION OF STRESS COMPONENTS ON π PLANE

vector σ_θ' projects on to this plane with a length of $\sqrt{2/3}\sigma_\theta'$. Fig. 5.8(a) shows the plane containing σ_θ'; IT - normal to the π plane and the projection of σ_θ' on the πplane. It is obvious from the figure that the projection of σ_θ' on the π plane is $\sqrt{2/3}\ \sigma_\theta'$. Fig. 5.8(b) shows the π plane as the plane of the paper and the projections upon this plane of the coordinate axes σ_θ', σ_r', σ_z'. Because of the fact that the sum of the deviatoric stress components $(\sigma_\theta' + \sigma_r' + \sigma_z')$ of any point M, for instance, is zero a simple construction such as shown in Fig. 5.8(b) makes it possible to determine the deviatoric stress components uniquely.In this figure MJ is parallel to $I\sigma_z'$ and IJ is perpendicular to it; KJ = $\frac{1}{3}$MJ and KU is parallel to $I\sigma_r'$. Under these conditions IU=UV, VK=KM and σ_θ', σ_r', σ_z' are represented by IU, UK and KM respectively. It can be seen that σ_r' = UV + VK is negative and $\sigma_\theta' + \sigma_z'$ = IU + KM is positive. Thus σ_r' is numerically equal to $\sigma_\theta' + \sigma_z'$ and the algebraic sum $\sigma_\theta' + \sigma_r' + \sigma_z' = 0$.

If one of the stress components, say σ_r, is zero, then $\bar{\sigma} = -\sigma_r'$ is represented by the length UK which is equal to UN and NK. Therefore, lengths IN and MN represent $\sigma_\theta (=\sigma_\theta'+\bar{\sigma})$ and $\sigma_z (=\sigma_z'+\bar{\sigma})$ respectively. This is, therefore, possible to determine the actual magnitudes of two stress components, if the third component is zero. This fact has been used in plotting the elastic loading (σ_r is assumed to be zero) paths of top and bottom fibres of the sheet.

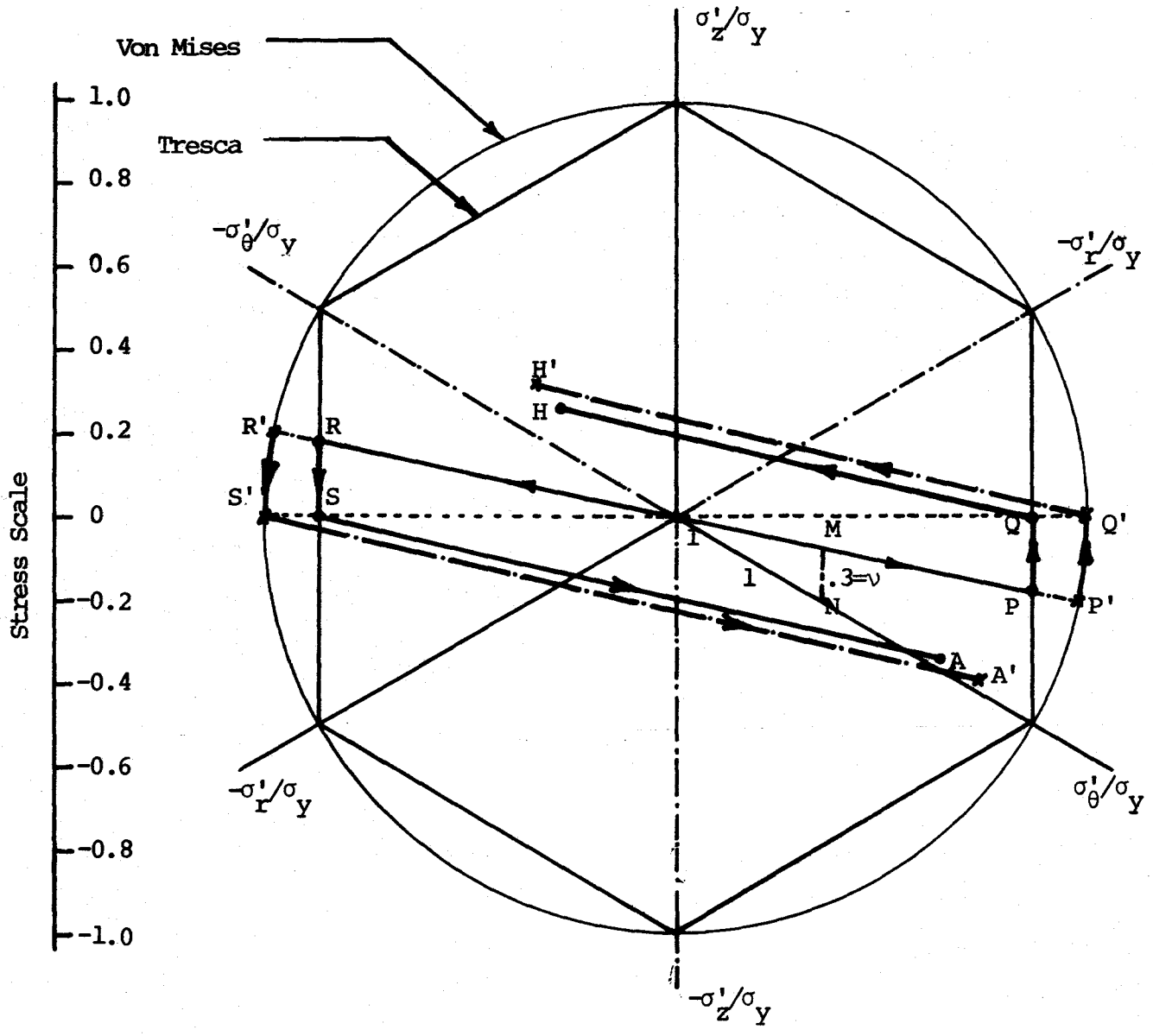

Stress Paths

IPQ- Bending T.F. (Tresca)

QH - Spring Back T.F. (Tresca)

IP'Q'- Bending T.F. (Mises)

Q'H' - Spring Back T.F. (Mises)

T.F. = Top Fibre

FIG. 5.9 STRESS PATHS OF EXTREME FIBRES DURING BENDING AND SPRING BACK (a/t=1.5,ν=.3)

Fig. 5.9 shows the stress paths of extreme fibres during bending and spring back for a/t=1.5 and ν=0.3. For convenience the actual values of the deviatoric stress components have been plotted which is the same as saying that the actual diagram has been enlarged by a scale factor of $\sqrt{3/2}$. Under these conditions the Von Mises yield criterion which is regarded as a circular cylinder of radius $\sqrt{2/3}\sigma_y$ and its axis coinciding with the line of hydrostatic states of stress, appears as a circle of radius σ_y on the π plane. The yield locus for the Tresca maximum shear criterion is a regular hexagon inscribed in the Von Mises circle.

In Fig. 5.9 point I represents the state of zero stress at the fibres of the sheet before bending starts. As bending progresses and whilst the material is still elastic the points representing the state of stress will lie within the hexagon (Tresca) or circle (Von Mises). Under elastic conditions the radial stress component σ_r may be neglected. Therefore, for plane strain bending (ε_z=0), the relation

$$\varepsilon_z = \frac{\sigma_z}{E} - \frac{\nu}{E}(\sigma_\theta+\sigma_r) \quad \text{gives}$$

$$\sigma_z = \nu\sigma_\theta$$

IP and IR represent the elastic loading paths for top and bottom fibres during bending operation. Due to the reasons mentioned earlier a point M, for instance, on IP or IR is such that MN = $\nu\times$IN. Primed points represent the corresponding positions for the Von Mises yield criterion. Points Q and S

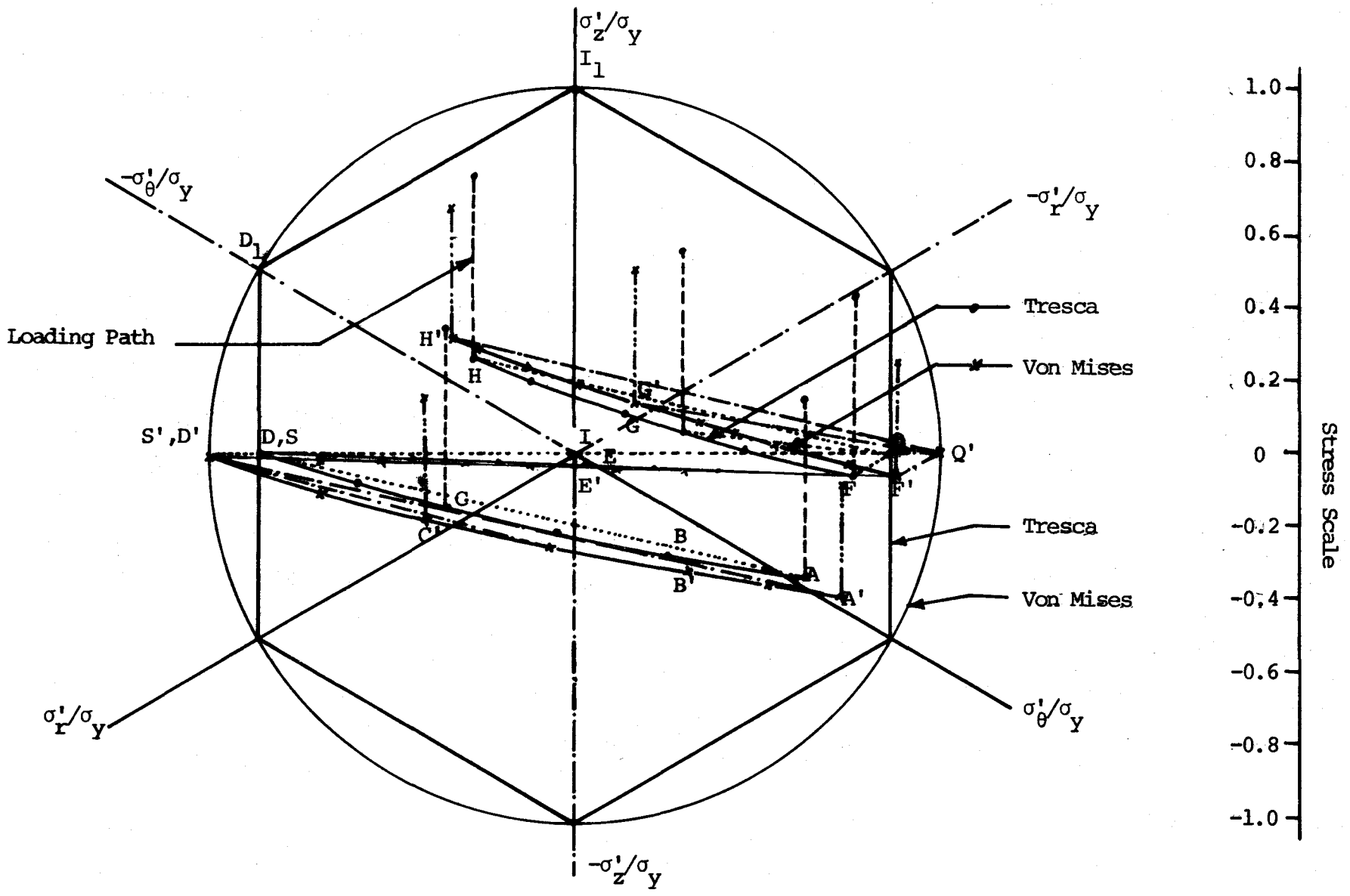

FIG. 5.10 GEOMETRIC REPRESENTATION OF RESIDUAL STRESS DISTRIBUTION ON THE PLANE OF DEVIATORIC STATES OF STRESS AND SUBSEQUENT STRETCHING FOR a/t=1.5,ν=.3

represent the fully plastic states of stress for top and bottom fibres respectively. During spring back top fibre follows the path represented by QH and bottom fibre follows the one represented by SA. Bottom fibre produces paths which would be a mirror image of the paths produced by top fibre if neutral plane were at mid plane.

Fig. 5.10 shows the state of stress at any point of the sheet, during spring back for a/t=1.5. ABCDEFGH represents the residual stress distribution across the thickness of the sheet, ABCD being that portion below neutral surface and FGH for the fibres above it. Point D represents the fully plastic state of stress for the fibres laying in the plastic core ($r=\rho$to r_n). During spring back or unloading the stress paths for various fibres, say represented by points A, B, C and D, follow the lines joining S to these points. Similarily for the fibres laying above the neutral surface the unloading stress state paths are those represented by the lines joining Q to the points such as F, G and H. S and Q represent the fully plastic states of stress after bending operation is complete (before spring back starts), for fibres below the neutral surface and those above the neutral surface respectively. For fibres in the plastic core the stress path follows the yield surface.

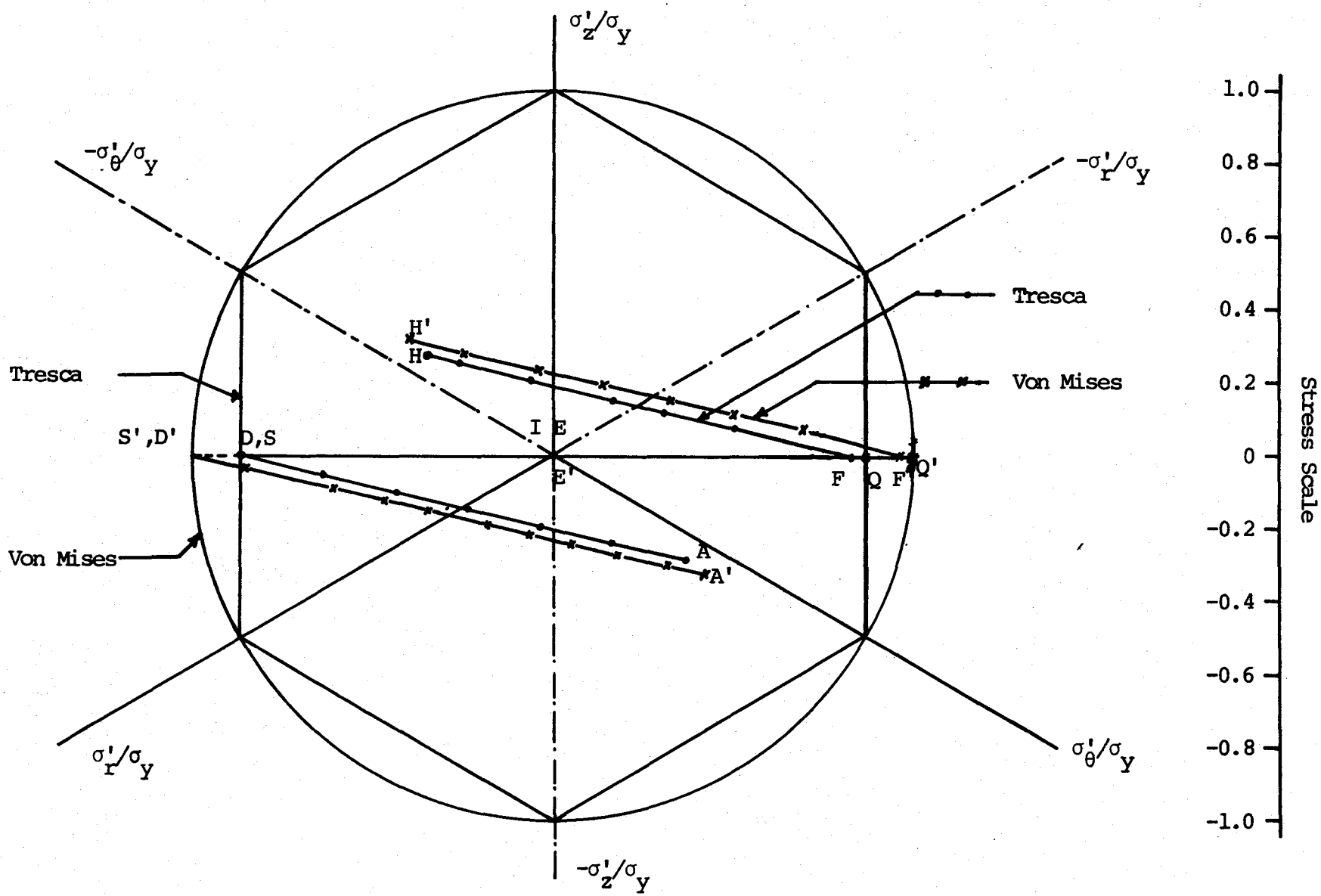

FIG. 5.11 GEOMETRIC REPRESENTATION OF RESIDUAL STRESS DISTRIBUTION ON THE PLANE OF DEVIATORIC STATES OF STRESS FOR a/t=25.0,ν=.3

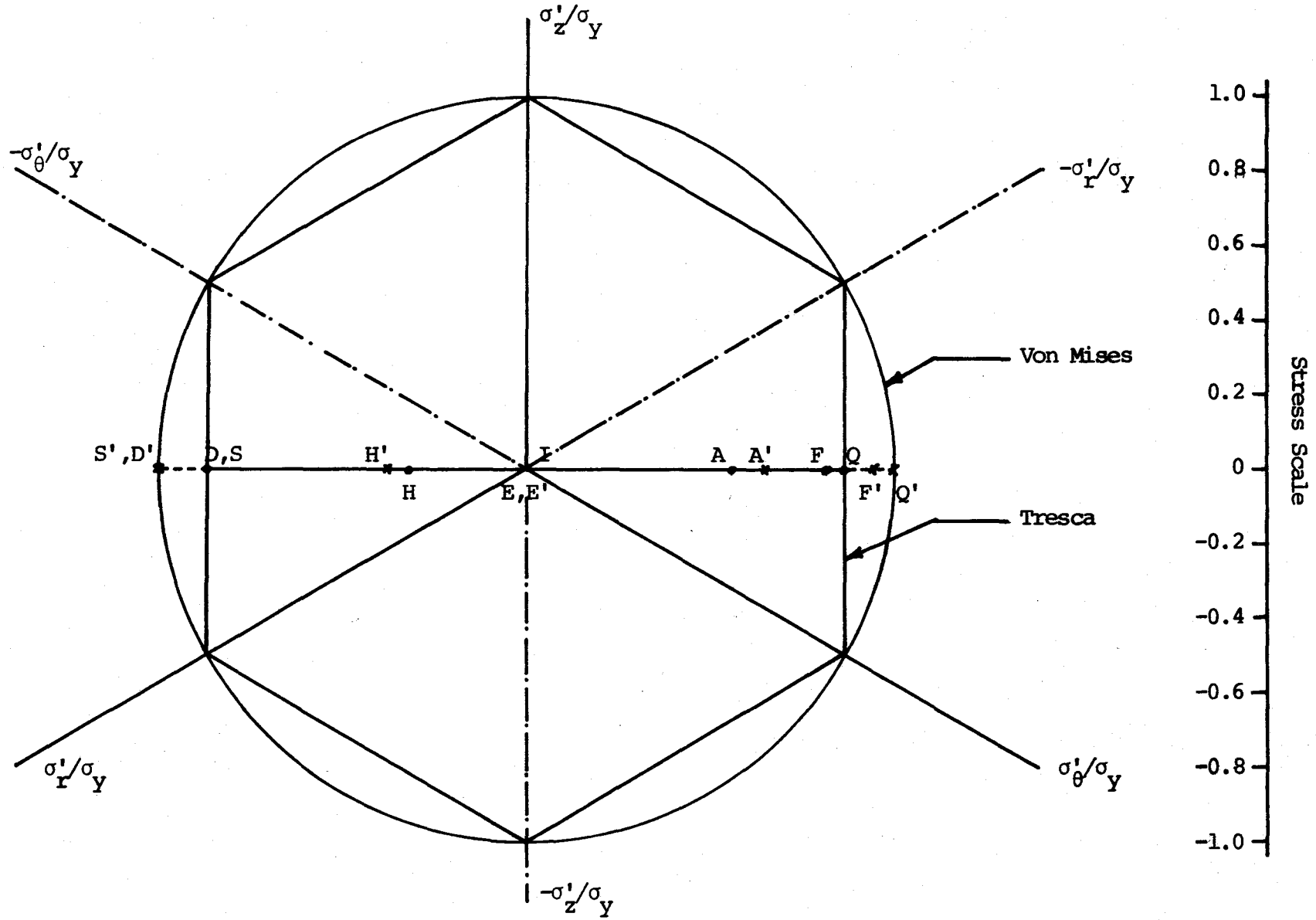

FIG. 5.12 GEOMETRIC REPRESENTATION OF RESIDUAL STRESS DISTRIBUTION ON THE PLANE OF DEVIATORIC STATES OF STRESS FOR a/t=1.5,ν=.5

To compare the stress paths and residual stress distributions for the case of severe bending (a/t=1.5) with those of moderate bending (a/t=25), the residual stress distribution for the later case has been plotted in Fig. 5.11. In this case the distribution curve FH is almost a straight line. It is to be noted that in this case radial stresses are very small as compared to those for any other case of severe bending. If radial stresses were neglected altogether, the shape of the residual stress distribution as obtained by Alexander[38] appears to be convex. It may therefore be concluded that the concave shape of curve FGH in Fig. 5.10 is due to the radial stresses of considerable magnitude.

For ν=0.5, $\sigma_z^R = 0.5\ (\sigma_\theta^R + \sigma_r^R)$

which gives $\sigma_\theta' = -\sigma_r'$ and $\sigma_z' = 0$. Therefore the residual stress distribution is a straight line bisecting the angle between the axes σ_θ'/σ_y and $-\sigma_r'/\sigma_y$ and between $-\sigma_\theta'/\sigma_y$ and σ_r'/σ_y. The residual stress distribution is as indicated by AD for the fibres below the neutral surface and by FH for the fibres above it as shown in Fig. 5.12.

5.3 Effect of Longitudinal Stretching on the Behaviour of Cold-Formed Sections

The residual stress distribution such as is illustrated by Fig. 5.10 may be usefully employed to study the behaviour of cold-formed sections loaded axially in tension. When the

cross section of a member, containing this type of residual stress distribution is loaded axially (in the lateral direction, z) in tension, each fibre remains elastic till it reaches the Tresca's hexagon (or Von Mises' circle). Pure tension in the z-direction produces no change in the stresses in θ and r directions in the elastic range. Therefore, an increment of $+\Delta\sigma_z$ in σ_z causes a change of $+\frac{1}{3}\Delta\sigma_z$ in the mean value $\bar{\sigma}$ which in turn produces a change of $-\frac{1}{3}\Delta\sigma_z$ in the values of σ'_θ and σ'_r plus a change of $+\frac{2}{3}\Delta\sigma_z$ in the value of σ'_z. It can now be shown graphically that to satisfy these increments the points A, B, C etc. should follow vertical paths (in the direction of σ'_z/σ_y axis) in the elastic range, as shown by vertical dotted lines, Fig. 5.10.

If it is assumed that all fibres are equally strained at the same rate during the loading of the member, the vertical ordinates will be of equal lengths and the basic form or shape of the residual stress distribution curve will not change until some fibre yields (i.e. until some point reaches the hexagon or circle).

In the case of Tresca the least ordinate is DD_1 and all the stress paths move in vertical straight lines till D reaches D_1. Point D_1 indicates the limit of proportionality of the cold bend member. If the member is stretched further, point D will move along D_1I_1 the side of the hexagon and other points will be deviated from vertical paths. In the case of

Von Mises' yield criterion point D' is already on the circle and stretching of the member will cause D' to move along the circle (not along vertical lines) and as such other points will also not move along vertical lines in order that force and moment equilibrium in the circumferential direction be satisfied. Therefore, theoretically the proportional limit for the Von Mises case is at zero stress level.

CHAPTER VI

CONCLUSIONS AND RECOMMENDATIONS FOR FURTHER RESEARCH

The object of this investigation was to find a method of computing the residual stress components in a wide sheet of elastic - perfectly plastic metal after spring-back. The spring-back occurs after a cold-forming process and it generates a rather complex stress and strain residuals in the cold-formed section. The analysis given herein takes into account the zone of plastic flow near the neutral surface. An approximate analysis which is much more simplified neglects the zone of plastic flow (i.e. assumes that the spring-back is completely elastic) and is also presented to provide a comparison between the two methods.

It is observed that the approximate analysis gives results which are comparable with those given by exact analysis for the cases of moderate and less severe bending. The differences in maximum positive and maximum negative values of circumferential stresses σ_θ^R computed by the two analyses are .12% and .80% respectively for a/t=25. The same values for a/t=1.5 are 3.14% and 12.00%. The equivalent values for σ_z^R are .01% and 1.52% for a/t=25 and 2.51% and 20.73% for a/t=1.5.

Therefore it is suggested that the approximate analysis can only be used for bending slightly more severe than moderate bending and the difference in stress components is

quite appreciable for severe bends of a/t 3.0 and less. Radial stress components can be neglected for moderate bending cases.

It is found that spring-back is not completely elastic and plastification occurs in a small zone of thickness just below the neutral surface. The thickness of this plastic zone decreases as the a/t ratio increases. The thickness of the plastic core is only 0.24% of the total sheet thickness for a/t=25. The thickness of this core increases to 3.28% for a/t=1.5.

Further it is found that all the stress components for Von Mises yield criterion are $(2/\sqrt{3})$ times the components for Tresca yield criterion. As such it is concluded that the yield criterion does not have any effect whatsoever on the present analysis and the stresses simply differ by a constant factor $(2/\sqrt{3})$. It should be noted however that the Prandtl-Reuss equations relating increments of stress and strain with stresses are based on the normality requirement of Von Mises material but were nevertheless used with Tresca as well.

The condition of plane strain in the wide sheet bending is confirmed by a simple bending test. Furthermore it is deduced that the dimensions of the sheet do not change appreciably during spring-back.

The difference in the stress paths for the current analysis (severe bending) and the analysis for moderate bending (neglecting radial stresses) is observed to have the

same basic form but a direct comparison is not possible since a significant elastic core was employed in Alexander's work[38]. The study of the effect of lateral stretching on the behaviour of cold-formed sections shows that severe bending lowers the proportional limit considerably below that computed for moderate bending. In fact it becomes zero for Von Mises criterion.

Recommendations for Further Research

1. It might be worthwhile to reinvestigate the problem as stated herein and to modify the analysis by taking into account the influence of work hardening on spring-back.

2. Theoretically it is found that the proportional limit is at a zero stress level for Von Mises yield criterion, i.e. no apparent elastic behaviour even initially. It is expected that conventional experiments will not confirm this analytical prediction as the zone of plastic flow is very small. Some very sophisticated experiments with a high level of stress and strain control would need to be conducted to show a proportional limit that tends toward a zero stress state since most of the sheet is still elastic.

3. It is recommended that an analysis be performed on the stretching characteristics of a severely bent sheet to simulate behaviour of the corners of square and rectangular hollow structural sections acting as beams or columns as well as for decking material such as is used in roofing.

APPENDIX A

COMPUTER PROGRAMS FOR CALCULATING BENDING, SPRING-BACK RESIDUAL AND DEVIATORIC STRESS COMPONENTS

Two programs were developed, one for approximate method and the other for exact method outlined in Chapter III.

A.1 Designations

The meaning of the variables used in the Fortran Programs are as given below. The different constants, variables and stress components were calculated in the order they are written and by using the equations indicated in [ ]. The details of operation and how the stress components were calculated are shown in the programs by comment cards and by flow charts drawn in Appendices A.2 and A.3.

BRATIO = a/t

T = t

PR = ν

A = a

RN = r_n [2.11]

M = m

D = d

VM = $2/\sqrt{3}$, a factor which when multiplied by stresses by Tresca Criterion gives stresses by Von Mises Criterion

$$BETA = \beta \qquad [3.21.2]$$

$$B = c \qquad [3.37]$$

$$X = x \qquad [3.21.4]$$

$$R = r \qquad \sigma^{s}_{r_j}$$

$$SR(J) = \left(\frac{}{\gamma}\right) \quad \text{where } J=j+1 \qquad [3.36]$$

$$S(J) = \left(\frac{\sigma^{s}_{\theta_j}}{\gamma}\right) \qquad [3.38]$$

$$STRRN = \left(\frac{\sigma^{s}_{r_{r_n}}}{\gamma}\right) \qquad \text{by } [3.36]$$

$$F = -\left(\frac{\sigma^{s}_{r_{r_n}}}{\gamma}\right) = \frac{1}{\beta}\left(\frac{c-\rho}{\rho}\right) \qquad [3.29]$$

$$RO = \rho \qquad [3.28]$$

$$F1 = F_1/\gamma \qquad [3.31]$$

$$F2 = F_2/\gamma \qquad [3.32]$$

$$AM1 = M_1/\gamma \qquad [3.33]$$

$$AM2 = M_2/\gamma \qquad [3.34]$$

$$AZ = \gamma/\sigma_y \qquad [3.39]$$

$$ALK = \ln(ak) \qquad [3.40]$$

$$STR = \varepsilon^{s}_{\theta_i}/\varepsilon_y \qquad [3.42]$$

$$F3 = -F_3/\sigma_y \qquad [3.32.1]$$

$$AM3 = -M_3/\sigma_y \qquad [3.34.1]$$

$$SUMF = \Sigma F/\sigma_y \qquad [3.30]$$

$$SUMM = \Sigma M/\sigma_y \qquad [3.35]$$

SSR(J),SIGR2,STR = σ_r^s/σ_y

SST(J),SIGT2,STT = σ_θ^s/σ_y

SSZ(J),SIGZ2,STZ = σ_z^s/σ_y

BSR,SIGR1 = σ_r/σ_y

BST,SIGT1 = σ_θ/σ_y

BSZ,SIGZ1 = σ_z/σ_y

RESR = σ_r^R/σ_y

REST = σ_θ^R/σ_y

RESZ = σ_z^R/σ_y

SIGMN = $\bar{\sigma}/\sigma_y$

DEVR = σ_r'/σ_y

DEVT = σ_θ'/σ_y

DEVZ = σ_z'/σ_y

MOM = M_p [2.18.2]

C = b

N = N [3.10]

Other are work variables only

A.2 Flow Chart for Approximate Analysis' Program

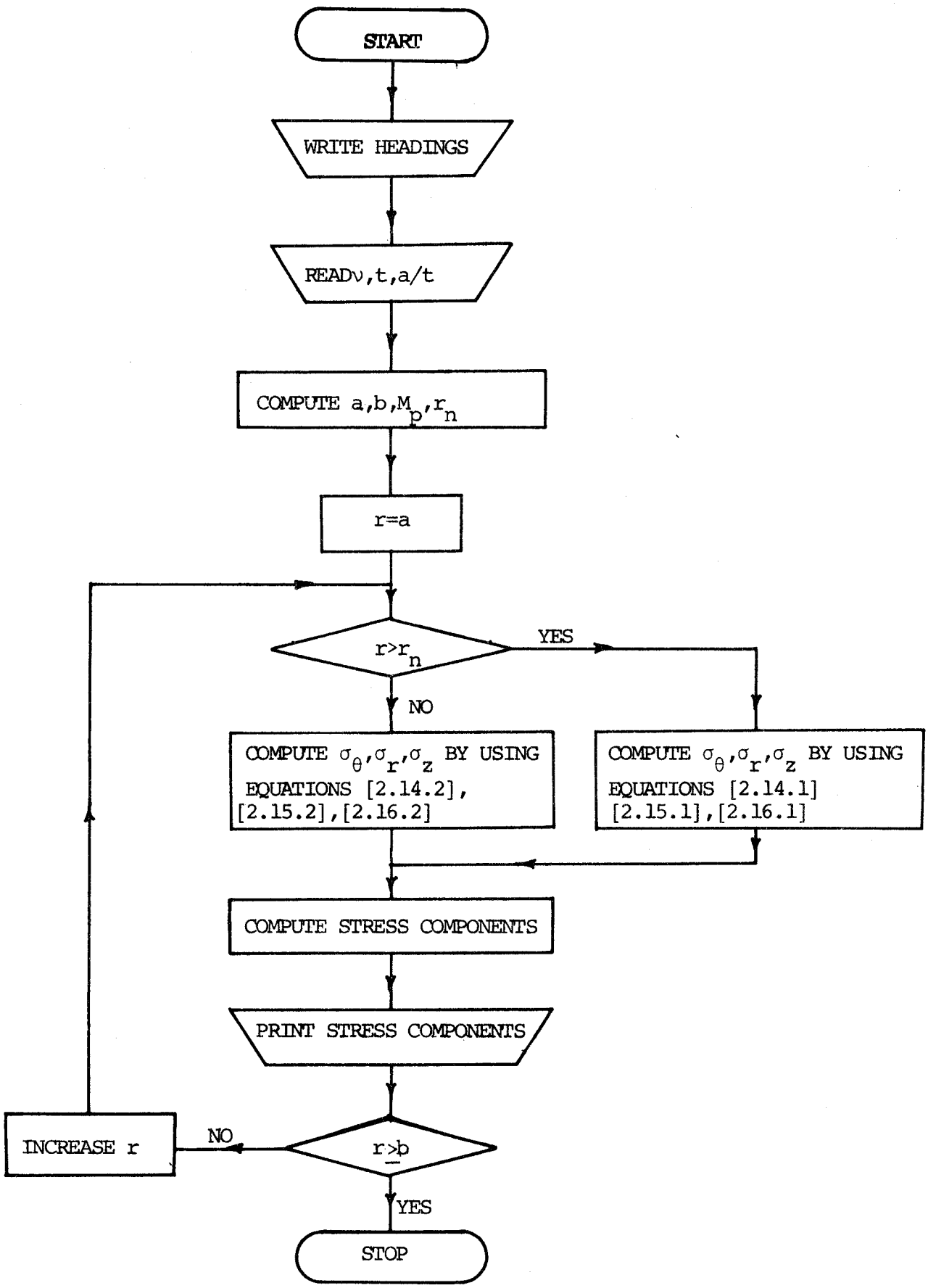

A.3 Flow Chart for Exact Analysis' Program

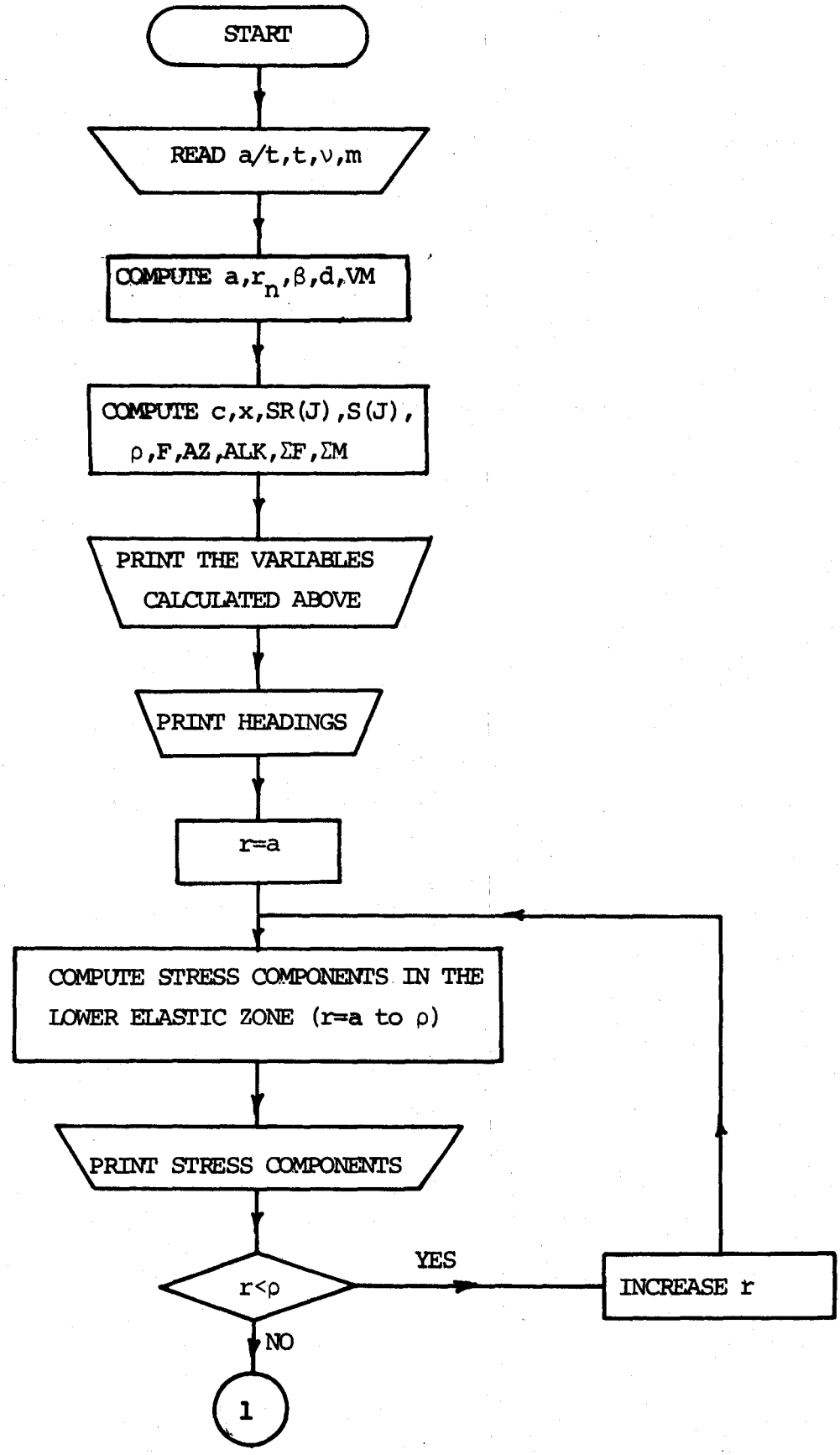

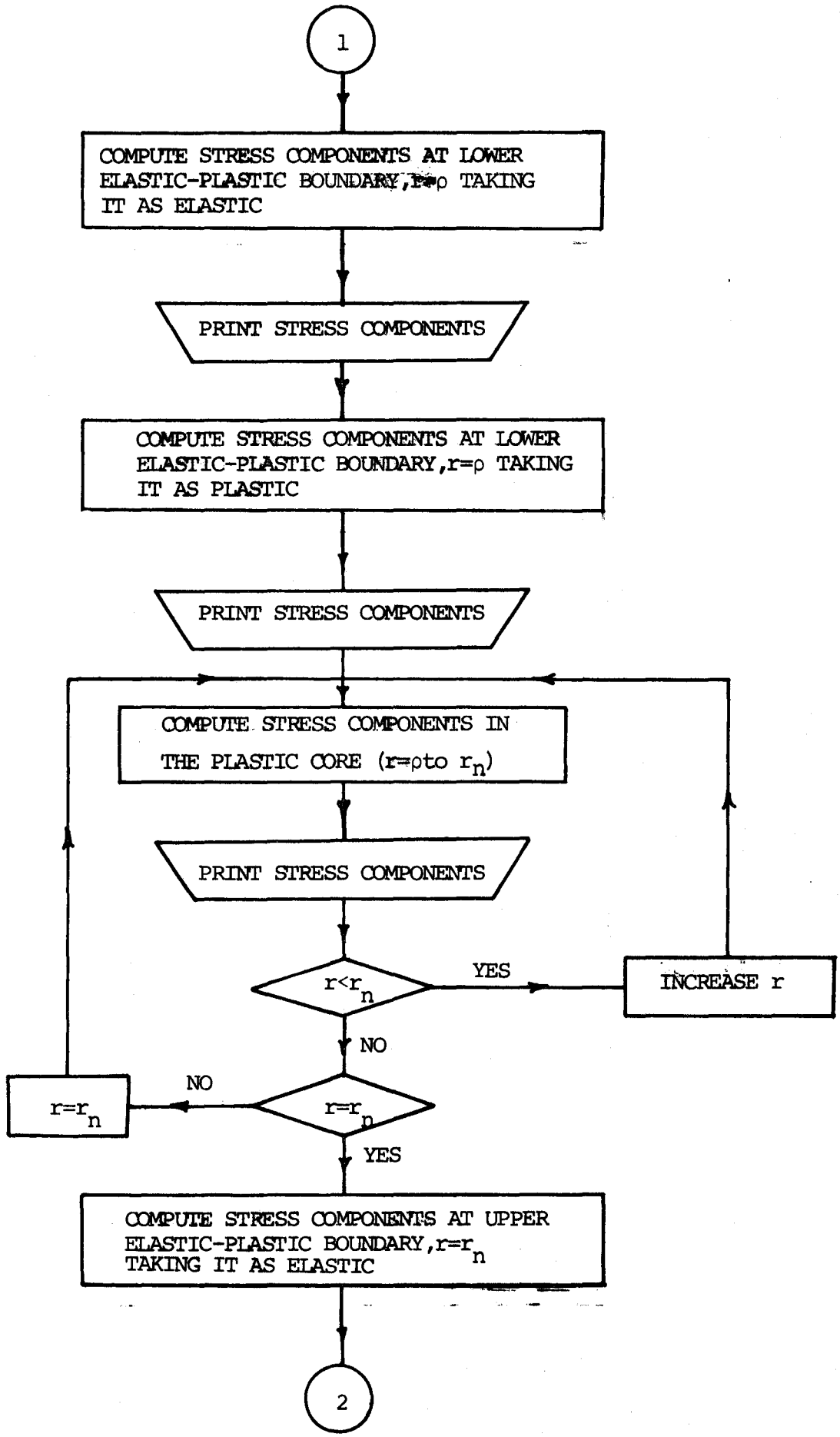
1
COMPUTE STRESS COMPONENTS AT LOWER ELASTIC-PLASTIC BOUNDARY, r=ρ TAKING IT AS ELASTIC
PRINT STRESS COMPONENTS
COMPUTE STRESS COMPONENTS AT LOWER ELASTIC-PLASTIC BOUNDARY, r=ρ TAKING IT AS PLASTIC
PRINT STRESS COMPONENTS
COMPUTE STRESS COMPONENTS IN THE PLASTIC CORE (r=ρ to r_n)
PRINT STRESS COMPONENTS
$r<r_n$
YES
INCREASE r
NO
$r=r_n$
NO
$r=r_n$
YES
COMPUTE STRESS COMPONENTS AT UPPER ELASTIC-PLASTIC BOUNDARY, $r=r_n$ TAKING IT AS ELASTIC
2

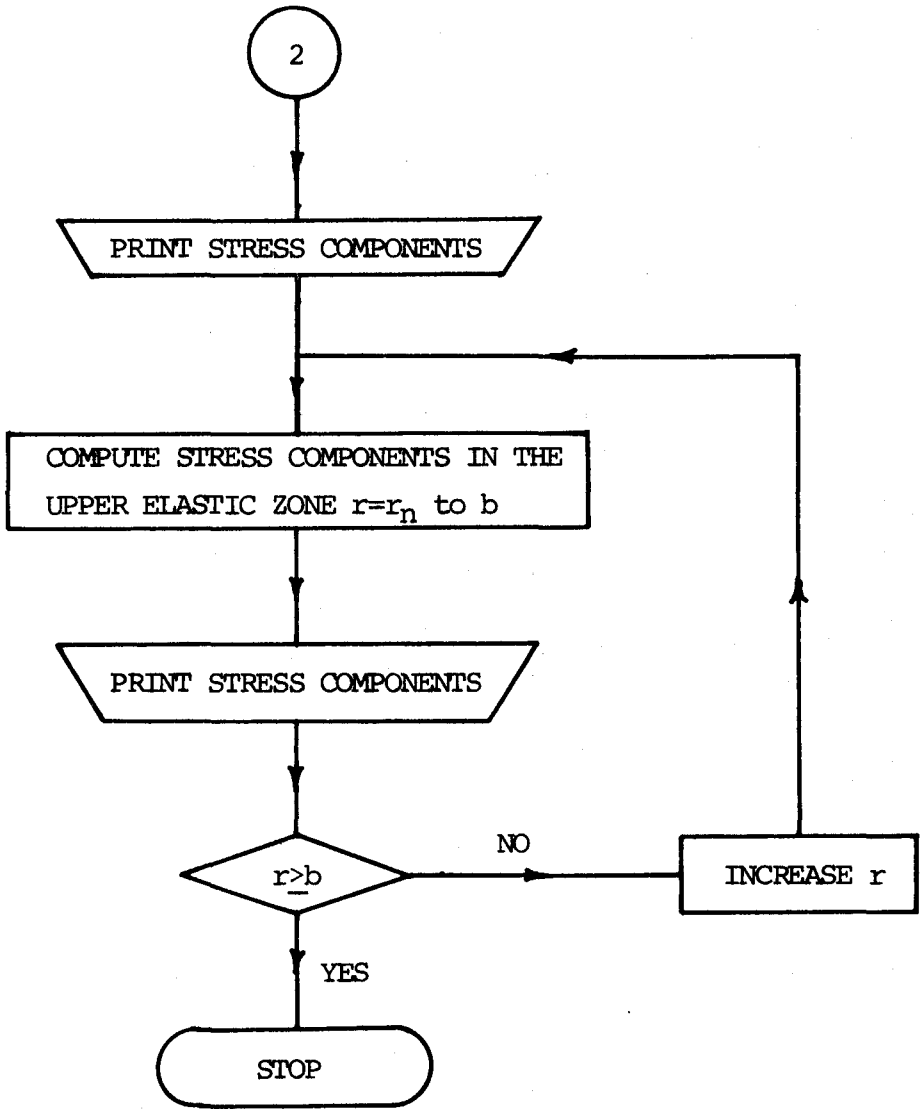
2
PRINT STRESS COMPONENTS
COMPUTE STRESS COMPONENTS IN THE UPPER ELASTIC ZONE r=r_n to b
PRINT STRESS COMPONENTS
r≥b
NO
INCREASE r
YES
STOP

```
HRK4.                                                          TYAGI DEV
RUN(S)
SETINDF.
REDUCE.
LGO.
'          6400 END OF RECORD
      PROGRAM TST (INPUT,OUTPUT,TAPE5=INPUT,TAPE6=OUTPUT)
C     TO CALCULATE THE STRESS COMPONENTS BY APPROXIMATE ANALYSIS
C     SPRING-BACK IS COMPLETELY ELASTIC
C     VARIABLES NOTATIONS AS DEFINED IN APPENDIX A.1
C     CHANGING THE VALUE OF BRATIO(OR A/T) IN THE DATA STATEMENT
     *WOULD ENABLE TO GET THE STRESSES FOR ANY RATIO OF A/T
C     STRESS COMPONENTS ARE THE COEFFICIENTS OF YIELD STRESS
C     STRESSES GIVEN BY TRESCA YIELD CRITERION,WHEN MULTIPLIED BY A
     *COEFFICIENT (2./SQRT(3.)) GIVE STRESSES FOR VON-MISES CRITERION
      REAL MOM,N
      WRITE(6,100)
  100 FORMAT(8X,*R*,6X,*RES R*,5X,*RES T*,5X,*RES Z*,5X,*DEV R*,5X,*DEV
     1T*,5X,*DEV Z*,5X,*SIGR1*,5X,*SIGT1*,5X,*SIGZ1*,5X,*SIGR2*,5X,*SIGT
     12*,5X,*SIGZ2*,///)
   10 FORMAT(1X,13F10.5,/)
   20 FORMAT(3F10.0)
      READ(5,20)BRATIO,T,PR
      A=(BRATIO)*T
      C=A+T
      MOM=(T**2)/4.
      RN=SQRT(A*C)
```

```
C       COMPUTE BENDING STRESSES FOR FIBRES BELOW NEUTRAL AXIS
        R=A
 11     IF(R.GT.RN)GO TO 22
        BSR=-ALOG(R/A)
        BST=BSR-1.
        BSZ=0.5*(BSR+BST)
        GO TO 33
C       COMPUTE BENDING STRESSES FOR FIBRES ABOVE NEUTRAL AXIS
 22     BSR=ALOG(R/C)
        BST=BSR+1.
        BSZ=0.5*(BSR+BST)
 33     CONTINUE
C       COMPUTE SPRING-BACK STRESSES
        N=((C*C-A*A)**2)-4.*A*A*C*C*((ALOG(C/A))**2)
        STR =-(4.*MOM/N)*(((A*A*C*C)/(R*R))*ALOG(C/A)+C*C*ALOG(R/C)+A*A*AL
      1 OG(A/R))
        STT =-(4.*MOM/N)*(-((A*A*C*C)/(R*R))*ALOG(C/A)+C*C*ALOG(R/C)
      1 +A*A*ALOG(A/R)+C*C-A*A)
        STZ=PR*(STR+STT)
C       COMPUTE RESIDUAL AND DEVIATORIC STRESS COMPONENTS
        RESR=STR+BSR
        REST=STT+BST
        RESZ=STZ+BSZ
        SIGMN=(RESR+REST+RESZ)/3.
        DEVR=RESR-SIGMN
        DEVT=REST-SIGMN
        DEVZ=RESZ-SIGMN
        WRITE(6,10)R,RESR,REST,RESZ,DEVR,DEVT,DEVZ,BSR,BST,BSZ,STR,STT,STZ
```

```
      IF(R.GE.C) GO TO 44
      R=R+.01
      GO TO 11
 44   STOP
      END
'        END OF RECORD
   1.5        0.25       0.3
'          END OF FILE
```

CD TOT 0065

```
HRK4,CM60000,T500.                                          TYAGI DEV
RUN(S)
SETINDF.
REDUCE.
LGO.
'          6400 END OF RECORD
      PROGRAM TST (INPUT,OUTPUT,TAPE5=INPUT,TAPE6=OUTPUT)
C     TO CALCULATE THE STRESS COMPONENTS BY EXACT ANALYSIS
C     PLASTIC CORE IS CONSIDERED
C     VARIABLE NOTATIONS AS DEFINED IN APPENDIX A.1
C     SHEET HAS BEEN DIVIDED IN TO 2500 PARTS
C     CHANGING THE VALUE OF BRATIO(OR A/T) IN THE DATA STATEMENT
     *WOULD ENABLE TO GET THE STRESSES FOR ANY RATIO OF A/T
C     STRESS COMPONENTS ARE THE COEFFICIENTS OF YIELD STRESS
C     STRESSES GIVEN BY TRESCA YIELD CRITERION,WHEN MULTIPLIED BY A
     *COEFFICIENT (2./SQRT(3.)) GIVE STRESSES FOR VON-MISES CRITERION
C     STRESS COMPONENTS IN FIRST ROW AGAINST ANY VALUE OF R ARE FOR
     *TRESCA YIELD CRITERION AND THOSE IN THE SECOND ROW ARE FOR
     *VON-MISES YIELD CRITERION
      DIMENSION S(2501),SR(2501),SSR(2501),SST(2501),SSZ(2501)
      READ(5,80)BRATIO,T,PR,M
      A=(BRATIO)*T
      RN=SQRT(A*(A+T))
      BETA=(2.*PR-1.)/(1.-PR)
      MM=M+1
      D=T/FLOAT(M)
      VM=2./SQRT(3.)
```

```
      AN=M
 10   FORMAT(6X,5F16.6,//////)
 20   FORMAT(6X,6E16.6,///)
 30   FORMAT(6X,5E16.6)
 40   FORMAT(1H1)
 50   FORMAT(8X,*R*,6X,*RES R*,5X,*RES T*,5X,*RES Z*,5X,*DEV R*,5X,*DEV
     1T*,5X,*DEV Z*,5X,*SIGR1*,5X,*SIGT1*,5X,*SIGZ1*,5X,*SIGR2*,5X,*SIGT
     12*,5X,*SIGZ2*,///)
 60   FORMAT(1X,13F10.5,/)
 70   FORMAT(11X,12F10.5,//)
 80   FORMAT(3F10.0,I5)
C     COMPUTE B AND X
      PROD1=1./(A+(AN-1.)*D)
      PROD2=PROD1/(A+(AN-1.)*D)
      SUM1=PROD1
      SUM2=PROD2
      DO 1 I=2,M
      AI=M-I+1
      PROD1=PROD1*(A+(AI+BETA)*D)/(A+(AI-1.)*D)
      PROD2=PROD1/(A+(AI-1.)*D)
      SUM1=SUM1+PROD1
 1    SUM2=SUM2+PROD2
      B=SUM1/SUM2
      X=B-A
C     COMPUTE S(J),SR(J),STRRN,RO AND F
      DO 3 J=2,M
      AN=J-1
      PROD1=1./(A+(AN-1.)*D)
```

```
      PROD2=PROD1/(A+(AN-1.)*D)
      SUM1=PROD1
      SUM2=PROD2
      IF(J.EQ.2) GO TO 11
      DO 2 I=3,J
      AI=J-I+1
      PROD1=PROD1*(A+(AI+BETA)*D)/(A+(AI-1.)*D)
      PROD2=PROD1/(A+(AI-1.)*D)
      SUM1=SUM1+PROD1
    2 SUM2=SUM2+PROD2
   11 SR(J)=D*(B*SUM2-SUM1)
    3 S(J)=(B-(A+AN*D))/(A+AN*D)+(BETA+1.)*SR(J)
      SR(1)=0.0
      SR(MM)=0.0
      S(1)=B/A-1.
      S(MM)=B/(A+T)-1.
      AK=(RN-A)/D
      K=AK+1.
      STRRN=SR(K)
      RO=B/(1.-BETA*STRRN)
      F=(1./BETA)*(B/RO-1.)
      WRITE(6,10)B,X,STRRN,RO,F
C     COMPUTE AZ AND ALK
      F2=0.0
      AM2=0.0
      DO 4 I=K,M
      F2=F2+D*(S(I)+S(I+1))/2.
    4 AM2=AM2+D*(S(I)+S(I+1))/2.*(A+(FLOAT(I)-.5)*D)
```

```
      F1=0.0
      AM1=0.0
      AK=(RO-A)/D
      K=AK
      DO 5 I=1,K
      F1=F1+D*(S(I)+S(I+1))/2.
    5 AM1=AM1+D*(S(I)+S(I+1))/2.*(A+(FLOAT(I)-.5)*D)
      AZ=(T*T)/(2.*F*(RN*RN-RO*RO)-4.*(AM1+AM2))
      ALK=AZ*F
C     COMPUTE THE SUM OF FORCE AND MOMENT TO SEE WHETHER THEY ARE ZERO
     *OR VERY SMALL TO SATISFY EQUILIBRIUM
      F3=ALK*(RN-RO)
      AM3=(RN*RN-RO*RO)*ALK/2.-T*T/4.
      SUMF=AZ*(F1+F2)-F3
      SUMM=AZ*(AM1+AM2)-AM3
      STR=AZ*(1.-PR*PR)*(B-A)/A
      WRITE(6,20)F1,AM1,F2,AM2,F3,AM3
      WRITE(6,30)SUMF,SUMM,AZ,ALK,STR
      WRITE(6,40)
      WRITE(6,50)
C     COMPUTE STRESS COMPONENTS IN THE LOWER ELASTIC ZONE FOR TRESCA
      L=IFIX((RO-A)*100.)
      L=L*100+1
      DO 6 J=1,L,100
   22 AK=J-1
      R=A+AK*D
      SSR(J)=SR(J)*AZ
      SST(J)=S(J)*AZ
```

```
      SSZ(J)=(PR)*(SSR(J)+SST(J))
      BSR=-ALOG(R/A)
      BST=BSR-1.
      BSZ=(BSR+BST)/2.
      RESR=SSR(J)+BSR
      REST=SST(J)+BST
      RESZ=SSZ(J)+BSZ
      SIGMN=(RESR+REST+RESZ)/3.
      DEVR=RESR-SIGMN
      DEVT=REST-SIGMN
      DEVZ=RESZ-SIGMN
      WRITE(6,60)R,RESR,REST,RESZ,DEVR,DEVT,DEVZ,BSR,BST,BSZ,SSR(J),
     1SST(J),SSZ(J)
C     COMPUTE STRESSES FOR VON-MISES YIELD CRITERION
      BSR=(VM)*(BSR)
      BST=(VM)*(BST)
      BSZ=(VM)*(BSZ)
      SSR(J)=(VM)*(SSR(J))
      SST(J)=(VM)*(SST(J))
      SSZ(J)=(VM)*(SSZ(J))
      RESR=(VM)*(RESR)
      REST=(VM)*(REST)
      RESZ=(VM)*(RESZ)
      DEVR=(VM)*(DEVR)
      DEVT=(VM)*(DEVT)
      DEVZ=(VM)*(DEVZ)
    6 WRITE(6,70)  RESR,REST,RESZ,DEVR,DEVT,DEVZ,BSR,BST,BSZ,SSR(J),
     1SST(J),SSZ(J)
```

```
C       COMPUTE STRESS COMPONENTS AT LOWER ELASTIC-PLASTIC BOUNDRY-TRESCA
        L=IFIX((RO-A)/D+1.)
        IF(J.EQ.L) GO TO 33
        J=L
        GO TO 22
 33     R=RO
 44     RESR=-ALOG(R/A)-ALK
        REST=RESR-1.
        RESZ=(RESR+REST)/2.
        SIGMN=(RESR+REST+RESZ)/3.
        DEVR=RESR-SIGMN
        DEVT=REST-SIGMN
        DEVZ=RESZ-SIGMN
        BSR=-ALOG(R/A)
        BST=BSR-1.
        BSZ=(BSR+BST)/2.
        STR=RESR-BSR
        STT=REST-BST
        STZ=RESZ-BSZ
        WRITE(6,60)R,RESR,REST,RESZ,DEVR,DEVT,DEVZ,BSR,BST,BSZ,STR,STT,STZ
C       COMPUTE STRESSES FOR VON-MISES YIELD CRITERION
        BSR=(VM)*(BSR)
        BST=(VM)*(BST)
        BSZ=(VM)*(BSZ)
        STR=(VM)*(STR)
        STT=(VM)*(STT)
        STZ=(VM)*(STZ)
        RESR=(VM)*(RESR)
```

```
      REST=(VM)*(REST)
      RESZ=(VM)*(RESZ)
      DEVR=(VM)*(DEVR)
      DEVT=(VM)*(DEVT)
      DEVZ=(VM)*(DEVZ)
      WRITE(6,70)  RESR,REST,RESZ,DEVR,DEVT,DEVZ,BSR,BST,BSZ,STR,STT,STZ
C     COMPUTE STRESS COMPONENTS AT LOWER PLASTIC-ELASTIC BOUNDRY-TRESCA
C     COMPUTE STRESSES FOR VON-MISES YIELD CRITERION
      L=IFIX((RO*1000.)+1.)
      AL=L
      AL=AL/1000.
      IF(R.GE.AL) GO TO 55
      R=AL
      K=0
      GO TO 44
C     COMPUTE STRESS COMPONENTS IN THE PLASTIC CORE FOR TRESCA
C     COMPUTE STRESSES FOR VON-MISES YIELD CRITERION
 55   L=IFIX(RN*1000.)-IFIX(RO*1000.+1.)
      IF(K.GE.L) GO TO 66
      R=R+0.0010
      K=K+1
      GO TO 44
 66   IF(R.GE.RN) GO TO 77
C     COMPUTE STRESS COMPONENTS AT UPPER PLASTIC-ELASTIC BOUNDRY-TRESCA
C     COMPUTE STRESSES FOR VON-MISES YIELD CRITERION
      R=RN
      GO TO 44
C     COMPUTE STRESS COMPONENTS AT UPPER ELASTIC-PLASTIC BOUNDRY-TRESCA
```

```
 77   L=IFIX((RN-A)/D+1.)
      J=L
      AK=J-1
      R=A+AK*D
      SSR(J)=SR(J)*AZ
      SST(J)=S(J)*AZ
      SSZ(J)=(PR)*(SSR(J)+SST(J))
      BSR=ALOG(R/(A+T))
      BST=BSR+1.
      BSZ=(BSR+BST)/2.
      RESR=SSR(J)+BSR
      REST=SST(J)+BST
      RESZ=SSZ(J)+BSZ
      SIGMN=(RESR+REST+RESZ)/3.
      DEVR=RESR-SIGMN
      DEVT=REST-SIGMN
      DEVZ=RESZ-SIGMN
      WRITE(6,60)R,RESR,REST,RESZ,DEVR,DEVT,DEVZ,BSR,BST,BSZ,SSR(J),
     1SST(J),SSZ(J)
C     COMPUTE STRESSES FOR VON-MISES YIELD CRITERION
      BSR=(VM)*(BSR)
      BST=(VM)*(BST)
      BSZ=(VM)*(BSZ)
      SSR(J)=(VM)*(SSR(J))
      SST(J)=(VM)*(SST(J))
      SSZ(J)=(VM)*(SSZ(J))
      RESR=(VM)*(RESR)
      REST=(VM)*(REST)
```

```
      RESZ=(VM)*(RESZ)
      DEVR=(VM)*(DEVR)
      DEVT=(VM)*(DEVT)
      DEVZ=(VM)*(DEVZ)
      WRITE(6,70)  RESR,REST,RESZ,DEVR,DEVT,DEVZ,BSR,BST,BSZ,SSR(J),
     1SST(J),SSZ(J)
C     COMPUTE STRESS COMPONENTS IN THE UPPER ELASTIC ZONE FOR TRESCA
      L=IFIX((RN-A)*100.+1.)
      L=L*100+1
      DO 7 J=L,2501,100
      AK=J-1
      R=A+AK*D
      SSR(J)=SR(J)*AZ
      SST(J)=S(J)*AZ
      SSZ(J)=(PR)*(SSR(J)+SST(J))
      BSR=ALOG(R/(A+T))
      BST=BSR+1.
      BSZ=(BSR+BST)/2.
      RESR=SSR(J)+BSR
      REST=SST(J)+BST
      RESZ=SSZ(J)+BSZ
      SIGMN=(RESR+REST+RESZ)/3.
      DEVR=RESR-SIGMN
      DEVT=REST-SIGMN
      DEVZ=RESZ-SIGMN
      WRITE(6,60)R,RESR,REST,RESZ,DEVR,DEVT,DEVZ,BSR,BST,BSZ,SSR(J),
     1SST(J),SSZ(J)
C     COMPUTE STRESSES FOR VON-MISES YIELD CRITERION
```

```
      BSR=(VM)*(BSR)
      BST=(VM)*(BST)
      BSZ=(VM)*(BSZ)
      SSR(J)=(VM)*(SSR(J))
      SST(J)=(VM)*(SST(J))
      SSZ(J)=(VM)*(SSZ(J))
      RESR=(VM)*(RESR)
      REST=(VM)*(REST)
      RESZ=(VM)*(RESZ)
      DEVR=(VM)*(DEVR)
      DEVT=(VM)*(DEVT)
      DEVZ=(VM)*(DEVZ)
 7    WRITE(6,70)  RESR,REST,RESZ,DEVR,DEVT,DEVZ,BSR,BST,BSZ,SSR(J),
     1SST(J),SSZ(J)
      STOP
      END
'        6400 END OF RECORD
  1.5       0.25       0.3       2500
'          END OF FILE
```

CD TOT 0272

BIBLIOGRAPHY

1. Chajes, A., Britvec, S.J. and Winter, G.
"Effect of Cold-Straining on Structural Sheet Steels", Journal of Structural Division, ASCE, Vol. 89, No. ST2, Proc. Paper 3477, April 1963, pp 1-32.

2. Karren, K.W.
"Corner Properties of Cold-Formed Steel Shapes", Journal of Structural Division, ASCE, Vol. 93, No. ST 1, Proc. Paper 5112, Feb. 1967 pp 401-432.

3. Karren, K.W. and Winter, G.
"Effects of Cold-Forming on Light Gage Steel Members", Journal of Structural Division, ASCE, Proc. Paper 5113, Vol. 93, No. ST1, Feb. 1967 pp 433-469

4. Winter, G.
"Cold-Formed, Light-Gage Steel Construction", Journal of Structural Division, ASCE, Proc. Paper 2270, Vol. 86, No. ST9, Nov. 1959, pp 151-173.

5. Sangdahl, G.S., Aul, E.L. and Sachs, G.
"An Investigation of the Stress and Strain States Occuring in Rectangular Bars", Proceeding, Society for Experimental Stress Analysis, Cambridge, Mass., Vol. VI, No. I, 1948, pp 1-18.

6. Hill, R.

"The Mathematical Theory of Plasticity", Oxford Univ. Press, London, England, 1950.

7. Nadai, A.

"Theory of Flow and Fracture of Solids", Vol. 1, McGraw-Hill Book Co., Inc., New York, N.Y., 1950.

8. Rolfe, S.T.

Discussion of "Effect of Cold-Straining on Structural-Sheet Steel", By Chajes, A., Britvec, S.J. and Winter, G., Journal of the Structural Division, ASCE, Proc. Paper 3688, Vol. 89, No. ST5, Oct. 1963, pp333.

9. Lowe, J. and Garafalo, F., "Precision Determination of Stress-Strain Curves in the Plastic Range", Proceedings, Soc. for Experimental Stress Analysis, Cambridge, Mass. Vol IV, NO. II, 1947, pp16-25.

10. Hoffman, O. and Sachs, G.

"Plasticity", McGraw-Hill Book Co., Inc., New York, N.Y., 1953.

11. Mendelson, A.

"Plasticity:Theory and Application", The Macmillan Co., New York, 1968.

12. Daniels, L.R.

"The Influence of Residual Stress Due to Cold Bending on Thin-Walled Open Sections", M.Eng. Thesis, McMaster Univ. 1969.

13. Gursahani, M.
"Influence of Plastic Straining on a Yield Criterion", M.Eng. Thesis, McMaster Univ. 1970.

14. Osgood, W.R.
"Note on Plane Strain", Journal of Applied Mechanics, March 1942, Vol. 9, No. 1, ppA-26.

15. "Hydraulic Presses Versus Drop Presses",--Topical Discussion No. 579-101, Trans. of ASME, 1893-94, Vol. 15, pp591-592.

16. Riggs, J.D.
"Cold-Working Sheet Metal in Dies", and its discussion, ASME Tras. Paper 941, 1902, pp547-568.

17. Cook, D.P. "Pressed-Metal Engineering", Mechanical Engineering 1924, Vol. 46, pp123-128.

18. Crane, E.V.
"Cold-Press Finishing of Metal", Mechanical Engineering 1926, Vol. 48, pp899-906.

19. Schroeder, W. "Mechanics of Sheet Metal Bending", ASME Trans. 1943, Vol. 65, No. 1, pp817-827.

20. Thomsen, E.G.
"A New Approach to Metal-Forming Problems", ASME Transactions 1955, Vol. 77, pp515-522.

21. Crane, E.V.
"Plastic Metal Working", ASME Transactions 1956, Vol. 78 pp413-415.

22. Wagner, W.S.
"Plastic Working of Metals", ASME Transactions 1956, Vol 78, pp401-405.

23. Lee, E.H.
"The Theoretical Analysis of Metal-Forming Problems in Plane Strain", ASME Trans., Journal of Applied Mech. 1952, Vol. 19, pp97-108.

24. "Sandwich-Rolling Process", Mechanical Engineering Feb. 1958, Vol. 80, pp87.

25. Shaffer, B.W. and Ungar, E.E.
"Mechanics of Sheet-Bending Process", ASME Trans., Jour. of App. Mech. March 1960, Vol. 27, pp34.

26. Junker, A.T.
"Bending of Thick Steel Plates", ASME Trans., Jour. of Basic Engrg., June 1965, Vol. 87, pp290-292.

27. Gill, G.S. and Parker, J.
"Plastic Stress-Strain Relationships--Some Experiments on the Effect of Loading Path and Loading History", ASME Trans., Jour. of App. Mech., March 1959, Vol. 26, pp77-87.

28. Phillips, A. and Gray, G.A.
"Experimental Investigation of Corners in the Yield Surface", ASME Trans., Jour. of Basic Engrg., June 1961, Vol. 83, pp275-288.

29. May, I.L. and Nair, K.D.
"On Relative Validity of Two Current Cold-Rolling Theories", ASME Trans., Jour. of Basic Engrg. March 1967, pp69-75.

30. Rolfe, S.T., Haak, R.P. and Gross, J.H.
"Effect of State-of-Stress and Yield Criterion on the Bauschinger Effect", ASME Trans., Jour. of Basic Engrg., Sept. 1968, pp403-408.

31. Budiansky, B.
"A Reassessement of Deformation Theories of Plasticity", ASME Trans., Jour. of App. Mech., June 1958, Vol. 26, pp259-264.

32. Eason, G.
"The Elastic, Plastic Bending of a Simply Supported Plate", ASME Trans., Jour. of App. Mech., Sept. 1961, Vol. 28, pp.395-401.

33. Eason, G.
"The Elastic-Plastic Bending of a Curved bar by End Couples in Plane Stress", Quarterly Jour. of Mechanics and App. Mathematics, 1960, Vol. 13, pp334-358.

34. Hoffman, O., Sachs, G.
"Introduction to the Theory of Plasticity for Engineers", McGraw-Hill Book Co., Inc., New York N.Y., 1953.

35. Lubahn, J.D. and Sachs, G.
"Bending of an Ideal Plastic Metal", ASME Trans., Feb. 1950, pp201-208.

36. Shaffer, B.W. and House, R.N.
"Displacemet in a Wide Curved Bar Subjected to Pure Elastic-Plastic Bending", ASME Trans., Jour. of App. Mech., Sept. 1957, pp447-452.

37. Shaffer, B.W. and House, R.N.
"The Elastic-Plastic Stress Distribution Within a Wide Curved Bar Subjected to Pure Bending", ASME Trans. Jour. of App. Mech, Sept. 1955, pp 305-310.

38. Alexander, J.M.
"An Analysis of the Plastic Bending of Wide Plate and the Effect of Stretching on Transverse Residual Stresses", Proc. Inst. of Mech. Engrs. Vol. 173, No. 1, 1959, pp73-85.

39. Timoshenko, S. and Goodier, J.N.
"Theory of Elasticity", McGraw-Hill Book Company, Inc., New York, 1951.

40. Fung, Y.C. and Wittrich, W.H.
"A Boundary Layer Phenomenon in the Large Deflection of Thin Plates", Quart. Journal Mech. and App. Math., Vol. VIII, Pt. 2, 1955.

41. Drucker, D.C.

"Stress-Strain Relations in the Plastic Range", Graduate Div. of Applied Maths., Brown Univ., Providence, R.I., Dec. 1950.

42. Gardiner, F.J.

"The Spring Back of Metals", ASME Trans., Vol. 79, Jan. 1957, ppl-9.

43. Shaffer, B.W. and House, R.N.

"The Significance of Zero Shear Stress in the Pure Bending of a Wide Curved Bar", Jour. of the Aeronautical Sciences, Vol. 24, 1957, pp307-308.